DEVELOPMENT OF ENERGY EFFICIENT HYBRID POWER SYSTEM FOR GREEN CELLULAR BASE STATIONS

By

Md. Sanwar Hossain
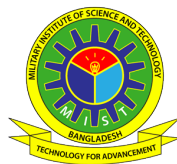
Student No - 1014160013 (P)

A THESIS SUBMITTED FOR THE DEGREE OF

MASTER OF SCIENCE

IN

ELECTRICAL, ELECTRONIC AND COMMUNICATION ENGINEERING

Department of Electrical, Electronic and Communication Engineering

MILITARY INSTITUTE OF SCIENCE AND TECHNOLOGY

Mirpur Cantonment, Dhaka-1216

March 2021

APPROVAL CERTIFICATE

The thesis titled **"DEVELOPMENT OF ENERGY EFFICIENT HYBRID POWER SYS-TEM FOR GREEN CELLULAR BASE STATIONS"** submitted by Md. Sanwar Hossain, Student No - 1014160013 (P), Session Oct/2014 has been accepted as satisfactory in partial fulfillment of the requirements for the degree of Master of Science in Electrical, Electronic and Communication Engineering on 04th March 2021.

BOARD OF EXAMINERS

1. _____   Chairman

   Dr. Md. Fayzur Rahman   (Supervisor)
   Professor
   Department of EEE, Green University, Dhaka-1207

2. _____   Member

   Brig Gen A K M Nazrul Islam, PhD   (Ex-Officio)
   Senior Instructor and Head
   Department of EECE, MIST, Dhaka-1216

3. _____   Member

   Lt Col Md. Tawfiq Amin, PhD
   Instructor Class A
   Department of EECE, MIST, Dhaka-1216

4. _____   Member

   Dr. Kazi Mujibur Rahman   (External)
   Professor
   Department of EEE, BUET, Dhaka-1205

DECLARATION

I hereby declare that this submission is my own work and to the best of my knowledge and belief, it contains no material previously published or written by another person, nor material which to a substantial extent has been accepted for the award of any other degree or diploma at MIST or any other educational institution, except where due acknowledgement is made in the thesis. I also declare that the intellectual content of this thesis is the product of my own work, except to the extent that assistance from others in the project's design and conception or in style, presentation and linguistic expression is acknowledged.

Signature of the Candidate

_____

Md. Sanwar Hossain

Dedicated to my parents and my wife

ACKNOWLEDGEMENT

First and foremost, my sincere gratitude goes to ALLAH, The Almighty God, the most Beneficent and Merciful. All praises are due to Him for giving His unlimited Mercy and Blessings throughout my MSc work.

I wish to express my sincere thanks and deepest appreciation to my supervisor, Professor Dr. Md. Fayzur Rahman, for his excellent supervision, invaluable advice, insightful discussions, continuous skilled guidance, encouragement and patience throughout this work. Despite his busy schedule, he always managed to schedule a meeting when needed and I greatly value his uncomplaining proofreading and polishing of all my papers.

I also express my warmest gratitude to Abu Jahid, for his help and support throughout my MSc candidature. I am sure it would have not been possible for me to complete this task without their invaluable generosity and commitment.

I would be pleased to extend my sincere thanks to all of my course teachers and staffs of EECE department, MIST for their cordial help and excellent support for successful completion of my research works.

Most importantly, none of this would have been possible without the love and patience of my family. I would like to express my heartfelt gratitude to my family for their unconditional love, encouragement, prayers and guidance.

ABSTRACT

A cellular base station (BS) powered by renewable energy sources (RES) is a timely requirement for the growing demand of wireless communication. Designing such a BS in Bangladesh poses some challenges due to the dynamic profile of the RES and traffic intensity in the tempo-spatial domain. Besides, generating energy from renewable energy sources (RES) plays an important role to cut the carbon footprints in the atmosphere by decreasing production of energy from conventional sources. Considering these issues, this thesis aims at developing a sustainable and environment-friendly cellular infrastructure using the locally available RES like hybrid solar photovoltaic (PV)/biomass generator (BG). The optimal system architecture and technical criteria of the proposed system are critically evaluated with the help of Hybrid Optimization Model for Electric Renewables (HOMER) optimization software for both on-grid and off-grid conditions to downsize the electricity generation cost and greenhouse gas (GHG) outflows while ensuring the desired quality of services over 20-year duration at the same time. Besides, the green energy sharing mechanism under the off-grid condition and the grid-tied condition has been critically analyzed for optimal use of green energy. Furthermore, a thorough investigation is conducted with the help of Monte-Carlo simulations to assess the wireless network performance in terms of throughput, spectral efficiency, and energy efficiency under the wide range of network configurations. A heuristic algorithm of load balancing technique among collocated BSs has been incorporated for elevating the spectral efficiency, and outage probability performance of the user equipment under various system configurations such as several simulations users, system bandwidth, and channel quality indicators (CQI). Simulation results reveal that the proper load balancing technique pledges zero outage probability with expected system performance whereas energy cooperation policy offers an attractive solution for developing green mobile communications through better utilization of renewable energy under the proposed hybrid solar PV/BG scheme. The research also finds that the energy-trading facility can achieve net present cost (NPC) and greenhouse gas saving up to 3.20% and 65.8%, respectively by ensuring the guaranteed continuity of power supply. The hybrid supply system has sufficient excess electricity and backup capacity that increase the system's reliability. In the end, the performance of the hybrid solar PV/BG system has been thoroughly compared with the standalone solar PV, hybrid PV/wind turbine (WT), and hybrid PV/diesel generator (DG) systems under on-grid and off-grid configurations for justifying the system validity.

CONTENTS

LIST OF FIGURES

LIST OF TABLES

LIST OF SYMBOLS

Symbols	Description
$\mathcal{BW}$	Bandwidth
$\mathcal{P}_{BS}$	Input power consumption of BS_i
$\mathcal{P}_{sleep}$	Power consumption on sleep mode of BS_i
$\mathcal{P}_0$	Power consumption at idle state
χ_i	Traffic demand of $\mathcal{B}S_i$
α	Path-loss exponent
d_0	Reference distance
d	Distance between transmitter and UE
X_σ	Random variable of shadow fading
σ	Standard deviation of shadow fading
$\mathcal{P}_{k,intra}$	Intra-cell interference of kth user
$\mathcal{P}_{k,inter}$	Intea-cell interference of kth user
$\mathcal{P}_N$	Additive white Gaussian noise (AWGN) power
$P_{tx}^{i,k}$	Transmitted power in i^{th} BS of kth user
$P_{rx}^{i,k}$	Received power in i^{th} BS of kth user
N	Total number of BSs
U	Total number of users
Δ	Slope of load dependent power consumption
N_{TRX}	Number of transceiver in a BS
P_1	Maximum power consumption in a sector
P_{TX}	RF transmit power
P_{BB}	Power consumption of baseband unit
P_{RF}	Power consumption of radio frequency unit
P_{PA}	Power consumption in the power amplifier
η_{PA}	Power amplifier efficiency
σ_{DC}	DC-DC power supply loss
σ_{MS}	Mains supply loss
σ_{cool}	Cooling loss
σ_{feed}	Feeder cable loss
R_{Total}	Total achievable throughput

$SINR_{i,k}$	Signal-to-interference plus noise ratio for k^{th} UE from BS_i
η_{EE}	Energy efficiency
$n_{RB}(t)$	Total number of resource blocks
E_{Loss}	Line loss energy
N_{batt}	Number of battery cells in the battery bank
B_{aut}	Battery bank autonomy
B_{life}	Battery bank lifetime
Q_{life}	Lifetime throughput of a single battery
Q_{tp}	Annual battery throughput
V_{bb}	DC bus-bar voltage
E_{Gen}	Total generated electricity
B_{Loss}	Battery loss
C_{Loss}	Converter loss
E_{Share}	Net energy transferred

LIST OF ABBREVIATIONS

Abbreviations	Description
AES	Average Energy Saving
BB	Basesband
BG	Biomass Generator
BS	Base Station
BW	Bandwidth
CQI	Channel Quality Indicator
DOD	Depth of Discharge
EE	Energy Efficiency
EMU	Energy Management Unit
GHG	GreenHouse Gas
GSM	Global System for Mobile Communications
HetNet	Heterogeneous Network
HOMER	Hybrid Optimization Model for Electric Renewables
IC	Initial Costs
ICI	Inter-Cell Interference
ICT	Information and Communication Technology
LTE	Long Term Evolution
LTE-A	LTE-Advanced
NPC	Net Present Cost
OFDMA	Orthogonal Frequency Division Multiple Access
OMC	Operation and Maintenance Costs
OPEX	Operational Expenditure
PA	Power Amplifier
PV	Photovoltaic
QoS	Quality of Service
RAN	Radio Access Network
RB	Resource Block
RC	Replacement Costs
RES	Renewable Energy Source
RF	Radio Frequency
RRH	Remote Radio Head

SV	Salvage value
SAM	System Advisory Model
SE	Spectral Efficiency
SG	Smart Grid
SINR	Signal-to-Interference-plus-Noise-Ratio
SOC	State of Charge
TRX	Transceiver
UE	User Equipment
VoLTE	Voice over LTE
WT	Wind Turbine

CHAPTER 1

INTRODUCTION

1.1   Introduction

With the remarkable increase in the number of mobile subscribers and high-speed data demand, cellular network operators are deploying a higher number of base stations throughout the world [1, 2]. According to the Ericsson survey, the number of the global mobile subscriber up to the first quarter of 2019 was around 7.9 billion, with 44 million new subscribers added during this quarter, wherein long term evolution (LTE) subscribers are 3.7 billion [3]. Currently, Bangladesh has 88 million unique subscribers and it is expected that at the end of 2025, this value will be 107 million [4]. Global system for mobile communications association (GSMA) mentions that at present, the number of universal base stations (BSs) is above 4 million and it is nearly double from 2007 to 2012 [5]. Over the last decades, the exponential evolution of information and communication technology (ICT) has significantly increased the power consumption by cellular networks. This rapid and radical deployment of cellular base stations is pushing up the total energy demand, resulting in an enormous burden on the power grid and triggering harmful greenhouse gas emissions. Base stations are the premier energy consumer of mobile networks which receive 57% of the total consumed energy [6]. In the year of 2007, the annual worldwide consumption of electricity by the telecom industry was 219 TWh that increased to 354 TWh in the year 2012 [7]. It is expected that energy consumption will be escalated at an additional yearly rate of 10% from 2013 to 2019. Till 2017 [8], Bangladesh has above 36679 Global system for mobile communications (GSM) BSs, which consume around 642 million kWh of energy and within this 14%, BSs are off-grid [8]. Additionally, 81% of the off-grid BSs in Bangladesh are powered by a diesel generator (DG) plus a battery system [8]. The international energy agency (IEA) has just released its latest global energy projection named the World Energy Outlook 2018 (WEO2018) where global energy demand is expected to grow by around 27% equivalent to 3,743 million tons oil from 2017 to 2040 [9]. According to [10], the information and communication technology sector consumes about 5%-10% of universal electricity production and produces about 2% to 4% of global carbon dioxide (CO_2) outflow, wherein BSs consume about 60% to 80% of the electricity consumed by the ICT sector.

Due to the aforementioned facts, telecom network operators are always trying to find out the alternative source of environment-friendly and cost-effective energy. As a consequence, harvesting energy from the locally available renewable energy sources has become one of the major concerns of academia and researchers [11–13]. Renewable energy sources (RES) such as solar, wind, biomass, hydro, geothermal, etc. are reusable and widely available in many places throughout the world [11–13]. Moreover, a huge amount of energy can be harvested from renewable energy sources with the help of modern technology by minimizing cost [14–16]. Being inspired by the potential benefits of renewable energy sources, telecom operators are progressively installing cellular BSs powered by the locally available RES. Despite the potential benefits, there are some challenges of harvesting energy from renewable energy sources due to the dynamic nature of RES and its dependency on the condition of weather [14–16]. Moreover, the use of renewable energy in the telecom industry may cause a shortage or outage of energy that may arise due to the intermittency nature of RES. The shortage or outage of energy is not allowed in the telecom industry which may degrade the continuity of power supply and reliability. However, the reliability of the renewable energy-based supply system can be ensured in the following ways: (i) by integrating the renewable energy sources with the non-renewable energy source, (ii) by integrating different types of renewable energy sources, and (iii) by integrating the renewable energy source or sources with the adequate energy storage devices. In [14, 17], authors examined the feasibility of deploying renewable energy-based cellular networks in different regions around the world and reported that approximately 320100 renewable energy-based off-grid BSs were installed till 2014 and around 389800 green energy enabled off-grid BSs would be in function within 2020.

Bangladesh is a tropical country that is situated between $20°34'$ and $26°38'$ north latitude and $88°01'$ and $92°41'$ east longitude with an area of 1,47,570 km^2 [17]. Bangladesh has the enormous potential of green energy generation from solar and biomass energy sources that create great opportunities for the fulfillment of present and future power demand. According to the national aeronautics and space administration (NASA) surface meteorology and solar energy database, the daily solar intensity of the country remain in the range of 4-6.5 kWh/m^2 with average solar radiation of 4.59 $kWh/m^2/day$ [18]. It has been reported that Bangladesh obtains around 70 PWh of solar energy each year which is 3000 times higher than the total electrical energy generation of the country [19]. Being motivated by the above potential solution, solar photovoltaic (PV) supplied base station has already been established

2

in Bangladesh [20]. Authors in [14] mentioned that up to 2015 above 521 solar PV powered base stations have already been installed in Bangladesh and telecom operators are trying to enhance the figure.

In the meantime, biomass is the fourth greatest energy source in the world, which contributes around 8.5% of the total world energy. In 2012, the United States produced around 15 GW of power from biomass which is almost 18% of the total biomass generated power in the world [21]. It is expected that within the next century, almost 50% of the world energy requirement will be supplied by biomass energy [22]. Nowadays, Bangladesh has also started generating energy from biomass on a small scale though most of the energy generated from the biomass is used for cooking and heating purposes only. Energy generation from biomass resources has a huge scope for Bangladesh because of the low cost of biomass and the high efficiency of energy conversion. At the same time, agriculture residue is the key source of biomass energy in Bangladesh where rice-husk constitutes a significant amount [23]. As reported by the 'Rice Mills Owners Association' in Bangladesh, there are around 540 rice mills throughout the country with an average capacity of 30 tons/day. They also report that 540 rice mills have the potential of producing 171 MW per day [24, 25]. According to [21], Bangladesh had approximate 90.21 million tons' of biomass available in fiscal year (FY) 2012-2013 whose energy potential is 1344.99 PJ equivalent to 373.71 TWh. Authors in [26] studied that Bangladesh will be able to generate 7682 GWh energy from the rice husk with a total capacity of 1066 MW in 2030. Moreover, around 13% of the total primary energy consumption came from renewable energy sources in 2012 [21]. Finally, GSMA reported that Bangladesh can save around 90 million USD per year by installing green energy harvesting technology instead of using the fossil fuel-based energy generation system [8].

It is always desirable to develop an energy-efficient green cellular network, which will minimize the capital cost, and greenhouse gas emission by maintaining the continuity of power services. Improving energy efficiency (EE) and maintaining continuity of power supply is quite challenging in the process of deploying renewable energy (RE) focused BSs [27, 28]. Typically conventional macrocell architectures are designed to cater to larger spectral areas that may often fail to attain the desired throughput to support seamless broadband service to uplink users. Besides, users move far away from the macro BS and often cause severe inter-cell interference. The weak indoor penetration and the appearance of dead spots

considerably reduce the indoor coverage under the traditional macrocell scenario. As a potential solution to overcome these issues, load balancing has appealed much consideration as a talented way out for higher resource allocation, better system enactment, and reduced operational expenditure as well. Load balancing is an efficient technique for adjusting the load and relieving the congestion among neighboring base stations in the modern cellular networks. With the introduction of load balancing techniques, a cellular network can gain in different ways, such as the effective exercise of frequency bands, improvement in coverage for cell-edge users, and boosting in overall network throughput [29].

However, the concept of load balancing can be applied for improving the spectral efficiency of mobile access setups. On the other hand, the load balancing mechanism flexibly adjusts BS coverage depending on experienced traffic density and enhances the service quality of an entire cellular network through balancing the traffic among surrounded BSs in a cluster. Thus, the continuity of the hybrid supply system can be improved by integrating the green energy sharing and load balancing mechanism. In this paper, the concept of load balancing is employed for improving the energy efficiency performance under optimal power supply scenarios. This chapter describes the background and motivation for this research work by briefly introducing the field and explaining the principal research problem. A summary of the contributions of this thesis is also presented. Finally, a concise outline of the thesis is provided at the end of the chapter.

1.2 Literature Review

Recently, several research works have been completed by the telecom operators and academia to develop an eco-friendly and sustainable green cellular network for the next-generation mobile communications utilizing the locally available renewable energy sources. The prime concern of green mobile communication is to enhance network performance in the field of throughput, energy efficiency, operational expenditure, and greenhouse gas discharge. Some of them advocate for the combination of renewable energy sources with the traditional non-renewable energy sources while others consider the integration of different RE sources or a single RE source with a battery unit.

Numerous research works related to the challenges and potential solutions to the problems of renewable energy-focused green cellular BSs have been presented in the literature. References [14, 19, 30] introduce a single renewable energy solar PV-based supply scheme along with an adequate battery bank addressing the key factors of designing solar PV-enabled

4

cellular BSs. In these works, various performance parameters such as energy yield, economic yield, and environmental aspects have been critically analyzed considering the dynamic nature of solar intensity. Although these works provide an exclusive method of harvesting energy from the standalone solar PV source, energy deficiency/outage may occur due to the single technology. The authors in References [31–33] investigated the optimal system architecture and technical criteria for installing hybrid solar PV/DG powered off-grid BSs throughout the world using the hybrid optimization model for electric renewables (HOMER) platform. The combined utilization of solar PV and DG could mitigate the fluctuations of renewable energy production and improve the quality of service (QoS) but it partially contains some DG-related difficulties such as high fuel cost, operation & maintenance costs (OMC), and CO_2 emission. Authors in [34], investigate the potential of hybrid solar PV and proton exchange membrane (PEM) fuel cells system for powering the remote off-grid base stations. Reference [2], proposed a renewable hydrogen-based supply system. Reference [23], introduced a solar PV and biomass gasifier focused energy supply. Ani and Nzeako et al. in [35], discussed the optimization of a hybrid (Solar & Hydro) and DG powered scheme for a remote BS. To reduce the net present cost (NPC), operational expenditures (OPEX), and greenhouse gas emission, authors in [10, 36, 37] mentioned a hybrid PV/WT system by integrating two renewable energy sources. Authors in [10, 36] explored the various key factors including the optimal sizing, net present cost, and greenhouse gas contents for assessing the system performance. Nevertheless, authors have not examined the sustainability of the designed system by considering the variation of bandwidth and BS transmission power. Generating energy from wind requires sufficient wind speed which is usually available in coastal areas and offshore islands.

Over the last decade, renewable energy-powered cellular network with a power grid line has drawn deep attention by the telecom operators because of the potential advantages and dynamic nature of renewable energy [38]. Moreover, due to the advancement of different energy management techniques [29, 39], renewable energy-focused grid-tied wireless networks can significantly improve the energy efficiency performance, network coverage area, and electricity exchanging facility. References [40, 41] introduce a grid-tied modern cellular base station that is primarily powered by the solar PV where backup power is provided by the battery bank and traditional grid supply. In these works, the authors propose a dynamic point selection and joint transmission coordinated multipoint transmission technique-based cellular networks, with dynamic inter-BS green electricity exchanging policy. Moreover, the

5

performance of the system has been analyzed critically using MATLAB-based Monte-Carlo simulations considering the realistic traffic pattern. The authors in Reference [42] introduce a grid-tied renewable energy-assisted heterogeneous cellular networks (HetNets) for which transmission power is optimized by the novel relay selection and power allocation algorithm. In these works, the key challenges of utilizing the maximum amount of renewable energy by reducing the grid energy consumption are critically analyzed by installing the different relay stations (RSs) in a network. References [43] evaluated the optimization of grid power consumption for hybrid renewable energy and the grid powered HetNets. The prime concern of this work is to reduce the grid power cost by controlling the transmitted power and stored energy considering the coverage probability constraint. These unique methods can overcome the drawback of using renewable energy and help to improve energy efficiency ensuring QoS, where the electrical power line is available.

Nowadays, modern cellular BSs are connected together to share the information to the control server, which will enhance the energy efficiency, spectral efficiency, and through-put performance of the wireless network. A lot of methods have been suggested by the researchers to improve energy efficiency and save energy though it is yet not saturated. A coordinated multipoint (CoMP)-based green cellular networks have been proposed in [44] that can substantially improve the spectral efficiency of the network by minimizing the inter-cell interference. However, the authors didn't consider the energy efficiency issue. Authors in [45], proposed a hybrid supply system where all the off-grid BSs are connected through a low resistive line to share the power among the neighboring BSs. In this work, the inter BSs energy sharing policy and optimal criteria are critically analyzed considering the in-termittency nature of renewable energy under different system bandwidth and transmission power. To increase energy efficiency, the infrastructure sharing concept is presented in [45–47], where the same radio access network (RAN) will be shared by the multiple network operators. For getting the same benefit, authors in [48], introduced a smart grid infrastruc-ture sharing mechanism. For improving the energy efficiency, Reference [49], proposed base station sleep mode provision, References [50, 51], proposed cell zooming concept. Although the sleep mode provision and cell zooming technique have many potential benefits, the sleep mode provision is not feasible for the populated areas and the implementation of the cell zooming technique involves a lot of challenges. In this trend, the authors in [52] proposed a distributed user association based load balancing algorithm to balance the load among the neighboring BSs. Reference [53] introduces an empirical load balancing algorithm that can

6

be used to optimize the range of heterogeneous networks. Therefore, the load balancing techniques are used for redistributing the load among the active BSs and can benefit in various ways including effective application of frequency bands, improvement in coverage for cell-edge users, and percentage increase in overall system throughput performance. In these papers, the idea of load balancing is employed for increasing the energy efficiency performance under optimal power supply scenarios. However, some of the above models fail to capture the load-dependent power consumption in BSs causing overestimations. Besides, many of them offered either very simple algorithms overlooking the real locations of users, or no algorithm at all.

1.3 Research Motivations

Due to the technological revolution and higher user data demand, the telecommunication industry is expanding at an exponential rate. Fulfilling the rapidly increasing demand of energy demand from the non-renewable energy sources has a hostile influence on both the economic and environmental implications resulting in higher capital cost and growth of greenhouse gas emission [10, 31]. As a result, green energy harvesting (EH) from different energy sources locally available has become an area of deep attention of the researchers with the aim to develop a sustainable and energy-efficient green cellular network [54, 55]. Locally available green energy sources such as sunlight, biomass, hydro, wind, etc. are re-useable, cheap, and pure in comparison with the non-renewable energy sources. Besides, renewable energy sources are available in many areas throughout the year. Renewable energy source becomes reliable if we can fulfill any of the following conditions. Firstly, it is to be combined with the conventional nonrenewable energy source. Secondly, the hybridization of two/three RE sources can also ensure reliability. Thirdly, it achieves reliability if a single renewable energy source is connected with a sufficient battery unit. Finally, renewable energy source becomes reliable when it is tied with the grid.

Energy sustainability and OPEX saving of a cellular network can be achieved by improving the energy efficiency and by establishing a dynamic traffic management network as reported in [56]. In this way, a great amount of electricity can be saved by introducing a higher energy-efficient component along with the guaranteed quality of services. For improving energy efficiency, numerous techniques have been proposed through research in this area but it is not yet saturated [6, 28]. According to [45, 48], transferring electricity among the neighboring base stations through a smart grid (SG) or low resistive line is a beneficial

technique for increasing the energy efficiency of BSs. Farooq et al. [48] developed a combined green energy sharing technique, where the physical power line is used to share energy among the BSs and the SG infrastructure to share the locally produced power. A framework of exchanging electricity between the two BSs via a low resistive conductor has been analyzed in [45]. Energy procurement within the BSs through SG is introduced in [57]. In order to improve the energy efficiency, the infrastructure sharing method has been mentioned in [46, 47], where the same radio access network (RAN) will be shared by the multiple network operators. Moreover, the concept of cell zooming, load balancing, dynamic sectorization of BSs [58], dynamic cell reconfiguration [59], and the traffic-aware intelligent cooperation among BSs [60] have shown a remarkable aptitude for improving energy efficiency. Dynamic traffic management network adapts the transceivers transmission power based on the traffic density and particular element of the network such as power amplifier (PA) unit, radio frequency (RF) unit, and baseband (BB) unit. Even the entire BSs can be switched off during the low traffic density [56]. If the traffic density is high, this method cannot be executed. In this case, a certain number of BSs must always be in an active position in order to support the basic operation of the network [6].

1.4   Research Methodology

In this work, we consider a cellular network whose base stations are powered by hybrid energy sources. Under the proposed model, each BS is equipped with a solar PV panel, biomass generator, battery bank, converter, etc. The system architecture will decompose into two parts: (i) hybrid power supply and (ii) telecommunication load (i.e. BS energy demand). The operation of the network can be divided into the following three states: Firstly, energy is supplied to the BS by the hybrid solar PV/biomass scheme where excess electricity is stored in the battery bank. Secondly, if the solar PV/biomass energy is not sufficient due to the deficiency of solar/biomass resources or seasonal change, the storage device will provide backup electricity. Thirdly, it will share the energy to the neighboring needy BS or electrical grid system if the excess electricity is greater than the threshold level (10% of load requirement). On the other hand, it will also receive energy from the nearest BS or electrical grid in case of an energy shortage. This sharing technique is aimed at the maximum utilization of renewable energy sources without scarifying their own energy demand. Integrated use of different energy resources reinforces the reliability and quality of services for envisaged green cellular networks with the reduction of capital cost and pollution rate. An extensive simulation will be carried out by HOMER software for evaluating optimal system architecture,

energy yield analysis, and cost assessment in the context of downlink LTE cellular networks varying different system parameters such as system bandwidth, and solar radiation. Besides, the wireless network has extensively been evaluated using Matlab based Monte Carlo simulations in terms of performance metrics such as throughput, spectral efficiency, and energy efficiency taking into account the tempo-spatial variation of traffic profile. In addition, the load balancing technique has been incorporated for improving the spectral efficiency and outage probability of the user equipment. The hybrid energy system design problem is formulated as an optimization problem with the objective function of minimizing net present cost (NPC) subject to various design and operational constraints. Several parameters for the system components, such as the operational lifecycle, component efficiency, and associated cost will be considered for the efficient performance of the optimization process to formulate the optimal hybrid power system. In this work, the zero loss of power supply probability, as well as sufficient excess electricity, is identified as a power reliability term. The ultimate goal is to identify the optimal solution aiming to minimize NPC satisfying all constraints with guaranteed reliability. Finally, a comprehensive comparison with other schemes will be carried out for further validation.

1.5 Research Challenges

The hybrid solar PV/BG-powered green cellular network with energy sharing and load balancing technique has many potential benefits but the implementation involves a lot of challenges. The key challenges and the possible solutions are listed below:

i) The implementation of a hybrid solar PV/BG system involves a greater amount of biomass resources, water, and land, which may not always be available in many countries. As tropical and fourth rice (the main source of biomass) producing country, Bangladesh has enough potential to harvest energy from the solar PV and biomass resources.

ii) The implementation of a hybrid solar PV/BG system may require to release of a negligible amount of carbon footprints due to the processing of biomass. With the advancement of modern technology, the higher volume of carbon footprints can be confined to a lower value. Moreover, the biomass generator indirectly reduces carbon footprints by minimizing the burning of rice husks in cooking and heating in Bangladesh.

iii) The implementation of a hybrid solar PV/BG system includes a huge number of energy storage devices for providing sufficient backup power in case of a shortage or outage of

9

renewable energy sources. This problem can be overcome by integrating the electrical grid system with the hybrid solar PV/BG system or by establishing inter-connection between the BSs via a low resistive power line in the case of off-grid conditions to facilitate sharing of power among the neighboring BSs.

iv) The implementation of the inter BSs energy sharing technique requires to trace the actual energy consumed by the individual BS and energy stored in the storage device. This problem can be overcome by sharing the source and load information to the control unit or control server.

v) The implementation of the load balancing technique also requires to trace the actual incoming traffic rate of the BSs. This problem can be solved by connecting the BSs to the control server where all the BSs will share their information with the control server and subsequently, the control server will sort the BSs according to the traffic density, transmission power, and stored energy.

1.6 Contributions

The major concern of this thesis is to develop a hybrid solar PV and biomass focused supply system for green powering the macro cellular network in Bangladesh considering the dynamic profile of renewable energy sources and traffic intensity. In this work, the selected off-grid site is Saldanga union Parishad of Debiganj Upazila under the Panchagarh district in the Rangpur Division of Bangladesh. The key challenges and potential solutions of designing a hybrid solar PV/BG powered green cellular network along with sufficient energy storage devices are critically analyzed as the output power of the renewable energy sources may be intermittent, and seasonal. A comprehensive simulation using HOMER software has been done over 20 years' project duration to calculate the techno-economic feasibility considering the real traffic by varying the solar radiation and bandwidth under different transmission power. Additionally, MATLAB-based simulation has been carried out to assess the performance of the wireless network. The major contributions of this paper can be summarized as follow:

i) The optimal system architecture and techno-economic feasibility of the solar PV and biomass focused supply system is determined using HOMER optimization software under various system bandwidth and transmission power endeavoring a green cellular network.

ii) The effectiveness of the energy sharing mechanism for saving energy by maximum utilization of renewable energy sources is evaluated. Particularly, we developed and analyzed the inter base station energy sharing algorithm via a low loss resistive power line for off-grid condition and energy trading policy with the electrical grid system for the grid-tied system. Based on the heuristic algorithms, we further analyzed the system reliability employing loss of power supply probability (LPSP) term and energy saving in terms of shared energy.

iii) In this thesis, we examined the performance of the wireless network in terms of through-put, spectral efficiency, energy efficiency, and energy efficiency gain considering a few limiting factors such as shadow fading and inter-cell interference using MATLAB-based Monte-Carlo simulations considering the dynamic traffic profile.

iv) A promising load balancing technique is developed for efficient utilization of resource blocks allocated in a cluster aiming to increase the spectral efficiency and reduce the outage probability metrics of the user equipment under various system configurations (e.g., channel bandwidth, channel quality indicator, and the number of simultaneous users).

v) To the end, a comprehensive feasibility comparison with other existing frameworks is conducted in the forms of performance metrics for justifying the network validity. Also, the breakeven point of the hybrid supply system is discussed for ensuring the cost-effectiveness of the proposed system.

1.7 Objectives of the Research

Telecom network operators are installing a higher number of BSs to meet the demand of ever-increasing data rate and the number of mobile subscribers across the world. The exponential growth of mobile networks and the corresponding demand of huge amount of energy has become a great challenge to the researchers and network operators due to the limited reservation, higher capital cost, and the negative impact of fossil fuel. Fulfilling the increasing demand of energy for the rising cellular networks has become a great challenge to the network operators because of the limited reservation of fuel energy sources and the growing concern about global warming. The prime objective of this thesis is to develop an energy-efficient hybrid supply system for green powering the cellular network considering the locally available renewable energy sources in Bangladesh. The whole research work is carried out to achieve the following specific goals:

i) To propose an energy sustainable hybrid-powered cellular networks emphasized long term reliability through green engineering solution.

ii) To evaluate an optimal solution of the proposed framework focusing on techno-economic analysis including energy yield and economic performance under a wide range of network scenarios.

iii) To investigate the system performance in terms of surplus electricity, carbon footprints, energy storage system, and cost of electricity varying different parameters such as solar radiation intensity, system bandwidth, and transmission power.

iv) Finally, a comprehensive comparison of system performance will be carried out with that of other power supply solutions to validate the effectiveness of the suggested system.

1.8   Outline of the Thesis

This thesis is divided into six chapters to clearly present the content. The rest of the thesis is organized as follows:

Chapter 2 provides a concise description of the system architecture along with major system components. The necessity of the hybrid supply system, mathematical modeling of the different system components, and the load profile of the base station are briefly explained for presenting a clear view to the reader.

Chapter 3 outlines the cost modeling and optimization formula of the hybrid supply system. The loss of power supply probability and green energy sharing policy are also discussed for ensuring guaranteed continuity of service by maximum utilization of renewable energy. Moreover, the performance of the wireless network is also analyzed in terms of performance metrics.

Chapter 4 demonstrates the analysis of the results including the simulation setup, optimal system architecture, energy yield analysis, battery capacity analysis, economic yield analysis, greenhouse gas emissions analysis, performance metrics analysis, and outage probability analysis via load balancing technique. The results are discussed with insightful comments. The results are found by simulation of the network with the help of HOMER optimization software and Matlab-based Monte Carlo.

Chapter 5 represents a comparison between the proposed system and other systems in terms of energy, economic, and cleanliness issues to justify network validity. The breakeven point of the hybrid supply system is also discussed in this chapter for identifying economic stability.

Chapter 6 concludes the thesis by summarizing the key findings and gives suggestions for the future improvement of the research works that can be carried out.

1.9 Conclusion

This chapter represents the prime research objectives of the research by addressing the key points. Moreover, the chapter provides a introduction, literature review, motivations, methodology, challenges, major contributions and a chapter-wise outline of the thesis for presenting a clear to the reader. The next chapter will discuss the system architecture and mathematical modeling of the major components of the proposed system.

CHAPTER 2

SYSTEM ARCHITECTURE AND MODELING

2.1 Introduction

The optimal system architecture and modeling of the different components of the hybrid supply system is a vital issue of developing a cost-effective sustainable solar PV/BG powered green cellular network. This chapter provides a concise description and corresponding mathematical modeling of the major system component of the hybrid supply system. Notably, the dimensioning of the hybrid supply system is done with the help of HOMER optimization software considering the tempo-spatial variation of renewable energy sources (solar PV and biomass) and traffic intensity under different network configurations. Oversizing the system components will enhance the output power as well as system cost. The optimal design ensures the lowest net present cost with high reliability of system operation. Based on the literature review and identified research gaps, this thesis explores the techno-economic feasibility of hybrid solar PV and biomass-based integrated renewable systems to powering long term evaluation (LTE) cellular BSs in Bangladesh.

2.2 Necessity of Hybrid Energy

Due to the technological revolution and higher user data demand, the telecommunication industry is expanding at an exponential rate. Fulfilling the increasing demand for energy by the single energy source may cause energy deficiency/energy outage which increases the loss of power supply probability by degrading the QoS. Therefore, the BSs of the next-generation cellular networks are provisioned to be powered by hybrid energy along with sufficient energy storage devices for ensuring the guaranteed continuity of power supply. Hybrid power systems are made to generate electrical power using different technologies and energy sources. The hybridization of energy can be made by the following ways: (i) hybridization of renewable energy with the non-renewable energy, (ii) hybridization of two/three renewable energy sources, (iii) hybridization of renewable energy with the electrical grid system, and (iv) hybridization of non-renewable energy with the electrical grid system. This paper investigates the hybridization of solar PV with the biomass resources for optimal powering the LTE cellular macro base stations in Bangladesh focusing on the technical, economic, and environmental issues. Energy harvesting from renewable energy sources (RES) has become

14

an overwhelming initiative to minimize energy deficiency and carbon footprints.

2.3 System Architecture

This section represents the concise description of the major components of the proposed system and the corresponding mathematical modeling in the context of green mobile communications. System activity can be classified into three parts: (i) hybrid solar PV/BG system independently supplies the BSs energy requirement, (ii) a certain amount of excess electricity is stored in the storage device and a major percent of excess electricity is shared to the neighboring BS or power grid, and (iii) if the solar PV/BG system is failed to support the BS energy demand primarily, backup power is provided by the storage devices, neighboring BS or power grid. A short description of the major components of the proposed model and the corresponding mathematical modeling are provided below:

2.3.1 Network layout

In this work, a two-tier downlink long term evaluation (LTE) cellular macro base station with a hexagonal shape has been considered. which acts as an access link between the mobile station and the core network. A typical BS consists of different types of power-consuming equipment such as digital signal processing or baseband unit (BB), transceiver (TRX) unit, radio frequency (RF) unit, power amplifier (PA) unit, and DC-DC regulator. The proposed network model is a combination of renewable energy harvester (solar & biomass), BS, converter, battery bank, and a smart energy management unit (EMU). The EMU primarily uses the generated power from RES and distributes the excess energy according to the BS requirement. In addition, EMU is used to prevent the overvoltage and overcurrent which enhances the battery lifetime by limiting the intensive discharging of the storage device. The BS is generally a DC load. It also includes some AC loads as auxiliary equipment such as air conditioning and lighting. In this model, we consider only one 30 W AC lamp which is connected to the BS from 6 PM to 6 AM. Macro BS with a remote radio head (RRH) does not require any cooling arrangement [37]. It is widely recognized that a 2/2/2 LTE macro BS operates at 20W (43dBm) and 40W (46dBm) [37]. However, 20W transmit power is broadly used [37]. The term 2/2/2 represents that a BS includes three sectors with each sector having two antennas.

2.3.1.1 Off-grid system

The architecture of the proposed hybrid solar PV/BG system for the off-grid condition is shown in Fig. 2.1. Under the off-grid condition, all the BSs are connected through a
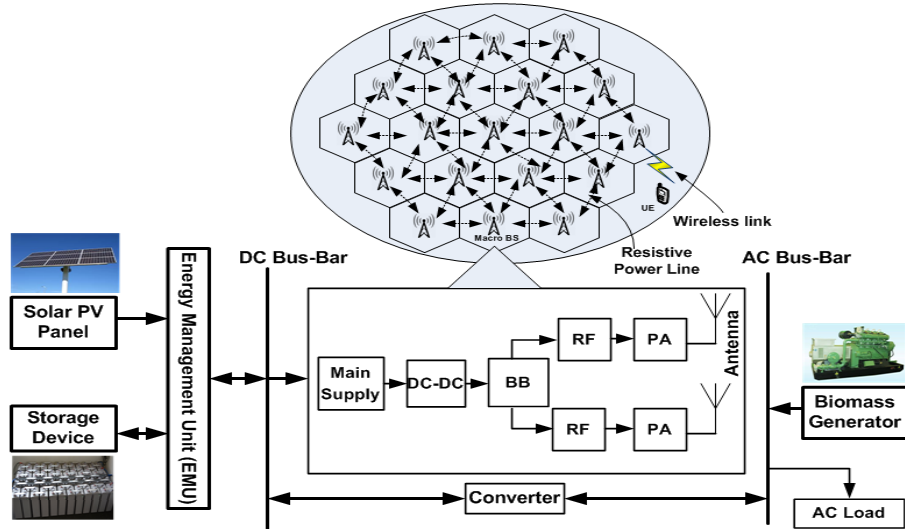
Figure 2.1: Architecture of the proposed hybrid solar PV/BG system for off-grid condition.

low resistive power line for sharing green energy among the interconnected BSs to ensure guaranteed continuity of power supply.

The algorithm of the introduced system is simplified in a flowchart as demonstrated in Fig. 2.2. The operation of the network can be divided into the following three states: Firstly, energy is supplied to the BS by the hybrid solar PV/biomass scheme where excess electricity is stored in the battery bank. Secondly, if the solar PV/biomass energy is not sufficient due to the deficiency of solar/biomass resources or seasonal change, the storage device will provide backup electricity. It is to be mentioned that the storage device can support the BS sufficient time. This support continues till it reaches the minimum depth of discharge which is sufficient time to fix the hybrid system. Thirdly, it will share the energy to the neighboring needy BS if the excess electricity is greater than the threshold level (10% of load requirement). It will also receive energy from the nearest BS in case of an energy shortage via a low resistive power line. This sharing technique is aimed at the maximum utilization of renewable energy sources without scarifying their own energy demand.

2.3.1.2 On-grid system

The architecture of the grid-connected hybrid solar PV/BG system is shown in Fig. 2.3. In the case of a grid-tied system, it can share energy directly to the electrical grid system.

2.3.2 Solar PV system

Solar is the most available, clean, and enormous renewable source of energy throughout the world. The solar PV panel collects solar energy and converts it into electrical energy.

16
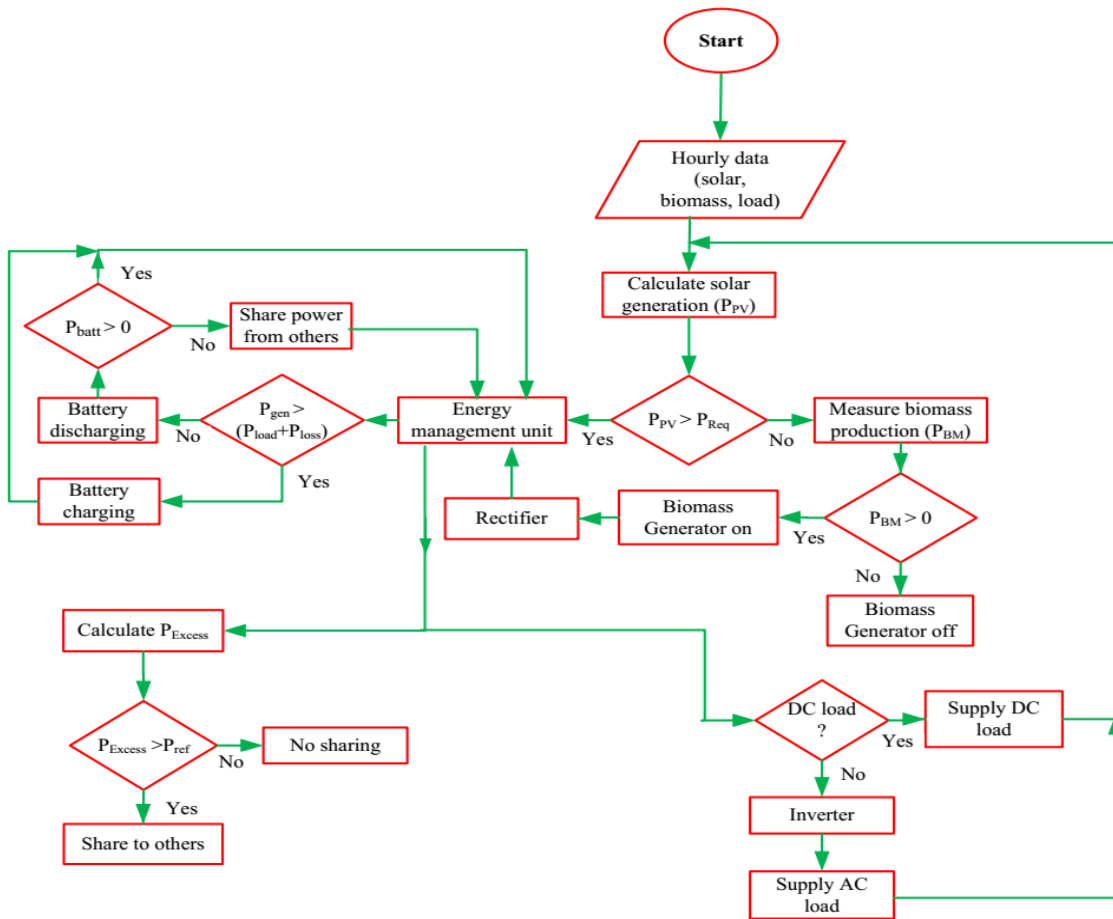
Figure 2.2: Flow chart of the proposed hybrid solar PV/BG system.
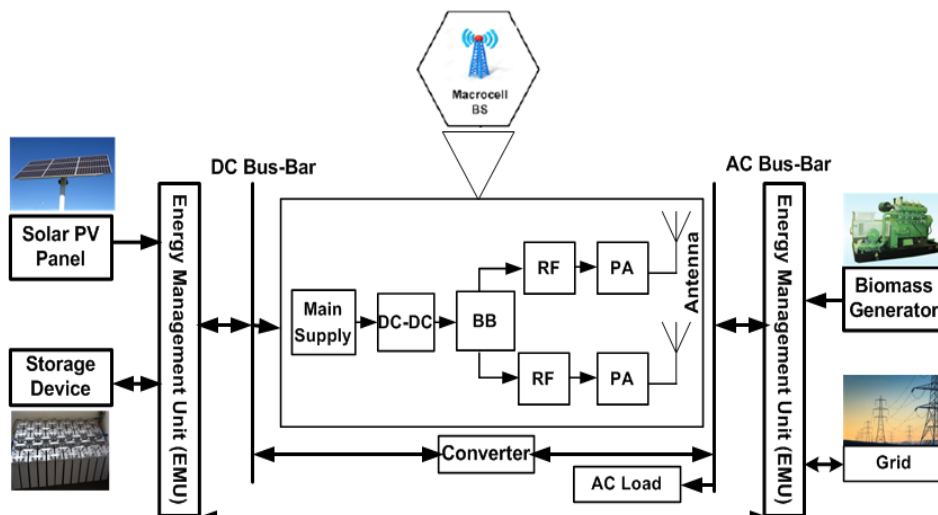
Figure 2.3: Architecture of the grid-tied hybrid solar PV/BG system.

Table 2.1: Specifications of the solar PV panel [37]

Parameters	Type (Value)
Solar module type	Sharp ND-250QCs (poly crystalline)
Nominal voltage (V)	29.80 V_{DC}
Nominal current (A)	8.40 Amp
Maximum power (P_{max})	250 $Watt$
Cell Configuration	60 in series
Open circuit voltage (V_{oc})	38.3 V_{DC}
Short circuit current (I_{sc})	8.90 Amp

Several solar PV cells are connected in series/parallel to form a solar PV array for harvesting more energy. Total renewable energy harvested by the solar PV panel can be found using the following equation [10]

$$E_{PV} = R_{PV} \times PSH \times \eta_{PV} \tag{2.1}$$

where R_{PV} is the rated capacity of the solar PV panel in kW. PSH is a peak solar hour in an hour which is equivalent to average daily sunlight intensity in $kWh/m^2/day$. η_{PV} is the derating factor that refers to the efficiency of the solar PV panel. There are many derating factors in a PV system design such as environmental, PV system, installation, cost, etc. In this work, a standard value of derating factor 0.9 is used for dimensioning solar PV panel. The term dimensioning of solar PV panels means the optimal sizing of the solar PV panel. The output power of the solar PV panels mostly depends on the solar radiation profile, geographical location, DC-DC loss factor, tracking mode, and the tilt of the solar PV panel.

The required number of solar PV panel (N_{PV}) to produce a specific output (P_p) can be formulated as follows [37]

$$N_{PV} = \frac{P_p}{P_{max}}, \tag{2.2}$$

where P_{max} is the maximum power of the solar PV panel. Table 2.1 represents the specification of the considered solar PV panel.

Fig. 2.4 represents the temporal variation of daily solar energy production by 1 kW solar PV panel, which is calculated with the help of the System Advisory Model (SAM). Fig. 2.5 depicts the average yearly solar energy generation for a given location in Bangladesh. The average value of sunlight intensity varies from one place to another; the highest sunlight intensity is 5.48 $kWh/m^2/day$ in April and the lowest intensity is 3.78 $kWh/m^2/day$ in July.

However, there are some difficulties and challenges of energy generation by the solar cell
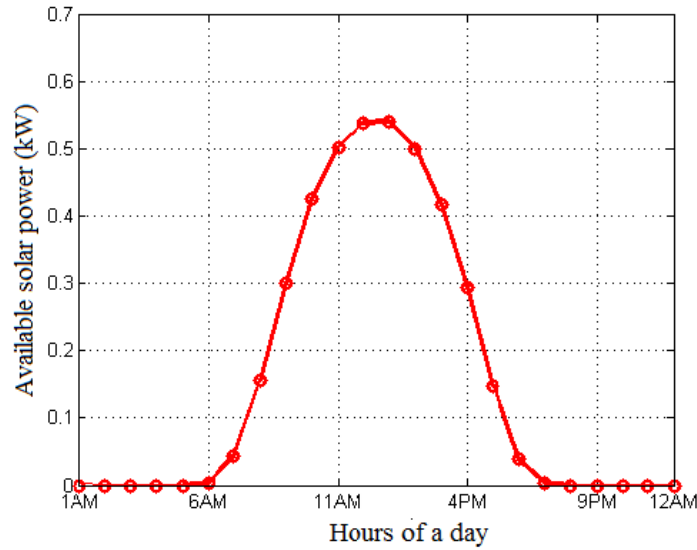
Figure 2.4: Average hourly solar power production over a day.
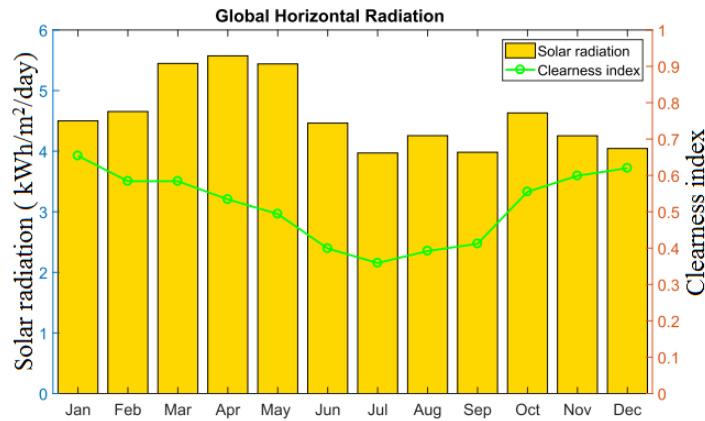
Figure 2.5: Average yarly solar radiation profile in Bangladesh.

due to the dirt, dust, tree debris, water spots, mould, tree shade, fog, cloud, and heavy rain in the tropical country. To overcome these problems, the hybridization of solar energy with biomass energy in remote areas can be a promising solution.

2.3.3 Biomass generator system

At present, energy harvesting from the biomass has become a mature technology and in our country, most of the available biomass resources are agriculture residue, animal dung, poultry dropping, etc. [17]. Moreover, as an agricultural country (over 60% production comes from fertile land), Bangladesh has enough potential for renewable energy harvesting from agricultural residue particularly from the rice husk and crop residue. Out of the agriculture residue, rice husk is a fine biomass whose average calorific value is around 14274 KJ/Kg (3411.33 KCal/Kg). Theoretically, one-ton paddy can produce around 200 Kg of rice husk but practically, the average amount is expected to 187 Kg [23]. Additionally, 1.5-4 Kg/hr
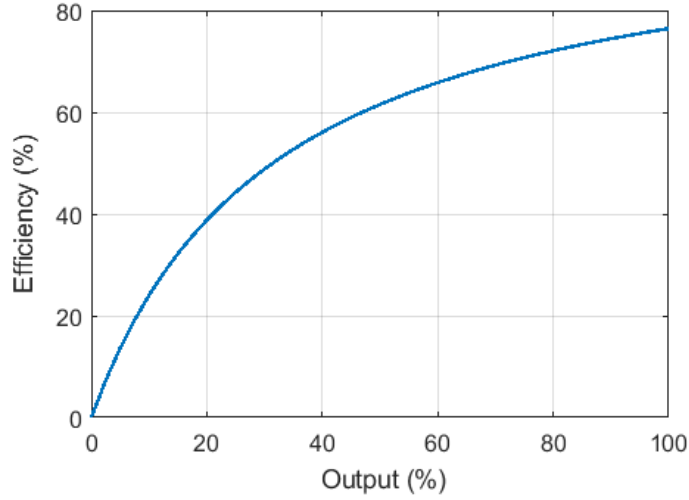
Figure 2.6: Characteristic curve of the biomass generator.

rice husk is required to produce 1 kWh energy. In this simulation, the maximum collection capacity of rice husk is considered around 20% (9 tons/day) of total rice husk available in the area, and the cost of biomass is taken as $30/tons [23].

The characteristic curve of the biomass generator is presented in Fig. 2.6. Power production from the biomass generator system depends on the various factors such as the calorific value of biomass (CV_{BM}), availability of biomass (T_{BM}), an operating hour of the biomass generator per day (t_{op}), and overall efficiency of the biomass conversion process (η_{BM}) which can be expressed as follows [17, 23].

$$P_{BG} = \frac{T_{BM}(tons/year) \times CV_{BM} \times \eta_{BM} \times 1000}{365 \times 860 \times t_{op}}. \tag{2.3}$$

Yearly energy generated by the biomass generator can be calculated as [17, 23]

$$E_{BG} = P_{BG}(365 \times 24 \times C_f), \tag{2.4}$$

where the C_f (capacity factor) is the ratio of actual electrical energy output to the maximum possible electrical energy output over a given period. In this work, the set capacity factor is 0.26.

In 2003, Bangladesh had around 74.128 million tons of biomass which are equivalent to 38.41 million tons of coal [22]. Fig. 2.7 depicts the yearly increasing coal equivalent biomass energy potential in Bangladesh. Additionally, Fig. 2.8 illustrates the biomass energy potential from different sources in Bangladesh [21].
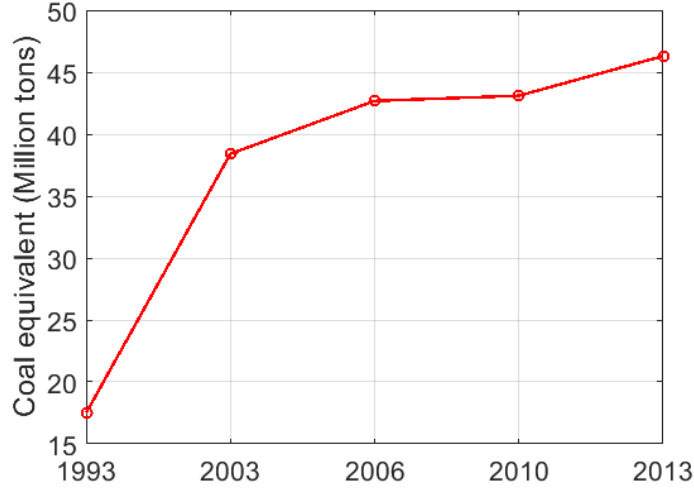
Figure 2.7: Biomass energy potential in Bangladesh.
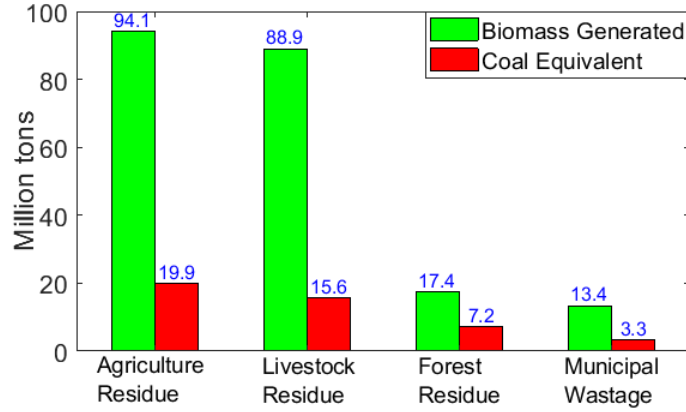
Figure 2.8: Biomass energy potential from different sources in Bangladesh.

2.3.4 Diesel generator system

The integration of DG with renewable energy sources plays a significant role in compensating the capital cost and BS energy demand during RES malfunction. This subsection represents the mathematical model of DG in order to compare the result of the suggested hybrid PV/BG system with the hybrid PV/DG system. Energy generated by a DG (E_{DG}) in kWh with rated power output (P_{DG}) can be determined as follows [37]

$$E_{DG} = P_{DG} \times \eta_{DG} \times t_{op}, \tag{2.5}$$

where η_{DG} is the efficiency of the DG and t_{op} is the operational time. However, the fuel consumption (F_C) is calculated by [37]

$$F_C = E_{DG} \times f_{sp}, \tag{2.6}$$

21

where f_{sp} is the specific fuel consumption (L/kWh). Generally, a DG set emits carbon footprint of 2.68kg/L [33].

2.3.5 Wind turbine system

The wind generator is integrated with the solar PV panel in the coastal area or hill track region intending to ensure the sustainable and reliable power supply. This subsection represents the mathematical model of WT in order to compare the result of the suggested hybrid PV/BG system with the hybrid PV/WT system. A wind turbine generates electrical energy in two steps: first, it converts the wind power into mechanical energy and then transforms into electricity. The electrical power produced by WT mainly relies on wind velocity, weather system, and hub height. The amount of electrical power generated by the WT can be calculated by [10]

$$P = \frac{1}{2}\rho V^3 C_P, \tag{2.7}$$

where V is the average velocity of wind (m/s), C_P is the coefficient of the Betz limit (typically 59% of maximum value), and ρ is the monthly air density (kg/m^3). However, a Whisper 200 wind generator model is installed to powering cellular BSs due to low capital cost and longer life span. The low solar power output during the rainy season is offset by the high power wind generation which leads to minimizing the fluctuation of hybrid RE production.

2.3.6 Electrical grid system

Generally, the power grid is an interconnected system that is used for supplying power to the load. In this work, the proposed hybrid solar PV/BG system has been connected to the utility grid for sharing the excess electricity to the grid, which ensures the maximum utilization of renewable energy by maintaining QoS.

2.3.7 Energy storage system

The battery bank is a backup device that acts as an energy buffer by compensating for the mismatch between energy generation and demand. On focusing the capital cost, and characteristics 'Trojan L16P' battery model is considered in this work. Additional information can be found in 'www.trojanbattery.com'.

The depth of discharge (B_{DOD}) is an important characteristic for selecting the battery bank capacity that tells how deeply the battery is discharged along with the battery state of charge (SOC). The battery state of charge is the indicator of the charging and discharging level of the battery which is expressed in percentage. The maximum state of charge (SOC_{max}) represents the nominal capacity of the battery bank and the minimum state of charge (SOC_{min})

represents the lower limit of battery discharge. The B_{DOD} of the Trojan L16P battery is 70% which implies that 70% of its energy has been delivered and 30% energy is reserved. The B_{DOD} can be calculated as follows [37]

$$B_{DOD} = (1 - \frac{B_{SOC_{min}}}{100}). \tag{2.8}$$

The backup time of the storage device is directly related to the capacity of the battery and can be expressed as [37]

$$B_c = \frac{P_{BS} \times D \times t_w}{B_{DOD} \times V_b \times K_b}, \tag{2.9}$$

where P_{BS} is the BS DC load in W, D is the backup time, t_w is the load working time, V_b is the battery voltage compatible at 48 V DC bus bar and K_b (1.14) is the battery capacity coefficient.

The storage capacity of the battery bank is a function of the number of batteries (N_{batt}), the nominal voltage of each battery (V_{nom}), nominal capacity of a single battery (Q_{nom}), and battery state of charge (B_{SOC}) that can be determined as follows [37]

$$E_{battmax} = \frac{N_{batt} \times V_{nom} \times Q_{nom}}{1000} \times B_{SOCmax}, \tag{2.10}$$

$$E_{battmin} = \frac{N_{batt} \times V_{nom} \times Q_{nom}}{1000} \times B_{SOCmin}, \tag{2.11}$$

$E_{battmax}$ and $E_{battmin}$ denote the maximum and minimum storage capacity of the battery bank in kWh.

Battery bank autonomy (B_{aut}) illustrates the number of hours that the fully charged batteries can back up the load without any support from the external power source. B_{aut} can be defined as the ratio of battery bank size to the BS electrical load and is determined in HOMER by the following equation [37]

$$B_{aut} = \frac{N_{batt} \times V_{nom} \times Q_{nom} \times B_{DOD} \times (24h/day)}{E_{BS}}, \tag{2.12}$$

where E_{BS} average daily BS load in kWh.

Battery lifetime (L_{batt}) mainly depends on two factors: battery float life and lifetime throughput. In other words, batteries die either from the use or from the old age. Battery lifetime plays a significant role in order to minimize the total replacement cost within the project duration. Based on these two factors, the overall lifetime of a battery can be determined as follows [37]

$$L_{batt} = min(\frac{N_{batt} \times Q_{life}}{Q_{tp}}, B_f), \tag{2.13}$$

23

where Q_{life} is the lifetime throughput of a single battery in kWh, Q_{tp} is the annual battery throughput (kWh) and B_f is the battery float life in years. Throughput is defined as the change in the energy level of the battery bank, measured after charging losses and before discharging losses. Lifetime throughput is the amount of energy that can be cycled through the battery bank before it dies and annual throughput is the amount of energy that cycles through the battery per year. The float life of the battery is the maximum length of time that the battery will last before it needs replacement, regardless of how much or how little it is used.

The number of batteries connected in series (N_{batt}^{series}) and connected in parallel ($N_{batt}^{parallel}$) can be found by the following equation

$$N_{batt}^{series} = \frac{V_{bb}}{V_{nom}}, \tag{2.14}$$

$$N_{batt}^{parallel} = \frac{N_{total}}{N_{batt}^{series}}, \tag{2.15}$$

where V_{bb} is the DC bus-bar voltage and V_{nom} is the nominal voltage of the battery.

2.3.8 Converter

When a system is compatible with both AC and DC loads a converter is required to obtain the desired frequency and uninterruptible power supply to the load with high efficiency. A converter can act as an inverter, rectifier, or both of them, wherein the AC to DC converter is known as the rectifier and the DC to AC converter is known as an inverter. Depending on the output power, output voltage and installation type inverter may be different and the capacity of the inverter can be determined by [10]

$$C_{inv} = (\frac{L_{AC}}{\eta_{inv}}) \times \sigma_{sf}, \tag{2.16}$$

where L_{AC} is the maximum AC load in kW, η_{inv} is the efficiency of the inverter, and σ_{sf} is the safety factor.

2.4 Base Station Power Profile

In order to determine the dimension and analyze the performance of the hybrid PV/biomass system, it is very momentous to assess the energy consumption of the BS considering the incoming traffic rate. The power consumption of a typical BS is dynamic in nature and mostly depends on the traffic profile of the BS, which varies over time and space. As refer to the [61, 62], the power consumption of a BS can be expressed as an affine function of the transmission power. In other words, the consumption contains a load-independent static power
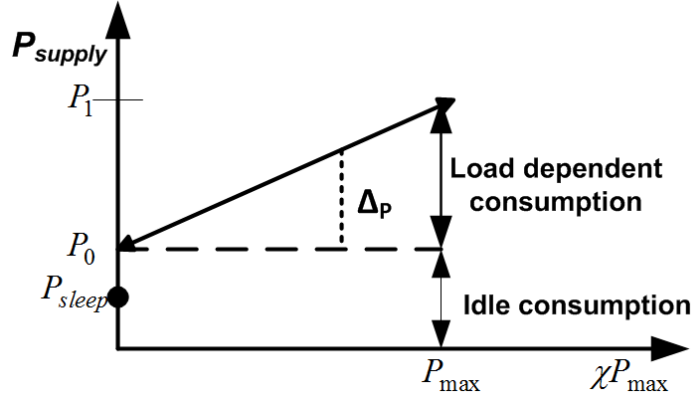
Figure 2.9: Base station power consumption.

P0 and load-dependent linearly raising power P1 as displayed in Fig. 2.9. Additionally, Fig. 2.10 illustrates the base station traffic profile which is approximated by using the Poisson distribution model and can be expressed as follows [61, 62]

$$\lambda(t) = \frac{p(t, \alpha)}{max[p(t, \alpha)]}, \tag{2.17}$$

$$p(t, \alpha) = \frac{\alpha^t}{t!} e^{-\alpha}, \tag{2.18}$$

where $\lambda(t)$ is the normalized traffic distribution, $p(t, \alpha)$ is the Poisson distribution function of traffic demand at a particular point of time, and α is the mean value where the maximum amount of traffic arrivals occur at 5 PM.

The total power consumption of a BS as a function of traffic intensity is shown in Fig. 2.10 and can be represented as follows [61, 62]

$$P_{BS} = \begin{cases} N_{TRX}[P_1 + \Delta_p P_{TX}(\chi - 1)], & \text{if } 0 < \chi \leq 1, \\ N_{TRX} P_{sleep}, & \text{if } \chi = 0, \end{cases} \tag{2.19}$$

where $P_1 = P_0 + \Delta_p P_{TX}$ is the height of power consumption of a BS, N_{TRX} is the total number of the transceiver, Δ_p is the load dependency power gradient and P_0 is the consumption at idle state [61, 62]. The scaling parameter χ is the load share, where $\chi = 1$ indicates that a fully loaded system and $\chi = 0$ indicates an idle system. Furthermore, a BS without any traffic load enters into sleep mode with lowered consumption, P_{sleep}. Table 2.2 represents the key parameters of a BS.

The power consumption of each element of the macrocell with RRH for both P_{TX}=20W and P_{TX}=40W is summarised in Table 2.3. Power losses in BSs primarily occur in the DC-DC regulator, main supply, and active cooling system which are linearly rising with the
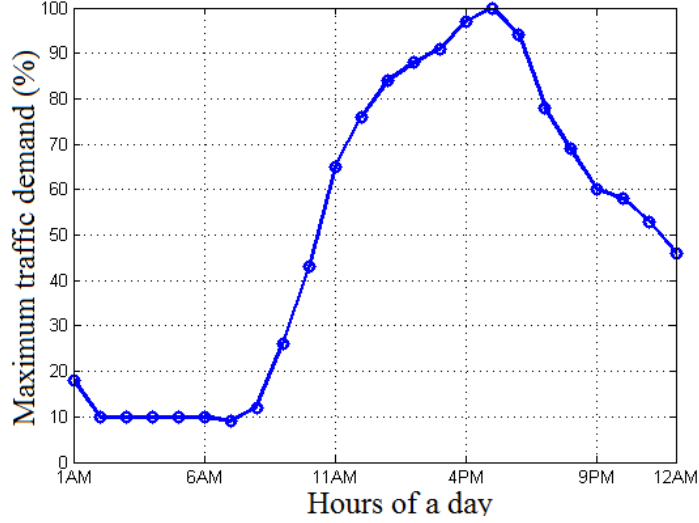
Figure 2.10: Dynamic traffic profile over a day.

power consumption of the other component. These three aspects are respectively symbolized by σ_{DC}, σ_{cool}, and σ_{MS}. The active cooling system is essential only for the macro BS. It is not necessary for the RRH and microcell type BS. In macrocell BS with RRH, the power amplifier (PA) is placed near the transmit antenna for saving power by eliminating feeder and active cooling losses. The maximum power consumption of a BS is determined as [61, 62]

$$P_1 = \frac{P_{BB} + P_{RF} + P_{PA}}{(1 - \sigma_{DC})(1 - \sigma_{MS})(1 - \sigma_{cool})} \tag{2.20}$$

where P_{BB}, P_{PA} and P_{RF} respectively refer to the baseband, power amplifier and RF power consumption for the given 10MHz transmission bandwidth as obtained from Table 2.3. The amount of power received by the power amplifier (P_{PA}) mainly depends on the maximum transmission power per antenna (P_{TX}), feeder losses (σ_{feed}) and the efficiency of the power amplifier (η_{PA}), which can be represented as follows [61, 62]

$$P_{PA} = \frac{P_{TX}}{\eta_{PA}(1 - \sigma_{feed})}, \tag{2.21}$$

where the efficiency and loss factor can be defined as:
$\eta = \frac{P_{out}}{P_{in}}$ and $\sigma = 1 - \eta$.

The power consumption by the baseband and radio frequency linearly varies with the bandwidth (BW) and a number of transceiver antenna (D) while the other parameters remain the same. The power consumption can be expressed as follows [61, 62]

$$P'_{BB} = N_{TRX}\frac{BW}{10MHz}P_{BB}, \tag{2.22}$$

26

$$P'_{RF} = N_{TRX} \frac{BW}{10MHz} P_{RF}, \qquad (2.23)$$

where P'_{BB} and P'_{RF} are respectively the baseband and RF power consumption for the desired bandwidth.

Table 2.2: Key parameters of the macro base station [61, 62].

BS Type	N_{TRX}	$P_{TX}[W]$	$P_0[W]$	Δ_P	$P_{sleep}[W]$
Macro RRH	6	20 and 40	84	2.8	56

Table 2.3: Macro BS power breakdown under peak load and 10MHz bandwidth [61, 62].

Components	Parameters	BS Type-1	BS Type-2
BS	P_{TX} [W]	20	40
	Feeder loss σ_{feed} [dB]	0	0
PA	Back-off [dB]	8	8
	Max PA out [dBm]	51	51
	PA efficiency η_{PA} [%]	31.1	31.1
	Total PA, $\frac{P_{Tx}}{\eta_{PA}(1-\sigma_{feed})}$[W]	64.4	128.6
RF	P_{TX} [W]	6.8	6.8
	P_{RX} [W]	6.1	6.1
	Total RF, P'_{RF} [W]	12.9	12.9
BB	Radio (inner Tx/Rx) [W]	10.8	10.8
	Turbo code(outer Tx/Rx) [W]	8.8	8.8
	Processors [W]	10	10
	Total BB, P'_{BB} [W]	29.6	29.6
DC-DC	σ_{DC} [%]	7.5	7.5
Cooling	σ_{cool} [%]	0	0
Mains Supply	σ_{MS} [%]	9	9
Sectors		3	3
Antennas		2	2
Total power [W]		**754.8**	**1219.6**

2.5 Conclusion

This chapter represents detailed discussions of the system architecture of the proposed system including the mathematical modeling of major system components. The necessity of a hybrid supply system has been explained for justifying the choice of thesis topic. Moreover, a concise discussion of the power profile of the BS is provided. In the next chapter, we will discuss the optimization problem and performance metrics in order to evaluate the performance of the proposed system with the objective function of minimizing NPC.

CHAPTER 3

OPTIMIZATION FORMULATION AND PERFORMANCE METRICS

3.1 Introduction

This chapter represents the mathematical modeling of cost parameters, and wireless performance metrics along with focusing the reliability, loss of power supply probability, and energy generation of the hybrid supply system. The basic concept of the wireless propagation model and the formulation of signal to the interference plus noise ratio (SINR) expression based on inter-cell interference is also discussed. Besides, the green energy sharing mechanism under the off-grid condition and the grid-tied condition has been formulated for optimal use of locally available green energy. Moreover, the heuristic algorithm of load balancing technique among collocated BSs has been incorporated for elevating the spectral efficiency and outage probability of the user equipment under different network conditions. Finally, the throughput, spectral efficiency, energy efficiency, and outage probability performance of the contemplated wireless network are presented in this chapter considering the tempo-spatial variation of traffic intensity.

3.2 Cost Modeling

In this work, HOMER optimization software has been used to determine the optimal architecture of the hybrid solar PV/biomass scheme that satisfies user-specified constraints with the lowest net present cost (NPC) including the initial capital costs (CC), replacement costs (RC), operation and maintenance costs (OMC), and salvage value (SV) during the project lifecycle. The economic feasibility of the proposed model can be evaluated with the help of these costs. The net present cost of the system can be computed as follows [30]

$$NPC = \frac{TAC}{CRF} = CC + RC + OMC - SV \tag{3.1}$$

The terms TAC and CRF respectively represent the total annualized cost and capital recovery factor of the system, which can be determined by (3.2) and (3.3) [30]

$$TAC = TAC_{CC} + TAC_{RC} + TAC_{OMC} \tag{3.2}$$

$$CRF = \frac{i(1+i)^N}{(1+i)^N - 1} \tag{3.3}$$

where N is the lifetime of the project and i is the annual real interest rate.

The cost remaining at the end of the project is known as salvage value which is evaluated by [30]

$$SV = C_{RC}(\frac{C_{RL}}{C_L}) \tag{3.4}$$

where C_{RC}, C_{RL}, and C_L respectively are the replacement cost, remaining lifetime, and lifetime of the component.

The involvement of biomass and diesel generator includes a significant amount of fuel cost (FC). As a consequence, NPC of the BG and DG enabled system can be computed as follows

$$NPC = CC + RC + OMC + FC - SV. \tag{3.5}$$

Cost of electricity (COE) is defined as the ratio of the total annualized cost (TAC) to the annual electricity production (E_{gen}) by the system [37]. COE also measures the cost of unit electricity produced which can be represented as $\$/kWh$.

$$COE = \frac{TAC}{E_{gen}} = \frac{NPC \times CRF}{E_{gen}}. \tag{3.6}$$

3.3 Problem Formulation

The hybrid energy system design problem is formulated as an optimization problem with the objective function of minimizing NPC subject to various design and operational constraints. In other words, our prime goal is to minimize the energy shortage through maximum utilization of solar and biomass energy in conjunction with a battery bank which in turn reduces NPC [37]. The objective function of the system can be expressed as the hybrid energy system design problem is formulated as an optimization problem with the objective function of minimizing NPC subject to various design and operational constraints. In other words, our prime goal is to minimize the energy shortage through maximum utilization of solar and biomass energy in conjunction with a battery bank which in turn reduces NPC [37]. The objective function of the system can be expressed as

$$\min \quad NPC$$

$$\text{subject to} \quad E_{PV} + E_{BG} > E_{BS}$$

$$E_{PV} + E_{BG} + E_{batt} = E_{BS} + E_{Loss}$$

$$E_{Excess} = E_{Gen} - E_{BS} - E_{Loss}$$

$$E_{battmin} \leq E_{batt} \leq E_{battmax}$$

where E_{Loss} is calculated in kWh/year involving both the converter losses (C_{Loss}) and battery losses (B_{Loss}). The combined energy contribution by solar PV panels and biomass generators can certainly meet the annual BS demand to ensure power reliability mentioned in (1). The constraint in (2) ensures that the annual energy obtained by the integrated renewable energy sources carries the annual BS consumption with its associated losses. The amount of excess electricity is preserved for future use as described by the constraint (3). The reserved energy also satisfies the power reliability constraint. The constraint (4) implies that the battery bank storage capacity should not exceed the maximum limit and not reach below the threshold level.

HOMER is the optimization software employed in this study to examine the optimal hybrid power system that satisfies user-specified constraints with the lowest net present cost. HOMER decides at each time step to meet the energy requirements at the lower net present cost, subject to the constraint from the dispatch strategy chosen in the simulation. HOMER starts an hourly simulation of every possible configuration, computing the available energy from the solar PV array, sizing of PV capacity, biomass generator, number of batteries comparing it to the BS load demand and losses, and deciding to store the surplus renewable energy in times of excess. An integrated renewable-powered hybrid scheme must be designed to meet the desired BS load demand at a defined level of security over the expected lifetime. The system must supply sufficient electricity to both the BS load and the backup power system each hour.

3.4   Reliability Modeling

The term 'annual capacity shortage' (E_{CS}) is an indicator of power reliability and is explained as the ratio of annual energy deficiency (E_{ED}) to the annual BS load demand (E_{BS}).

$$E_{CS} = \frac{E_{ED}}{E_{BS}}, \tag{3.7}$$

where E_{BS} is expressed in kWh/yr and E_{ED} can be represented as follows

$$E_{ED} = E_{BS} - E_{gen}, \tag{3.8}$$

where E_{Gen} is the generated electricity which can be written as

$$E_{Gen} = E_{PV} + E_{BG}. \tag{3.9}$$

A reliable system can be developed by fulfilling the base station demand with sufficient backup power over the entire project duration. For the suggested hybrid PV/BG scheme,

excess electricity (E_{Excess}) can be generated when total energy generation is over than the base station energy requirement that can be formulated by the following equation

$$E_{Excess} = E_{Gen} - E_{BS} - C_{Loss} - B_{Loss},$$
(3.10)

where C_{Loss} and B_{Loss} respectively represent the losses associated with converter and battery.

3.5 Loss of Power Supply Probability

Loss of the power supply probability (LPSP) is used to measure the system reliability over the intended project duration. LPSP can be defined as the ratio of supply energy shortage to the total BS demand for a given period that ranges from zero to one. However, LPSP can also be designated as loss of load probability (LOLP), load coverage rate (LCR), loss of power probability (LOPP) in some literature [63, 64]. Note that a higher value of LPSP signifies lower system reliability. In order to ensure zero outage as well as guaranteed quality of experience, sufficient excess energy should be reserved for backup supply during unexpected energy shortage. In this paper, the optimum design configuration is determined assuming the tangent of the partial derivative of RE supplies including storage devices with desired LPSP. The LPSP of the system can be projected as follows [65]

$$LPSP = \frac{\sum_{t=1}^{T} LPS(t)}{\sum_{t=1}^{T} P_{BS}(t)}$$
(3.11)

where loss of the power supply (LSP) identifies the power shortage while the power supply fails to satisfy the load demand ($P_{Tot} < P_{BS}$). Here, $P_{Tot} = P_{PV} + P_{BG} + P_{batt}$ for a given period of time (t ε T). The higher values of LSP degrade the system reliability whereas the LPSP = 0 indicates the contemplated supply system can fulfill the BS energy demand entirely.

3.6 Energy Cooperation Modeling

In this subsection, a heuristic green energy sharing technique has been proposed for ensuring the guaranteed continuity of supply by maximum utilization of renewable energy sources under different cases. In the case of the off-grid condition, the hybrid supply system can share green energy among the neighboring base stations. On the other hand, it can share energy to the electrical grid system for a grid-connected system. For both off-grid and on-grid conditions have three different cases are the following:

Case I: Generation is higher than demand ($E_{Gen} > E_D$)

If $E_{Gen} > E_D$, then the harvested green energy is sufficient to fulfill the BS's energy demand, and excess energy is stored in the battery bank for providing backup power and the remaining energy is used for sharing. Here, E_{Gen} refers to the sum of energy generated by renewable energy sources (solar PV, and BG) while E_D includes both the energy demand for the base station and associated losses. In this case, there is no need of receiving energy from the other BSs and the loss of the power supply (LPS) will be zero as $E_{Gen} > E_D$. The generated, excess, and shared energy can be expressed as follows [37]

$$E_{Gen} = E_{PV} + + E_{BG} \tag{3.12}$$

$$E_D = E_{BS} + E_{Loss} \tag{3.13}$$

$$E_{Share} = E_{Gen} - E_D - E_{Excess} \tag{3.14}$$

$$LPSP(t) = 0 \tag{3.15}$$

where E_{Loss} involves both the converter and battery losses.

For an on-grid condition, it can share energy directly to the electrical grid system. But, under the off-grid condition, it can share energy to the neighboring needy BSs via a low resistive power line. If R is the resistance of the entire line, then the line losses (E_{Line}) for the time t can be estimated by the following equation [37]

$$E_{Line} = I^2 R(l) \times t_r = \frac{P_{Share}^2 R(l)}{V^2} \times t_r \tag{3.16}$$

where I is the current flowing through the transmission line, V is the DC 48 volt and P_{Share} is the shared power. Hence, the total shared energy and average energy saving (AES) by the inter BS sharing mechanism can be determined as follows [37]

$$E_{Share} = P_{Share} \times t_r \tag{3.17}$$

$$E_{Saving} = \frac{\sum_{i=1}^{N} E_{Share}(t)}{\sum_{i=1}^{N} E_{BS}(t)} \times 100\% \tag{3.18}$$

where N is the number of sharing BS, typically 19 for the two-tier configuration, and E_{BS} is the required energy of ith BS.

Case II: Generation is equal to demand ($E_{Gen} = E_D$)

If $E_{Gen} = E_D$, then the base station will be served by the generated green energy and

backup power will be supplied by the battery bank, hence E_{Share}=0, and $LPS(t)$=0. The reserved capacity of the battery bank (Bc) that is required for supporting the BS energy demand for t (in hours) time can be determined using (2.9).

Case III: Generation is lower than demand ($E_{Gen} < E_D$)

If $E_{Gen} < E_D$, then the harvested green energy cannot fulfill the BS energy demand entirely. Hence, the BS will receive energy from the electrical grid system (for the grid-tied system) or the neighboring over generated BS (via the low resistive power line for the off-grid interconnected system) as mentioned in case I. In this case, the loss of power supply will arise. The LPS and the total amount of energy needed for the ith BS at time t can be estimated as follows

$$LPS(t) = E_D^i(t) - E_{Gen}^i(t) = E_{Need}^i(t) \tag{3.19}$$

where, $E_{Need} = E_{Grid}$ for grid-tied system and $E_{Need} = E_{Share}$ for off-grid system.

For off-grid conditions, all the BSs are interconnected through a low resistive power line. Moreover, all the BSs are sorted according to the generated energy and traffic intensity as follows: $BS_i = BS_{i,1}, BS_{i,2}, \ldots\ldots, BS_{i,M}$, where M is the number of the adjacent base station of BS_i. Now, if the base station $BS_{i,1}$ has sufficient excess energy then BS_i can receive this green energy in the case of shortage or outage of energy. However, a needy BS_i will search all the neighboring BSs to find out the over generated BSs to fulfill the required energy. If the base station BS_i takes green energy from the neighboring base station $BS_{i,M}$, the total amount of energy consumed from the neighboring BSs can be estimated as follows [37]

$$E^i(t) = \sum_{m=1}^{M} E_{Share}^{i,m}(t) \tag{3.20}$$

Table 3.1: Algorithm of off-grid energy sharing algorithm for i^{th} base station BS_i

1: Initialize: $E_{Gen}(t)$, $E_D(t)$, $E_{BS}(t)$, $E_{Loss}(t)$, and $B_c(t)$
2:   **if** $E_{Gen}(t) > E_D(t)$
3:     Find $E_{Excess}(t)$, $E_{Share}(t)$, and $B_c(t)$
4:     Start charging the battery bank
5:       **if** $B_c(t) = 1$ then
6:         Allowed sharing to the neighboring BSs
7:         **else** stop sharing and go to Step 3
8:       **end if**
9:   **if** $E_{Gen}(t) \leq E_D(t)$
10:     Coordinate with the neighboring over generated BSs
11:     Sort the neighboring M BSs with respect to stored energy
        i.e., find the set $BS_i = BS_{i,1}$, $BS_{i,2}$, ...,$BS_{i,M}$
12:       **for** m=1:M
13:         Calculate $E^i(t) = \sum_{m=1}^{M} E_{Share}^{i,m}(t)$
14:           **if** $E^i(t) = E_{Need}^i(t)$
15:             Stop the algorithm and go to Step 19
16:           **else**
17:             m = m + 1 and go to Step 12
18:           **end if**
19:       **end for**
20:   **end if**

Table 3.2: Algorithm of on-grid energy sharing.

1:   Initialize: $E_{Gen}(t)$, $E_D(t)$, $E_{BS}(t)$, $E_{Loss}(t)$, and $B_c(t)$
2:   **if** $E_{Gen}(t) > E_D(t)$
3:     Find $E_{Excess}(t)$, $E_{Share}(t)$, and $B_c(t)$
4:     Start charging the battery bank
5:       **if** $B_c(t) = 1$ then
6:         Start sharing to the electrical grid
7:         **else** stop sharing and go to Step 3
8:       **end if**
9:   **end if**
10: **if** $E_{Gen}(t) \leq E_D(t)$
11:     Discharge battery bank to supply shortage energy
12: **end if**

Table 3.3: Key parameters for MATLAB based Monte-Carlo simulation setup [37].

Parameters	Value
Resource block (RB) bandwidth	180 kHz
System bandwidth, BW	5,10,15,20 MHz
Carrier frequency, f_c	2 GHz
Duplex mode	FFD
Cell radius	1000 m
BS Transmission power	46 dBm
Noise power density	-174 dBm/Hz
Number of sectors	3
Number of antennas	2
Reference distance, d_0	100 m
Path loss exponent, α	3.574
Shadow fading, X_σ	8 dB
Access technique, DL	OFDMA
Traffic model	Randomly distributed

The algorithms of the green energy sharing model for both off-grid and on-grid conditions are presented in Table 3.1 and Table 3.2 respectively. In this algorithm, $B_c(t)$ is the energy stored in the battery bank, and $B_c(t)$=1 indicates that the battery bank is fully charged.

3.7 Performance Metrics

The throughput and energy efficiency performance of the proposed networks is performed with the help of MATLAB software, which is commonly known as Monte-Carlo simulation. The simulations are executed by averaging above ten thousand iterations considering the dynamic traffic pattern. We also assumed that every user is linked with one resource block (RB). The basic parameters of the simulation setup are summarized in Table 3.3.

3.7.1 System model

In this work, a shadow fading channel model with log-normally distributed has been considered. Path loss is calculated in dB for the interval of d between the transmitter and receiver. Path loss can be defined as follows [37]

$$PL(d) = PL(d_0) + 10\alpha log_{10}\left(\frac{d}{d_0}\right) + X_\sigma, \tag{3.21}$$

where $PL(d_0)$ is the path loss for the reference distance (d_0), α is the exponent of path loss. Path loss for reference distance can be evaluated from the free-space path loss equation.

For k^{th} user equipment (UE), the received power at a distance $d = d^{i,k}$ from i^{th} BS β_i is given by [37]

$$P_{rx}^{i,k} = P_{tx}^{i,k} - PL(d) + X_\sigma \tag{3.22}$$

where $P_{tx}^{i,k}$ is the transmitted power in dBm and X_σ is the amount of shadow fading modeled

as a zero-mean Gaussian random variable with a standard deviation σ dB. The transmit power $P_{tx}^{i,k}$ from BS i to UE k satisfies $\sum_{k\epsilon U} P_{tx}^{i,k} \leq P_i^{max}$, where P_i^{max} is RF output power of BS β_i at its maximum traffic load and U is the number of active UE in this BS.

The inter-cell interference (ICI), $P_{k,inter}$, can be determined by [37]

$$P_{k,inter} = \sum_{m \neq i}(P_{rx}^{m,k}) \tag{3.23}$$

Then, the received signal to interference plus noise ratio (SINR) at k^{th} UE from BS β_i can be given by [37]

$$SINR_{i,k} = \frac{P_{rx}^{i,k}}{P_{k,inter} + P_{k,intra} + P_N} \tag{3.24}$$

where $P_{k,intra}$ is the intra-cell interference, P_N is the additive white Gaussian noise (AWGN) power given by $P_N = -174 + 10log_{10}(BW)$ in dBm with BW is the bandwidth in Hz. Notwithstanding, orthogonal frequency division multiple access (OFDMA) technique in the LTE system includes zero intra-cell interference.

3.7.2 Energy efficiency

In this work, the term 'energy efficiency' is defined as the ratio of total network throughput to the total power consumed by the network. Energy efficiency measures the performance of the wireless network, which is expressed as the number of bits transmitted per Joule of energy. According to Shanon's information capacity theorem, total achievable throughput in a wireless network at time t can be modeled as follows [37]:

$$C_{Total}(t) = \sum_{k=1}^{U}\sum_{i=1}^{N} BWlog_2(1 + SINR_{i,k}) \tag{3.25}$$

where N is the number of transmitting BSs and U is the total number of user equipment (UEs) in the wireless network. Thus, the EE metric denoted as N_{EE} for time t can be modeled as follows [37]:

$$N_{EE} = \frac{C_{total}}{P_{BS}}, \tag{3.26}$$

where P_{BS} is the total power consumed in all the BSs at time t and can be calculated by using (2.19).

3.7.3 Spectral efficiency

The spectral efficiency determines how efficiently a limited frequency can be utilized in wireless communication. Spectral efficiency measures the data rate that can be transmitted over a given system bandwidth. The spectral efficiency of the wireless network can be expressed by the following equation

$$\eta_{SE} = \frac{R_{total}(t)}{BW} \tag{3.27}$$

3.7.4 Outage probability

The term 'outage probability' determines the probability of outage of the user equipment in the wireless network and it arises when the required data rate is less than the threshold level of the data rate. We consider that $SINR_{i,k}$ is the threshold level of SINR for effective communication of UE from class j, then the outage probability of uth UE U_u from j^{th} class C_j location in i^{th} BS can be expressed as [66]

$$P_{i,u}^{j,out} = Pr\{SINR_{i,u}^{j} \leq SINR_{j,th}|U_u \in C_j\} \tag{3.28}$$

where $Pr\{U_u \in C_j\}$ is the probability that user u is from class C_j.

3.7.5 Resource allocation

A resource block (RB)is the lowest unit of physical resources that are assigned to every user. In the time domain, the resource block is one slot long. In the frequency domain, the resource block is 180 kHz wide and either 12 x 15 kHz subcarriers or 24 x 7.5 kHz subcarriers wide. For most of the channels, the number of subcarriers associated per RB is 12. As an example, a 5 MHz downlink signal can be expressed as 25 resource blocks wide or 301 subcarriers wide (DC subcarrier is not involved in an RB). In the LTE network, 10% of the available bandwidth is used as a guard band for avoiding overlapping [67]. The standard bandwidth and corresponding resource block and subcarriers for both uplink and downlink conditions are presented in Table 3.4.

Table 3.4: Frequency measurement.

Bandwidth	Resource Blocks	Subcarriers (downlink)	Subcarriers (uplink)
1.4 MHz	6	73	72
3 MHz	15	181	180
5 MHz	25	301	300
10 MHz	50	601	600
15 MHz	75	901	900
20 MHz	100	1206	1200

The number of resource blocks allocated for the individual BS is determined based on the operating bandwidth. The individual BS use their allocated RBs according to the user requirement. In every time slot, this decision has been taken by the allocation algorithm. If one RB cannot fulfill the target requirement of a UE throughput then another RB is allocated according to the availability of free RBs. So, the total bandwidth allocated for a single user

Table 3.5: Traffic steering Resource Block allocation algorithm.

1:   Initialize: $n_{RB}, \chi_{i,j}, \chi_{th}, \forall_j \in U, \forall_j \in N$

2:   Set n_{RB}=0, $\forall_j \in U$

3:   **for** $k = 1 : T$

4:     **for** $i = 1 : N$

5:       **if** $\chi_{i,j}$ ¡ χ_{th} **then**

6:         Position of $U = \chi_{i,j}$, n_{RB} are updated

7:         **for** $j = 1 : U$

8:           Compute $\rho_j = \sum_{i \in N} \chi_{i,j} \beta_{i,j} log_2(1 + SINR_{i,j})$

9:           **if** $\chi_{i,j} = 1$ && $\rho_j < R_t$ **then**

10:             Increment n_{RB}

11:             $\beta_{i,j} = n_{RB} W_{RB}$

12:           **end if**

13:         **end for**

14:         Assigned all RBs or R_t is reached by all active UEs; updated $\chi_{i,j}$

15:       **end if**

16:     **end for**

17:   **end for**

18:   **if** all UEs are satisfied and residual RBs remains than

19:   share equally in candidate space

20:   **end if**

---

can be calculated from the multiplication of total RB allocated for the user and the BW of a single RB. The detailed procedure of the resource block algorithm is presented in Table 3.5.

In the resource block algorithm, k=UE_1, UE_2,. . . UE_m = set of m users that have to be served, R_t= total throughput target for UEs, n_{RB} = number of resource blocks, W_{RB} = BW of a single RB, $\beta_{i,j}$ = bandwidth assigned by BS_i to UE_j. Binary variable $\chi_{i,j}$ signifies the association policy between BSs and UEs, as in the following

$$\chi_{i,j} = \begin{cases} 1, & if \quad UE_j \quad is \quad served \quad by \quad BS_i \\ 0, & otherwise; \forall_i \in N, \forall_j \in U \end{cases} \tag{3.29}$$

3.7.6   Load balancing algorithm

In this subsection, we propose a traffic-aware load balancing algorithm, which has the potential to exchange the peak traffic among the nearby base stations. An example of traffic-guided load balancing is shown in Fig. 3.1. In this load balancing concept, all the nineteen BSs in a two-tier macro cellular network will be sorted according to their arrival of traffic rate. The higher traffic density BS will search the neighboring BSs to find out the lower
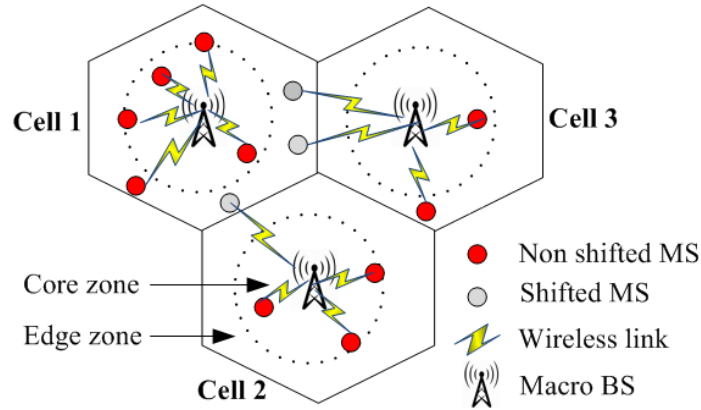
Figure 3.1: Traffic guided load balancing model.

traffic density BSs to shift the peak load (beyond the threshold value) to the neighboring lower density BS. This shifting of peak load increases the spectral efficiency and decreases the outage probability of the network. The detail of the load balancing algorithm is presented in Table 3.6. The operation of the algorithm can be divided into two modes: Firstly, the base stations are not allowed to shift the core zone load to the neighboring BSs. Secondly, if there is any high traffic density BS and the neighboring BSs can receive the load, the higher traffic density BS will shift the load to minimize the outage probability. Moreover, the amount of load received by the low traffic density BSs depends on their unused resource blocks and renewable energy generation.

However, the load balancing has appealed much consideration as a talented way out for higher resource allocation, better system enactment, and reduced operational expenditure as well. Load balancing is an efficient technique for adjusting the load and relieving the congestion among the neighboring BSs. With the introduction of load balancing techniques, a cellular network can gain in different ways, such as the effective exercise of frequency bands, improvement in coverage for cell-edge users, and boost in overall network spectral efficiency and outage probability.

Table 3.6: Traffic guided load balancing algorithm.

1:	Initialize: $\chi_{i,j}$, χ_{th},RBs
2:	Sort the BSs according to the traffic intensity and stored energy
3:	**if** $\chi_{i,j}$ ¿ χ_{th}
4:	**for** m=1:M
5:	Find the neighboring lower density BS from the set BS_i =$BS_{i,1}$, $BS_{i,2}$, ...,$BS_{i,M}$
6:	Shift 1% of edge zone load to the neighboring lower density BS
7:	**if** $\chi_{i,j}$ = χ_{th}
8:	Stop the algorithm and go to Step 11
9:	**else**
10:	m=m+1 and go to Step 4
11:	Update $\chi_{i,j}$
13:	**end if**
14:	**end for**
15:	**end if**

Here, χ_{th} is the threshold level of traffic intensity that can be efficiently carried out by the ith base station BS_i. In the load balancing algorithm, RB (resource block) is the smallest unit of resources that is assigned to the user. It is considered that at least one RB should be allocated for every user. On the other hand, multiple RBs are connected to a single user in the case of higher data demand and higher system bandwidth.

3.8 Conclusion

This chapter entails a detailed discussion of the different cost parameters in order to assess the economic feasibility of a hybrid supply system subject to various design parameters and operational constraints. The reliability issue and loss of power supply probability of the hybrid supply system are also discussed. Thereafter, inter base station energy sharing technique, energy trading policy with the electrical grid system, and balancing the load among the neighboring the base station has been modeled aiming to ensure the guaranteed continuity of power supply. In the next chapter, we will discuss the results of the proposed solar PV/BG powered cellular network addressing the key points.

CHAPTER 4

RESULTS AND DISCUSSIONS

4.1 Introduction

In this chapter, the results of the hybrid solar PV/BG-powered macro cellular network are critically analyzed focusing on the various key parameters such as optimal system architecture, energy issues, economic issues, energy efficiency issues, outage probability via load balancing, and greenhouse gas emissions. The optimal system architecture and technical criteria of the hybrid supply system are evaluated with the help of the Hybrid Optimization Model for Electric Renewables (HOMER) optimization software for both on-grid and off-grid conditions to downsize the electricity generation cost and greenhouse gas emissions over 20 years duration. The simulation setup of HOMER software and the capacity of the battery bank is also presented in this chapter. Besides, the green energy sharing mechanism under the off-grid condition and the grid-tied condition has been critically analyzed for optimal use of green energy while ensuring the guaranteed continuity of power supply. On the other hand, the wireless network has extensively been evaluated using Matlab based Monte Carlo simulations in terms of performance metrics such as throughput, spectral efficiency, and energy efficiency metrics under various system configurations taking into account of uneven incoming traffic intensity, and inter-cell interference. Thereafter, we discussed the load balancing technique for efficient utilization of resource blocks allocated in a cluster aiming to increase the spectral efficiency of the wireless network and decrease the outage probability metrics of the user equipment under different channel quality indicators (CQI) factor, and channel bandwidth.

4.2 Simulation Setup

The project lifetime and annual interest rate are the vital issues for evaluating the economic feasibility of the project, because of their direct effect on total project cost. In this simulation, the project duration is 20 years that represents the lifetime of the BS equipment and the long-term feasibility of the proposed system. The annual interest rate is 6.75%, which is the interest rate of Bangladesh bank. Energy shortage or outage is not acceptable in the telecom sector; thus, the sources must supply power to both the BS system and the backup system. As a consequence, 10% power is reserved for ensuring 0% annual capacity shortage
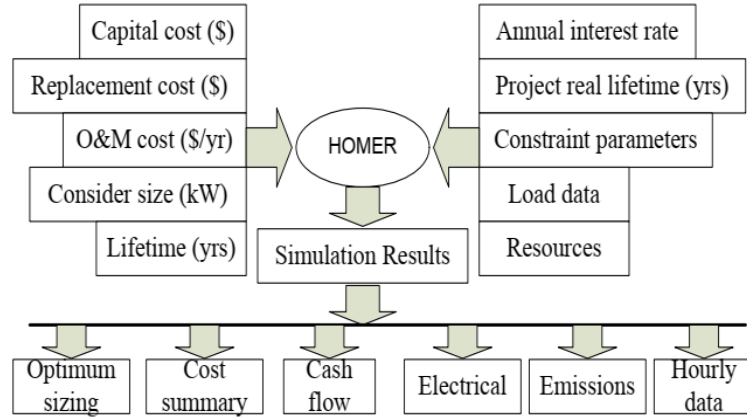
41

Figure 4.1: Flow diagram of the HOMER optimization software.

and for providing backup power to the BS load under a certain decrease in the renewable energy output. Moreover, several sets of size, cost parameters of different components such as solar PV panel, biomass generator, converter, battery unit, and solar/biomass resource profile of the chosen area are set in HOMER software to find out the optimal criteria. HOMER is optimization software that decides at each time step to satisfy the BSs load requirement that is related to traffic density and keep provision for backup power at the lowest NPC. The flow diagram of the HOMER software is shown in Fig. 4.1. The technical specifications, economic parameters, and system constraints that are used in this simulation setup are summarized in Table 4.1.

4.3 Optimal System Architecture

The schematic diagrams of the proposed grid-tied hybrid solar PV/BG system in the HOMER platform are illustrated in Fig. 4.2 and Fig. 4.3 respectively for P_{TX} = 20 W and P_{TX} = 40 W, while Fig. 4.4 and Fig. 4.5 represents the HOMER layout for an off-grid system. The seasonal DC load profiles of the proposed system for P_{TX} = 20 W and P_{TX} = 40 W are respectively shown in Fig. 4.6 and Fig. 4.7. In addition, a 30-W lamp is considered as an AC load for the night hours. Tables 4.2 and 4.3 summarize the optimal criteria for both on-grid and off-grid systems under P_{TX} = 20 W and P_{TX} = 40 W. The optimal size of different components has been found considering the average value of solar intensity (4.59 $kWh/m^2/day$) and average available biomass (9 tons/day) profile for the selected area. From the numerical data, it is seen that the battery bank capacity and BG size remain unchanged for all configurations, which indicates that the system is reliable. It is also observed that the grid-connected system requires an increased level of converter size in comparison with the off-grid system because the grid-connected system has to handle more energy. Moreover,

Table 4.1: Key parameters and their specifications for HOMER simulation setup [21, 68].

System Components	Parameters	Value
Resources	Solar intensity	4.59 kWh/m^2/day
	Biomass available	9 tons/day
	Wind speed	4.48 m/s
	Interest rate	6.75%
Solar PV	Operational lifetime	25 years
	Derating factor	0.9
	System tracking	Dual-axis
	Capital cost	$1/W
	Replacement cost	$1/W
	Operation and maintenance cost/year	$0.01/W
Biomass Generator	Efficiency	30%
	Operational lifetime	25,000 h
	Capital cost	$0.66/W
	Replacement cost	$0.66/W
	Operation and maintenance cost/year	$0.05/h
	Fuel Cost	$30/t
Grid	Energy purchase price	$0.122/kWh
	Energy sellback price	$0.110/kWh
	Demand charge	$0.350/kW/month
Wind Turbine	Size	1 kW
	Operational lifetime	25 years
	Hub height	10 m
	Capital cost	$1.6/Watt
	Replacement cost	$1.6/Watt
	Operation and maintenance cost/year	$0.05/Watt
Diesel Generator	Efficiency	40%
	Operational lifetime	25,000 h
	Capital cost	$0.66/W
	Replacement cost	$0.66/W
	Operation and maintenance cost/year	$0.05/h
Battery	Round trip efficiency	85%
	$B_{SoC_{min}}$	30%
	V_{nom}	6 V
	Q_{nom}	360 Ah
	Capital cost	$300/unit
	Replacement cost	$300/unit
	Operation and maintenance cost/year	$10/unit
Converter	Efficiency	95%
	Operational lifetime	15 years
	Capital cost	$0.4/W
	Replacement cost	$0.4/W
	Operation and maintenance cost/year	$0.01/W

Table 4.2: The optimal architecture of the proposed system for average solar radiation.

BW	PV (kW)		BG (kW)		Battery (units)		Converter (kW)	
(MHz)	20 W	40 W	20 W	40 W	20 W	40 W	20 W	40 W
5	3	3.5	1	1	64	64	1.5	1.5
10	3	3.5	1	1	64	64	1.5	1.5
15	3.5	4	1	1	64	64	1.5	1.5
20	3.5	4.5	1	1	64	64	1.5	1.5

Table 4.3: Summary of technical criteria of the proposed system for different solar intensity, R (kWh/m^2/day) under 10 MHz bandwidth.

R	PV (kW)		BG (kW)		Battery (units)		Converter (kW)	
	20 W	40 W	20 W	40 W	20 W	40 W	20 W	40 W
4.5	3	3.5	1	1	64	64	1.5	1.5
5	3	3.5	1	1	64	64	1.5	1.5
5.5	3	3.5	1	1	64	64	1.5	1.5

a linear rise of solar PV capacity with the system BW and transmission power is found to support the higher load requirement.
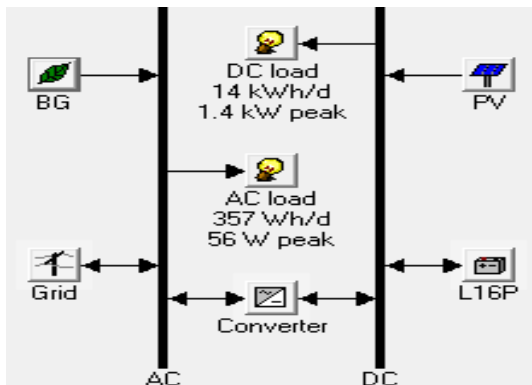

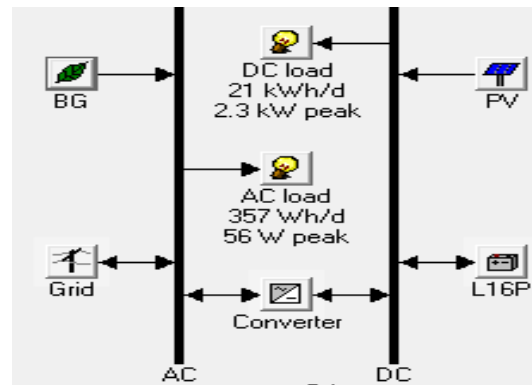**Figure 4.2:** Layout in HOMER for grid-tied BS under BW=10 MHz and P_{TX} = 20 W.

Figure 4.3: Layout in HOMER for grid-tied BS under BW=10 MHz and P_{TX} = 40 W.

The complementary effects of solar PV panel and biomass generators for the grid-connected scheme are demonstrated in Fig. 4.8 and Fig. 4.9, whereas Fig. 4.10 and Fig. 4.11 show the monthly statistic of power contribution for the off-grid system. The monthly statistic curve has been found considering the average solar radiation and biomass (rice husk) available under BW = 10 MHz. It is also considered that, for a grid-tied system, renewable energy sources supply the BS energy demand without receiving energy from the electrical grid system under normal conditions. All the monthly power contribution curves imply that a significant amount of power was contributed by the solar PV panel due to the higher value of the solar radiation profile. It is also noted that the maximum solar PV energy contribution occurs from
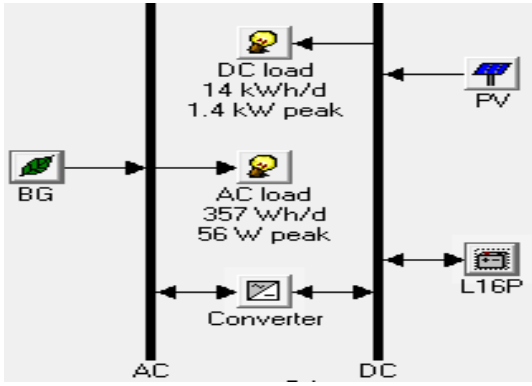
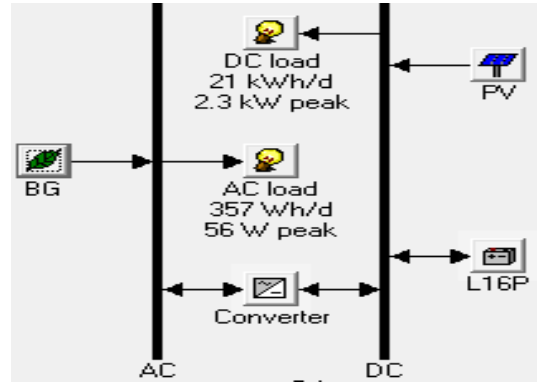**Figure 4.4:** Layout in HOMER for off-grid BS under BW=10 MHz and $P_{TX} = 20$ W.

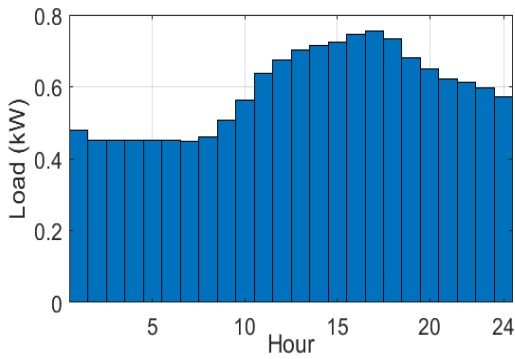**Figure 4.5:** Layout in HOMER for off-grid BS under BW=10 MHz and $P_{TX} = 40$ W.

Figure 4.6: DC load profile for macro-BS under BW = 10 MHz and $P_{TX} = 20$ W.
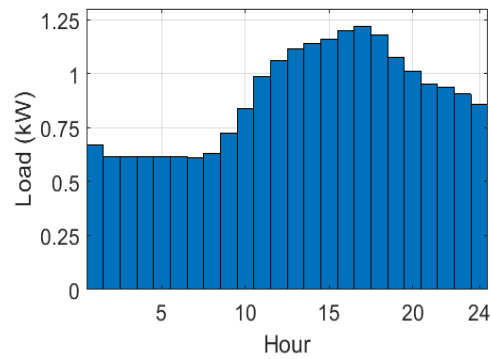

Figure 4.7: DC load profile for macro-BS under BW = 10 MHz. and $P_{TX} = 40$ W.

January to May and November to December when the solar radiation is maximum. Additionally, the minimum PV energy contribution takes place in the months when solar radiation is generally lower due to the rainy season. The rest of the demand is fulfilled by the biomass generator. On the other hand, for the grid-tied system, though the contribution of solar PV energy is a similar image of the yearly solar radiation graph, the contribution of BG is high as compared to the off-grid system. Moreover, a higher value of energy generation has been found for a grid-tied system because of selling excess electricity to the grid.

A clear view of the overall solar PV module size for diverse solar radiation is demonstrated in Fig. 4.12. In line with our expectation, the capacity of the solar PV panel is linearly related to the sunlight intensity for achieving a higher amount of renewable energy selling target. Additionally, the higher transmission power requires higher values of solar PV capacity for most of the cases.
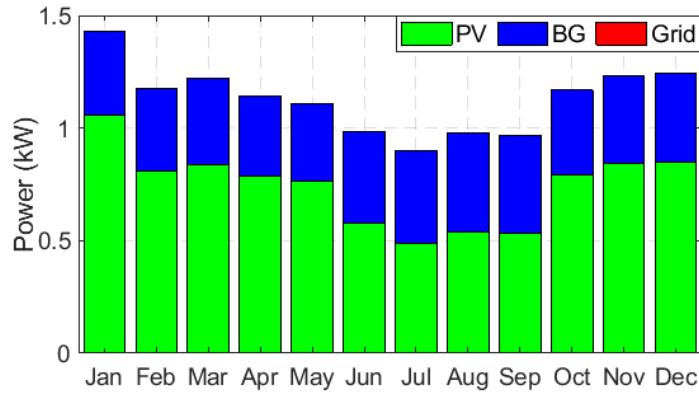
Figure 4.8: Monthly data of power contribution by on-grid hybrid PV/BG for P_{TX} = 20 W and BW = 10 MHz.
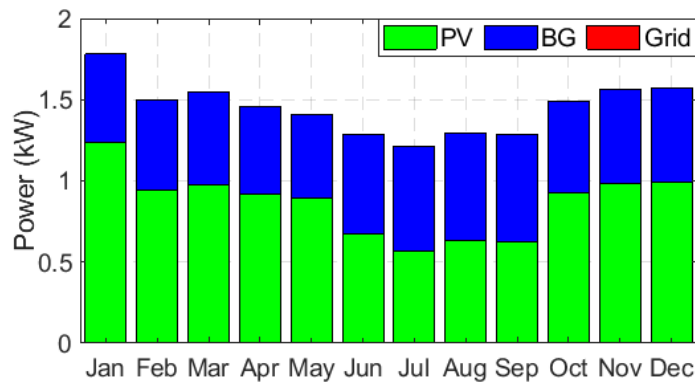

Figure 4.9: Monthly data of power contribution by on-grid hybrid PV/BG for P_{TX} = 40 W and BW = 10 MHz.
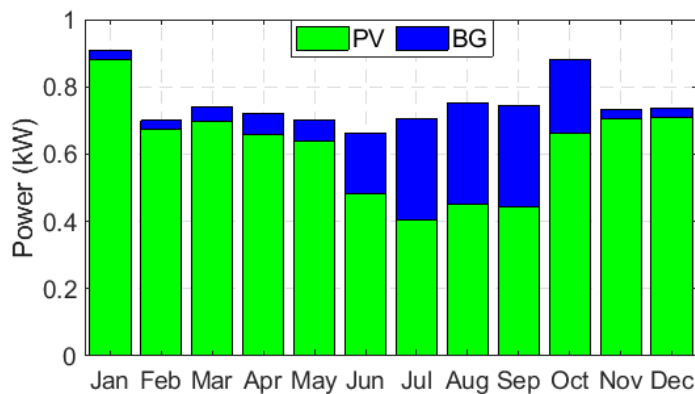

Figure 4.10: Monthly data of power contribution by off-grid hybrid PV/BG for P_{TX} = 20 W and BW = 10 MHz.
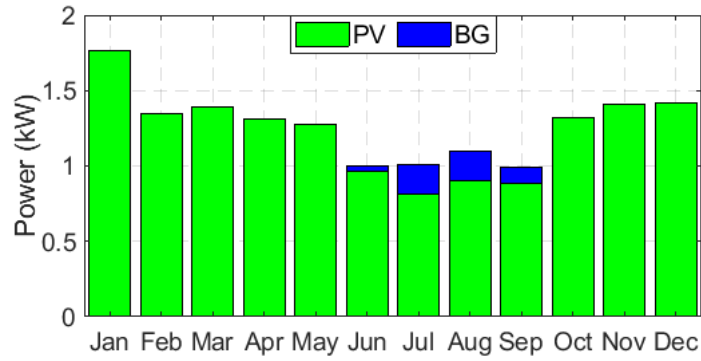
Figure 4.11: Monthly data of power contribution by off-grid hybrid PV/BG for $P_{TX} = 40$ W and BW = 10 MHz.
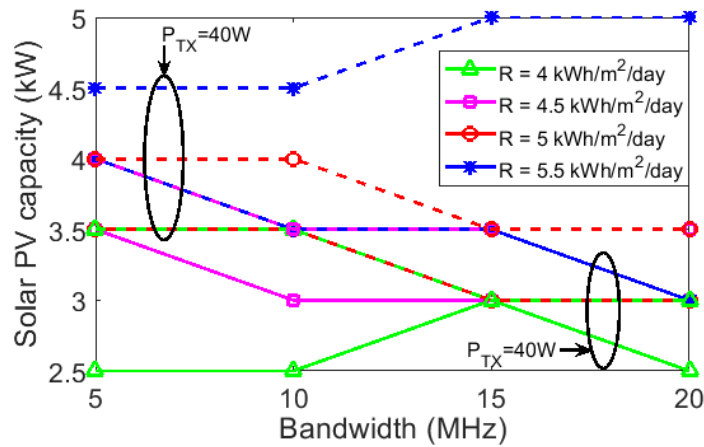
Figure 4.12: Solar PV panel capacity for the grid-tied hybrid PV/BG system under different solar intensity
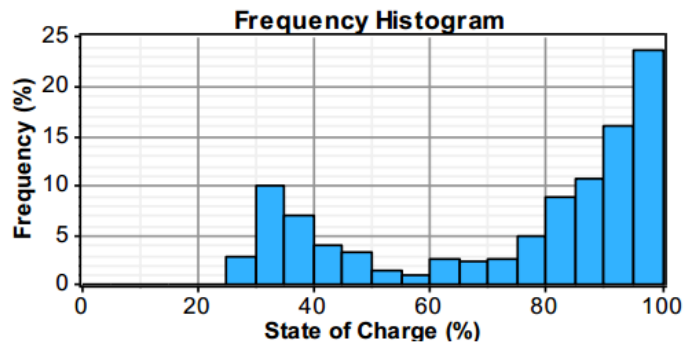
Figure 4.13: Annual frequency histogram of SOC for P_{TX}=20W, BW=10MHz, and R_{avg}.

Fig. 4.13 and Fig. 4.14 demonstrate the annual frequency histogram of a battery bank respectively for macro BS of P_{TX}=20W and P_{TX}=40W. The frequency histogram of P_{TX}=20W indicates that the battery bank is in a minimal SOC for approximately 2% of the year and high SOC for approximately 23% of the year. Thus, the battery bank replacement is essential during the project time.

Figure 4.14: Annual frequency histogram of SOC for P_{TX}=40W, BW=10MHz, and R_{avg}.

4.4 Energy Yield Analysis

In this section, the annual energy generated by the solar PV panel, BG, amount of excess electricity, and sold energy are critically analyzed based on the optimal design criter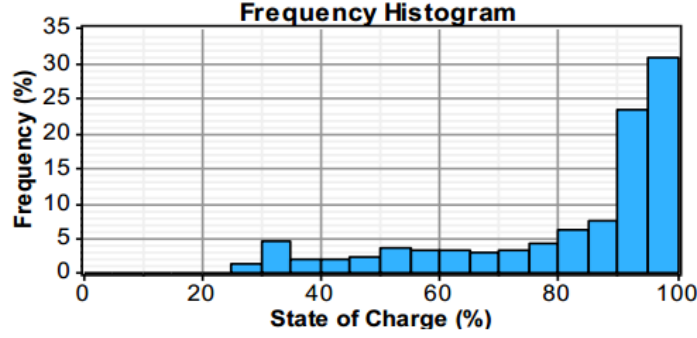ia. Moreover, the amount of energy saving by the green energy sharing mechanism has been thoroughly investigated under different network configurations.

The annual consumed energy (DC and AC load), excess energy, and shared energy for the macro cellular network under 10MHz bandwidth are shown in Fig. 4.15. On the other hand, the individual energy breakdown of the hybrid solar PV/BG system for on-grid and off-grid conditions is presented in Fig. 4.16 and Fig. 4.17 respectively. The data of this figure has been found considering the dynamic profile of the RES under 10 MHz bandwidth. In both cases the solar PV panel is the highest energy contributor, and the biomass generator is the lowest energy contributor. Fig. 4.16 also tells that no energy has been consumed from the electrical grid system for utilizing renewable energy sources at the maximum level. The main objective of the electrical grid system is to sell the excess renewable energy and receive energy back in case of a shortage or outage of RES.

4.4.1 Solar PV energy

The optimal size of the solar PV panel required for the hybrid PV/BG system is summarized in Tables 4.2 and 4.3. With reference to the tables for P_{TX} = 20 W and BW = 10 MHz, the proposed scheme consists of 12 (i.e., 3 kW) Sharp ND-250QCs solar modules: 4 connected in series and 3 connected in parallel to be compatible with the requirements of the charge controller. On the other hand, the proposed system consists of 14 (i.e., 3.5 kW) Sharp ND-250QCs solar modules for P_{TX} = 40 W and BW = 10 MHz, which is calculated
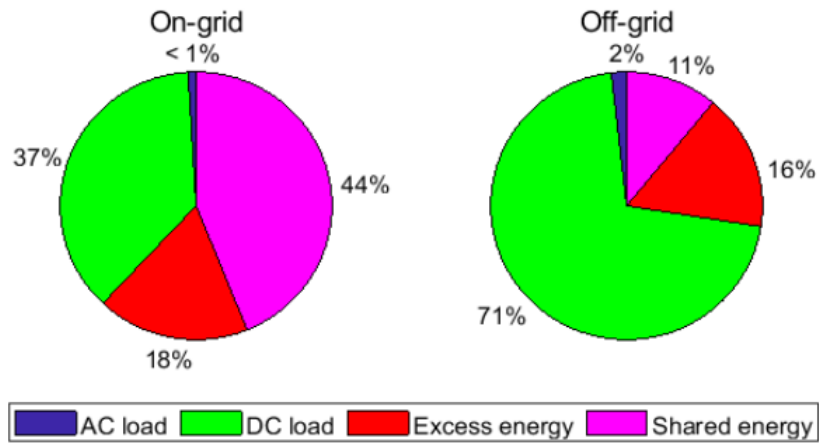
Figure 4.15: Energy breakdown for the 10 MHz system bandwidth.
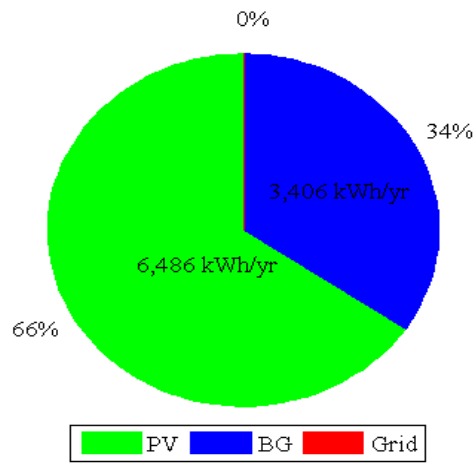

Figure 4.16: Energy breakdown for the on-grid condition under 10 MHz system bandwidth.
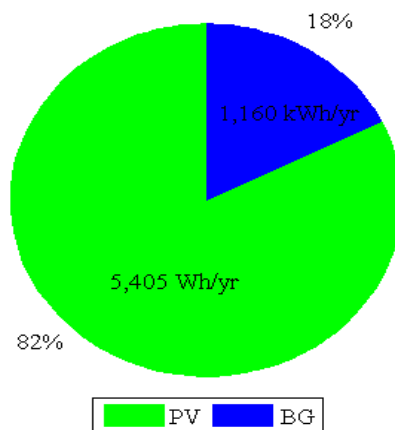

Figure 4.17: Energy breakdown for the off-grid condition under 10 MHz system bandwidth.
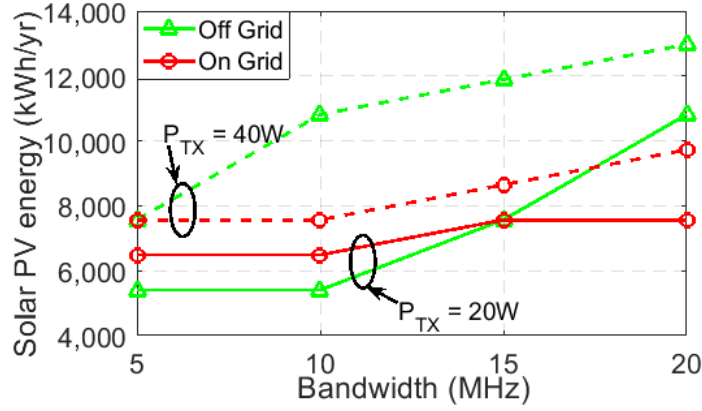
Figure 4.18: Solar energy generation for the proposed system under different bandwidth.

by (2.2):$N_{PV} = \frac{P_p}{P_{max}} = \frac{3.5\ kW}{250\ W} = 14$. Focusing on the characteristic curve, the Sharp ND-250QC solar module (polycrystalline) with a nominal voltage of 29.80V, nominal current of 8.40A and power of 250W is a good choice for this work.

The total amount of energy generated by the solar PV panel for P_{TX} = 20 W and BW = 10 MHz can be evaluated using (2.1): $E_{PV} = 3\ \text{kW}(R_{PV}) \times 4.59(PSH) \times 0.9(\eta_{PV}) \times 365$ days/year $= 4523.45$ kWh/year. Moreover, a two-axis tracking mode of solar PV panel enhances the solar energy generation by 43.4%, resulting in the production of 6486 kWh/year. In a similar process, energy generated for all other configurations is calculated. The yearly energy produced by the set of solar PV panels for dissimilar network arrangement is presented in Fig. 4.18 considering the average solar radiation profile. All the curves like Fig. 4.12 are showing escalation, which indicates that higher system BW and P_{TX} contribute to the higher yearly energy impact. Due to cost optimization, there is no fixed trend of solar energy generation for the on-grid and off-grid systems. In most of the cases of the off-grid system, the energy generations by the solar PV panel are higher due to the reservation of higher excess energy.

4.4.2 Biomass energy

According to the Tables 4.2 and 4.3, the optimal size of the biomass generator for all configurations is 1 kW. The amount of power produced and the corresponding yearly energy generated by the BG can be found by the Equations (2.3) and (2.4) in the following way: P_{BG} = 3.49 tons/year (T_{BM}) 3411.33 KCal/Kg (CV_{BM}) $\times$ 0.30 (η_{BG}) $\times$ 1000/(365 $\times$ 860 $\times$ 11.38 h (t_{op})) = 0.999 kW and E_{BG} = 0.999 kW (P_{BG}) $\times$ 365 $\times$ 24 $\times$ 0.389 (capacity factor) = 3406 kWh/year for macro BS, under average biomass available.
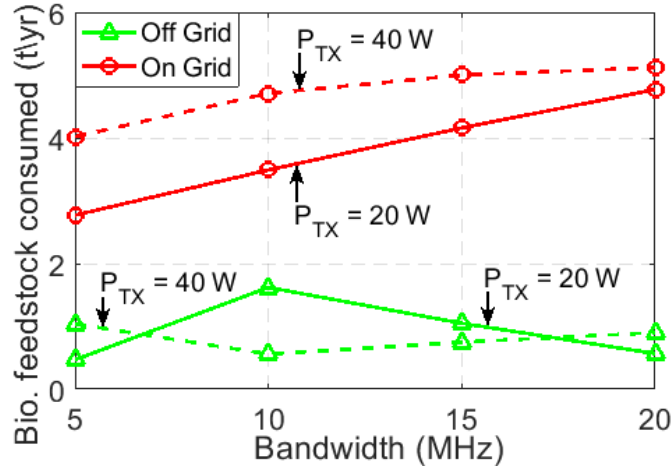
Figure 4.19: Bio-feedstock consumed for the proposed system under different bandwidth.

A quantitative comparison of bio-feedstock consumption with respect to the system BW under different grid conditions is presented in Fig. 4.19. Additionally, Fig. 4.20 signifies the effect of the biomass generator running hours on the BG lifespan. From the figures, it is found that a greater value of BG running time increases the consumption of bio-feedstock lowering the BG lifetime. Fig. 4.19 also depicts that a grid-tied system with P_{TX} = 40 W consumes more biomass than the off-grid system owing to the increased load demand by selling energy to the grid. The energy generated by the biomass generator is a similar pattern of bio-feedstock consumption as shown in Fig. 4.21. However, a lower value of BG functioning time upturns the BG lifetime and enhances the system performance by a substantial reduction of CO_2 emissions. On the other hand, a greater value of BG functioning time specifies the higher yearly energy contributions by the biomass generator, which improves the system reliability and grid capacity by maximum utilization of locally available renewable energy sources.

4.4.3 Energy breakdown

HOMER optimization software determines the generated energy (from solar PV and BG), compares it with the different types of demand such as electrical load (base station DC and AC load) and losses (battery and converter loss), and take decisions at each step about how to manage the excess electricity in terms of charging battery and selling to the grid. For BW = 10 MHz and P_{TX} = 20 W, HOMER calculates the excess energy using (3.10) as follows: E_{Excess}= 6486 kWh (E_{PV}) + 3406 kWh (E_{BG}) − 5240 kWh (E_{BS}) − 3141 kWh (E_{Sales}) − 16 kWh (B_{Loss}) − 493 kWh (C_{Loss}) = 1002 kWh/yr. By the analogous process, the annual excess electricity generated for another network setting can be determined.

51
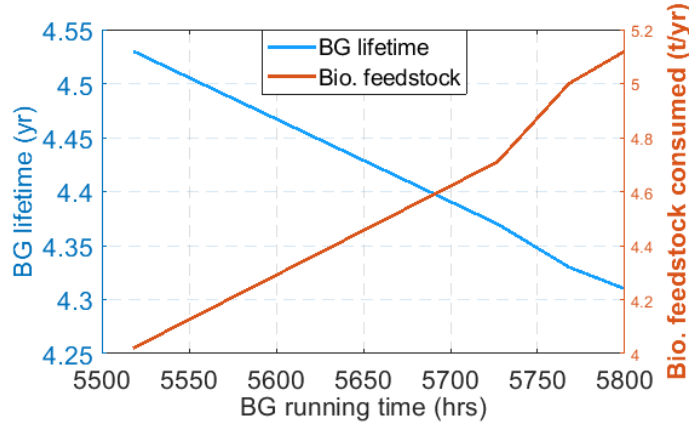
Figure 4.20: BG life and Bio-feedstock consumed for the proposed system with BG operating hours.
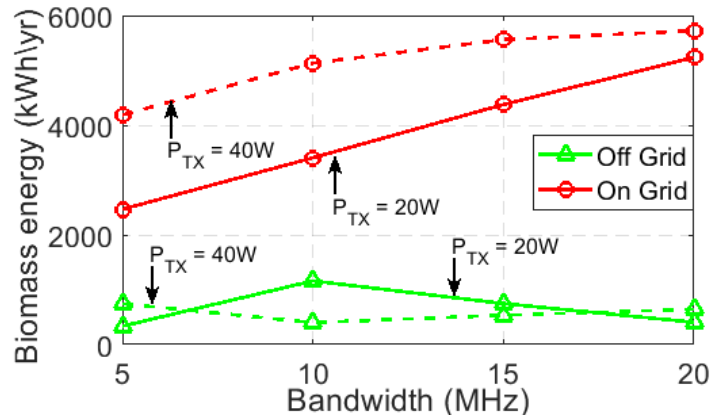
Figure 4.21: Energy generated by the BG for the proposed system under different bandwidth.

The annual energy breakdown for both on-grid and off-grid systems are respectively summarized in Fig. 4.22 and Fig. 4.23. The data presented in these figures have been found considering the average solar/biomass profile in the context of different transmission power and system BW. As is seen, the grid-tied system consists of a significant amount of excess electricity, which implies that the system can meet the BS load requirement independently. From the energy breakdown curves, it is also observed that the grid-tied system has the provision to transfer a higher amount of energy to the grid, which enhances the system reliability by maximizing the utilization of renewable energy sources and by maintaining zero energy shortage. A higher value of excess electricity is always desirable for ensuring better performance. Fig. 4.22 and Fig. 4.23 clearly depict that the proposed system has sufficient excess electricity for all configurations. Finally, a greater amount of excess electricity is found for the higher value of the P_{TX}.
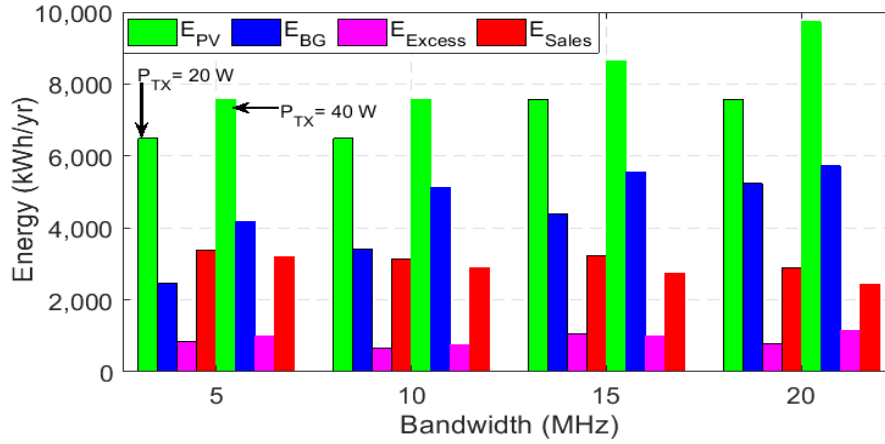
Figure 4.22: Annual energy breakdown for the grid-tied hybrid PV/BG system.
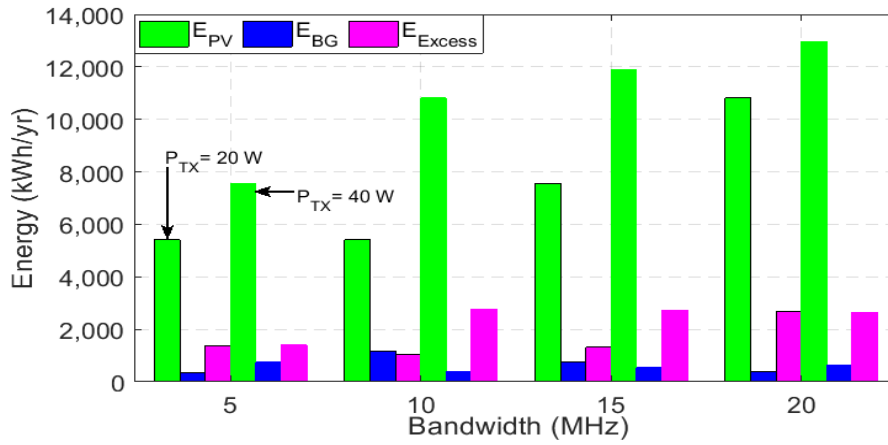
Figure 4.23: Annual energy breakdown for the off-grid hybrid PV/BG system.

4.4.4 Energy saving by sharing

4.4.4.1 Off-grid condition

Under the suggested network, the BSs would exchange energy among themselves in the possible shortest path to reduce the I^2R loss occurred in the conductor after fulfilling its own demand as shown in Fig. 4.24. In this model, we consider a transmission line whose resistance is 3.276 Ω per kilometer length that is found from the American Wire Gauge (AWG) standard conductor size table. The inter-site distance (ISD) is calculated as $\sqrt{3}$ times of cell radius (i.e. $\sqrt{3}R$) and the cell radius is 1000 m with 43 dBm transmit power. The total resistance of the transmission line between the two BSs is 5.67 Ω.

The green energy sharing model enhances network sustainability by forming a collaboration between the neighboring BSs. For remote sites, where the grid connection is not
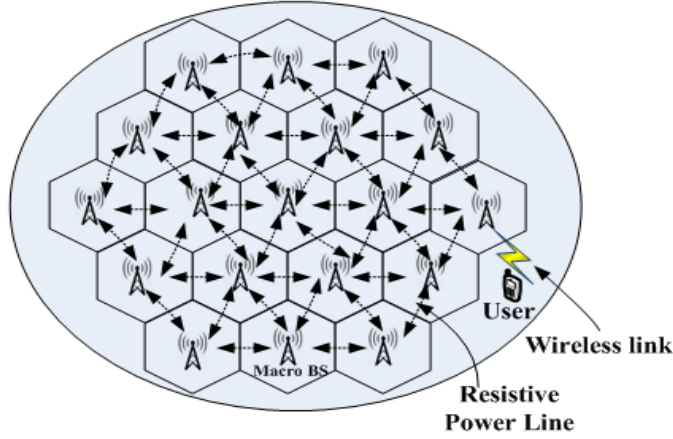
Figure 4.24: Energy sharing among the neighboring BS for the off-grid condition.

Table 4.4: Annual energy assessment for energy sharing mechanism.

BW (MHz)	E_{Excess} (kW)		I (Amp)		E_{loss} (kWh)		E_{share} (kWh)		E_{save} (%)	
	20W	40W	20W	40W	20W	40W	20W	40W	20W	40W
5	1386	1407	3.29	3.34	537	556.08	848.3	850.9	21.7	13.17
10	1034	2762	2.45	6.56	298.13	2137	735.8	625	14.85	8.35
15	1314	2724	3.12	6.47	485.05	2079	828.9	645	12.66	7.08
20	2687	2639	6.39	6.27	2028	1952.6	658.9	686.3	8.37	6.57

Table 4.5: Annual energy sharing for various resistance loss under P_{TX}=20W, and BW=10MHz.

| Resistance (%)	Resistance (Ω)	E_{loss} (kWh)	E_{share} (kWh)	E_{save} (%)
100	5.670	298.13	735.88	0 (reference)
95	5.386	283.2	750.8	2.03
90	5.103	268.3	765.7	4.06
85	4.819	253.4	780.6	6.08
80	4.536	238.5	795.5	8.11

available, the energy sharing technique assists the BSs for the harvesting energy from locally available energy sources by maximum utilization of RES through subsequent energy and cost-saving. Fig. 4.25 shows the amount of shared energy for 10MHz macro BS which is calculated using (3.17). The percentage of energy-saving by applying the energy sharing technique is determined by (3.18) and presented in Fig. 4.26. Fig. 4.25 and 4.26 depict that the amount of shared energy and percentage of energy-saving for macro BS is respectively 10 kWh and 4%. Table 4.4 summarizes the sharable energy, energy losses, and percentage of energy-saving for diverse BW considering the average solar intensity.

Fig. 4.27 and Table 4.5 illustrate the amount of transferred energy between the neighboring BSs with the variation of resistance of the power line. In line with our expectation, all the curves follow the analogous shape to reach their minimum values, which implies that a lower value of line resistance offers smaller line losses and incurs a higher amount of energy
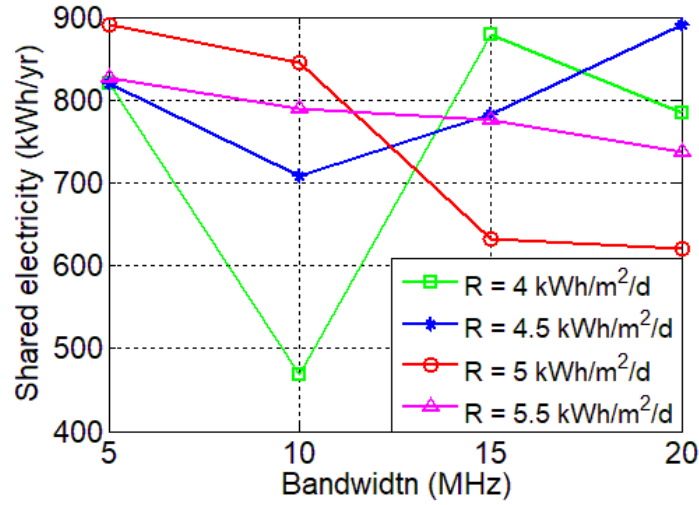
Figure 4.25: Shared electricity among neighboring BS for P_{TX}=20W, and BW=10MHz.
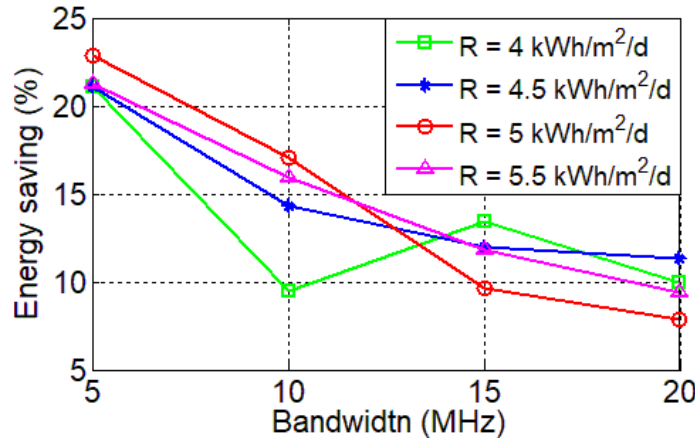
Figure 4.26: Energy-saving via energy cooperation mechanism for P_{TX}=20W.

sharing. Table 4.5 also expresses that 5% less resistance will save up to 5% energy and thus improves energy sharing up to 2.03%.

4.4.4.2 On-grid condition

Fig. 4.28 represents a monthly statistic of energy sold to the electrical grid system using the energy sharing mechanism. In line with our expectation, the grid-connected hybrid solar PV/BG system can transfer a significant volume of renewable energy to the electrical grid system after fulfilling the required energy demand of the macro BSs. The amount of sold energy for different system bandwidth is demonstrated in Fig. 4.29. It is seen that the curves of both the sold and excess energy are downward in trend because of the higher amount of energy consumed by the BS in higher system bandwidth. It is also remarkable that the sold energy curve is staying above the excess energy curve which implies that the proposed system
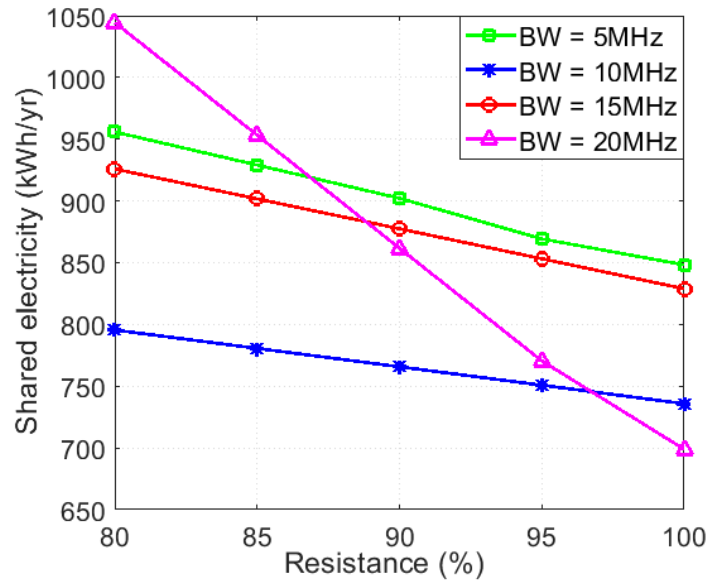
Figure 4.27: Shared electricity under different resistance for P_{TX}=20W.
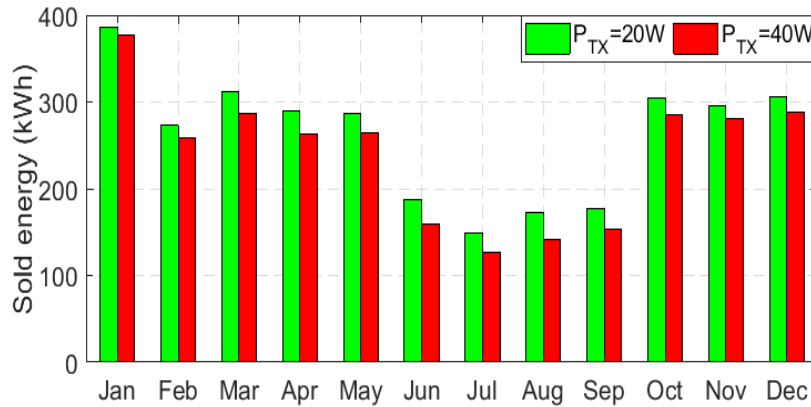
Figure 4.28: Monthly sold energy for the grid-tied hybrid PV/BG system.

has sufficient generation capacity and a greater amount of energy is transferred to the electrical grid system and a small portion of the energy is used for pack up protection. However, the generated energy can perform three functions: (i) a major portion of the generated energy is essential to fulfill the BS's load requirement, (ii) some amount of excess energy is stored in the battery bank to back up the system in the time of shortage or outage of renewable energy, and (iii) the remaining amount of energy is transferred to the electrical grid system for ensuring the continuity of power supply by maximum utilization of renewable energy sources.

4.5 Battery Capacity Analysis

The total number of battery units that are required for both $P_{TX} = 20$ W and $P_{TX} = 40$ W of the proposed configuration is 64: 8 connected in series and 8 in parallel to be compatible
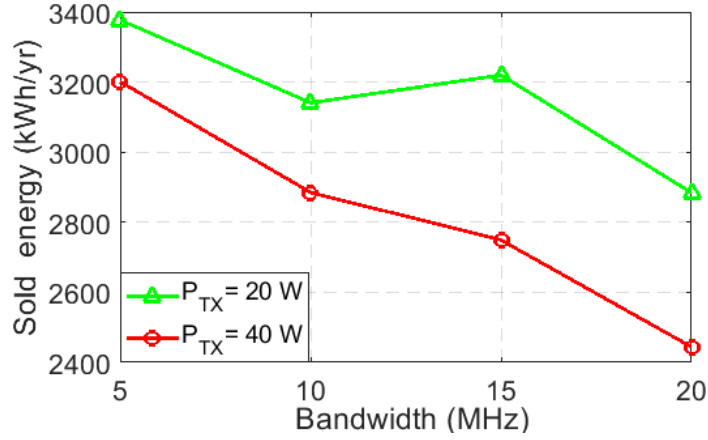
Figure 4.29: Sold energy for the grid-tied hybrid PV/BG system under different BW.
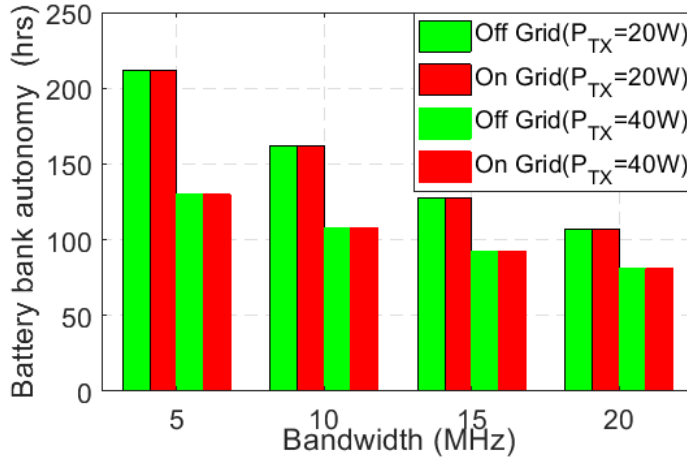
Figure 4.30: Battery bank autonomy vs. bandwidth.

with the 48-V DC bus bar. The storage device provides backup power for 162 h, which is determined using (2.12) for P_{TX} = 20 W, BW = 10 MHz, and R_{avg} configuration: (N_{batt} = 64 $\times$ V_{nom} = 6V $\times$ Q_{nom} = 360 Ah $\times$ B_{DoD} = 0.7 $\times$ 24hr)/daily BS load, E_{BS} = 14.93 kWh= 162 h. The autonomy of the battery bank for other configurations can also be determined by the analogous process. Additionally, lifetime (B_{life}) and annual throughput (Q_{thp}) of the storage device can be calculated using (2.13).

Fig. 4.30 represents the battery bank autonomy (B_{aut}) for both off-grid and on-grid systems under different system bandwidth and transmission power. The values of B_{aut} for off-grid and the on-grid systems are identical in both systems as the number of battery units is the same. However, it gradually decreases with the system bandwidth as the daily BS load consumption increases correspondingly. If any BS has to be upgraded from off-grid to an on-grid system, then no major battery backup system has to be changed. Other feasibility
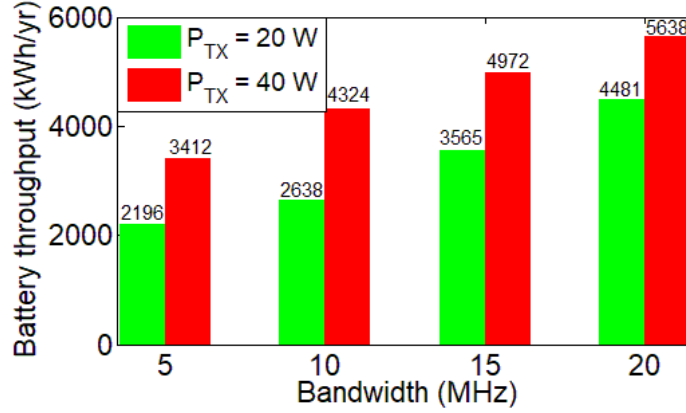
Figure 4.31: Variation of battery bank throughput with bandwidth for different P_{TX}.

calculations can also be done easily. A greater value of B_{aut} is preferable for designing sustainable system architecture to fulfill the BS demand for an elongated period of time. Improved performance of battery lifetime naturally reduces the replacement price, decreasing the overall net present cost.

Battery bank throughput (Q_{thp}) for various system BW which is presented in Fig. 4.31. It is noteworthy that the battery bank throughput is mostly affected by the BS energy demand and BW variation. As a result, a higher value of system bandwidth and transmission power increases the BS energy demand. As refer to (2.12), a higher value of E_{BS} uplifts the battery bank throughput. A higher value of Baut and Blife are preferable for reliable and cost-effective green mobile network to carry the BS load for a long time. The better performance of Blife inherently minimizes the replacement cost in terms of overall NPC.

4.6 Economic Yield Analysis

In this subsection, the economic feasibility of the proposed hybrid PV/BG scheme has been critically analyzed in terms of capital cost (CC), replacement cost (RC), operation and maintenance cost (OMC), salvage value (SV), fuel cost (FC), and total net present cost (NPC) that have to be maintained within the project duration. The cost breakdown of the individual components is performed considering the average renewable energy availability of the selected area.

The nominal cash flow summary of the hybrid PV/BG system in the HOMER platform for the grid-tied system under BW = 10 MHz and $P_{TX} = 20$ W is demonstrated in Fig. 4.32. The total NPC contains all types of costs that are necessary during the project lifetime and determined in each year of the project as follows: Capital cost $23,460 + Replacement cost
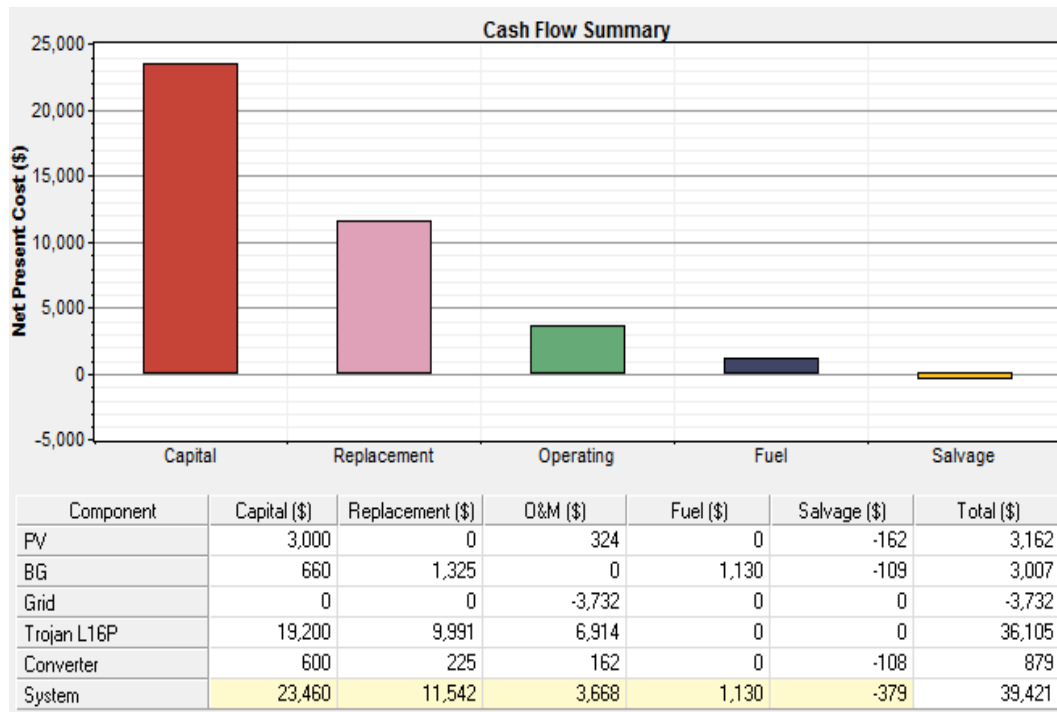
Figure 4.32: Cash flow summary for the grid-tied hybrid PV/BG system under 10 MHz bandwidth.

$11,542 + OMC $3668 + Fuel cost $1,130 − Salvage value $379, which equals $39,421. As is seen, the highest amount of cost is the capital cost, which is required at the beginning of the project, whereas replacement cost is the second-highest due to the smaller lifecycle of BG, battery, and converter. Additionally, a bulk amount of OMC and FC is included because of the continuous maintenance and biomass requirement, which uplifts the total NPC of the project. The leftover cost of each unit at the termination of the project period is counted as salvage value, which is indicated in the figure as negative.

On the other hand, the individual cost breakdown for the off-grid system keeping the grid system aside is shown in Fig. 4.33. All the systems have a significant amount of CC and OMC. The total number of the battery unit and the cost of battery per unit are the key factors for increasing the CC and OMC of the scheme. It is seen that an off-grid system without an energy-selling facility handles smaller energy as compared to the grid-tied system. An off-grid system also requires a smaller amount of biomass and converter size. As a consequence, the off-grid system has a decreased level of CC, RC, and FC though the NPC is high. It is also remarkable that a large amount of price will be paid back by selling the excess renewable energy to the public utility grid. In the end, the grid-tied system consists of a negative OMC, which represents the return of money, substantially reducing total NPC and cost of electricity.

Component	Capital ($)	Replacement ($)	O&M ($)	Fuel ($)	Salvage ($)	Total ($)
PV	2,500	0	270	0	-135	2,635
Generator 1	660	903	0	525	-162	1,926
Trojan L16P	19,200	9,991	6,914	0	0	36,105
Converter	40	15	11	0	-7	59
System	22,400	10,909	7,195	525	-304	40,725
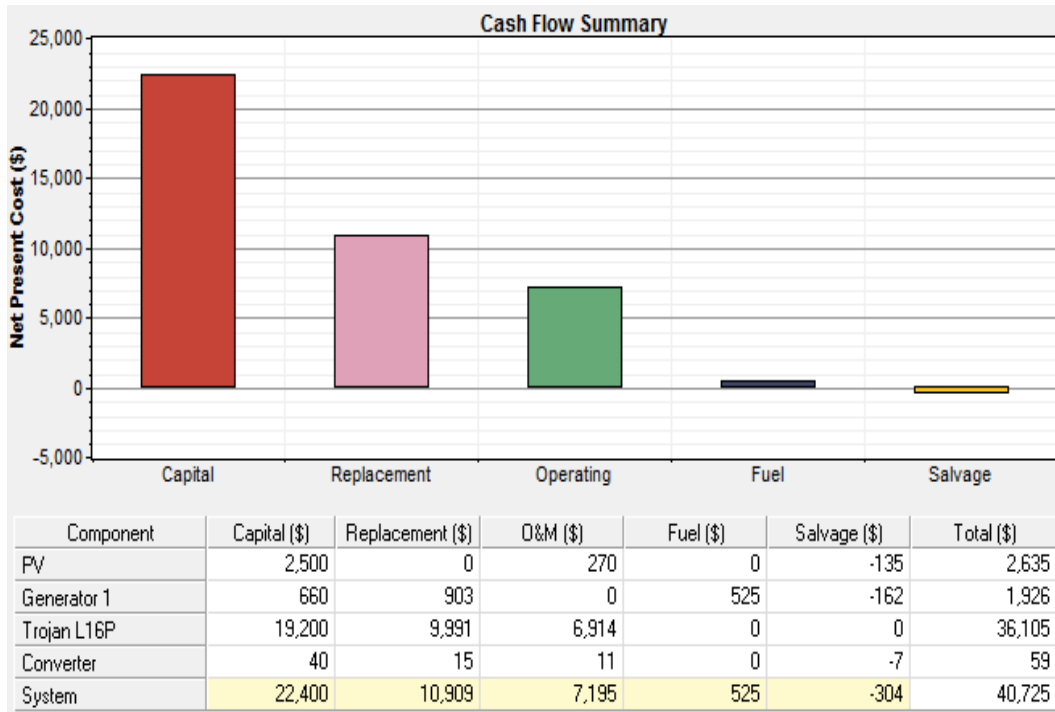
Figure 4.33: Cash flow summary for the off-grid hybrid PV/BG system under 10 MHz bandwidth.
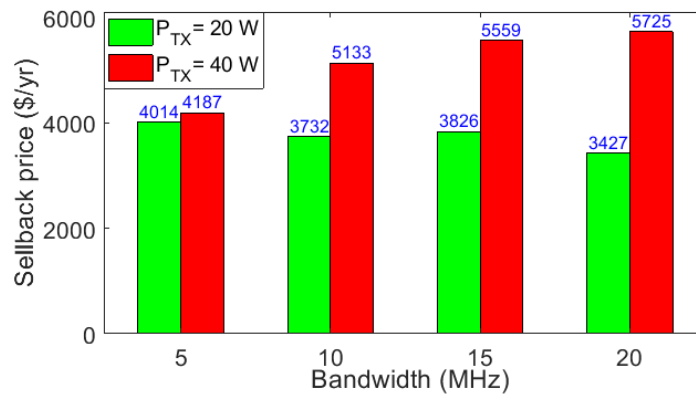
Figure 4.34: Sellback price for the grid-tied hybrid PV/BG system under different BW.

For more clarification, a short summary of the sale-back price under different transmission power and BW is presented in Fig. 4.34

The individual cost breakdown of the entire project for various system bandwidth and solar intensity is respectively summarized in Tables 4.6 and 4.7. In line with our expectation, a gradual increment of CC, RC, OMC, FC, and NPC is found for a greater value of system bandwidth and transmission power to cope up with the higher energy demand. Moreover, the capital expense is inversely related to solar radiation as shown in Table 4.7.

Table 4.6: Cost breakdown of the proposed system under various system BW.

BW	CC ($)		RC ($)		OMC ($)		FC ($)		SV ($)		NPC ($)	
(MHz)	20 W	40 W	20 W	40 W	20 W	40 W	20 W	40 W	20 W	40 W	20 W	40 W
5	23,460	23,960	11,479	11,546	3937	4246	897	1303	436	403	39,377	40,653
10	23,460	23,960	11,542	11,577	3668	4644	1130	1525	379	373	39,421	41,334
15	23,960	24,460	11,550	11,583	4226	4864	1347	1621	399	394	40,683	42,135
20	23,960	24,460	11,575	11,583	4646	5285	1548	1660	373	416	41,353	43,077

Table 4.7: Cost breakdown of the proposed system under various solar intensity, $R(kWh/m^2/day)$.

R	CC ($)		RC ($)		OMC ($)		FC ($)		SV ($)		NPC ($)	
	20 W	40 W	20 W	40 W	20 W	40 W	20 W	40 W	20 W	40 W	20 W	40 W
4.5	23,460	23,960	11,545	11,583	3965	4749	1135	1535	377	367	39,528	41,460
5	23,460	23,960	11,523	11,558	3293	4227	1108	1490	397	391	38,987	40,844
5.5	23,460	23,960	11,501	11,536	2928	3814	1048	1455	416	412	38,557	40,352
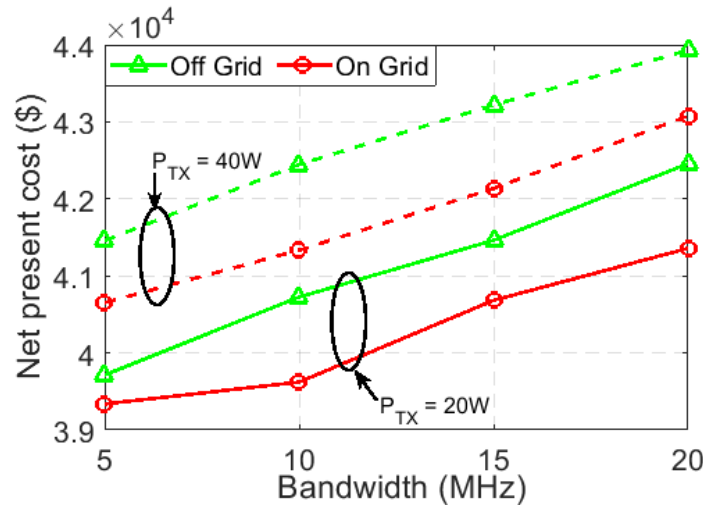
Figure 4.35: Net present cost vs. bandwidth for the proposed system.

Fig. 4.35 depicts the clear image of the net present cost for both on-grid and off-grid macro-BS varying the system BW and P_{TX}. The graph tells that higher BW and P_{TX} incurs greater NPC likewise Table 4.6. According to (2.19), the BS energy demand goes to the upper direction to support the higher system BW and P_{TX}, and hence, NPC curves follow a similar pattern. It is also observed that the off-grid curves lie above the on-grid curves, so the grid-tied hybrid solar PV/BG system is more cost-effective. In addition, the impact of biomass price on the total net present cost is illustrated in Fig. 4.36 under different network configurations. As is expected, all the NPC curves show an increasing trend with respect to the biomass price. This is happening because the biomass price is linearly related to the fuel cost as well as NPC.
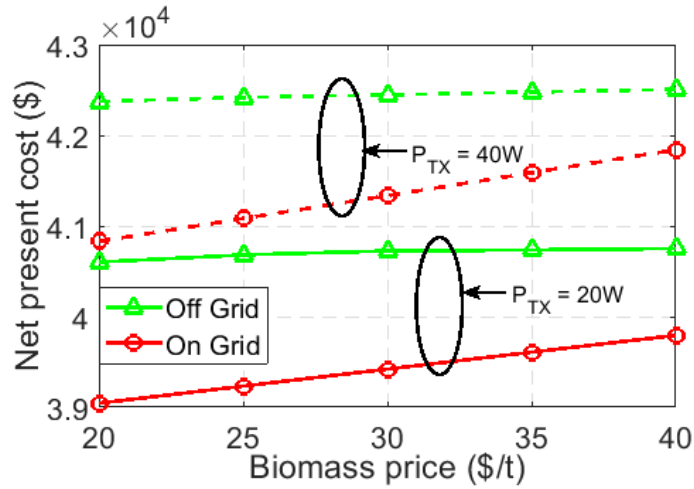
Figure 4.36: Net present cost vs. biomass price for the proposed system.
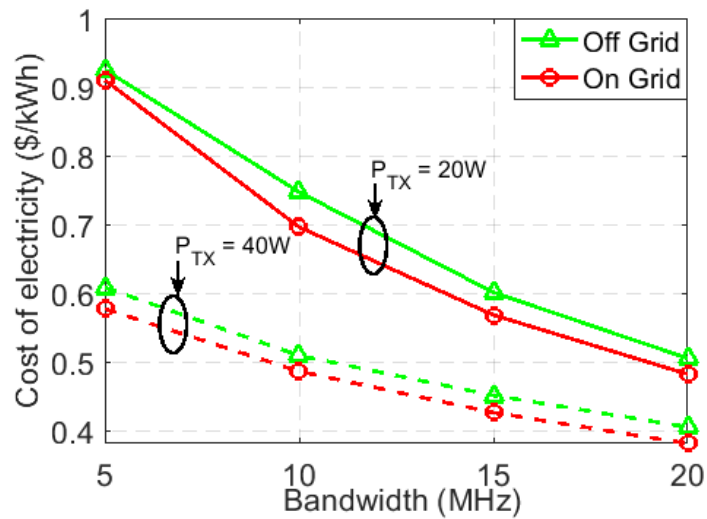
Figure 4.37: Cost of electricity vs. bandwidth for the proposed system.

The effect of P_{TX} and BW variation on the cost of electricity is shown in Fig. 4.37 for both off-grid and on-grid conditions. The electricity generation cost as well as the per-unit cost of electricity is gradually falling with the increment of system BW and P_{TX}. It is happening because of the higher amount of electricity generation, resulting in the decrement in total expenses. From the aforementioned analysis, it is concluded that a better value of COE can be obtained by installing the BS at higher system BW and higher transmission power. Additionally, the COE curves under different transmission power can be explored by varying the biomass price as shown in Fig. 4.38. It is noticed that lower transmission power and higher biomass price are responsible for poor economic performance.
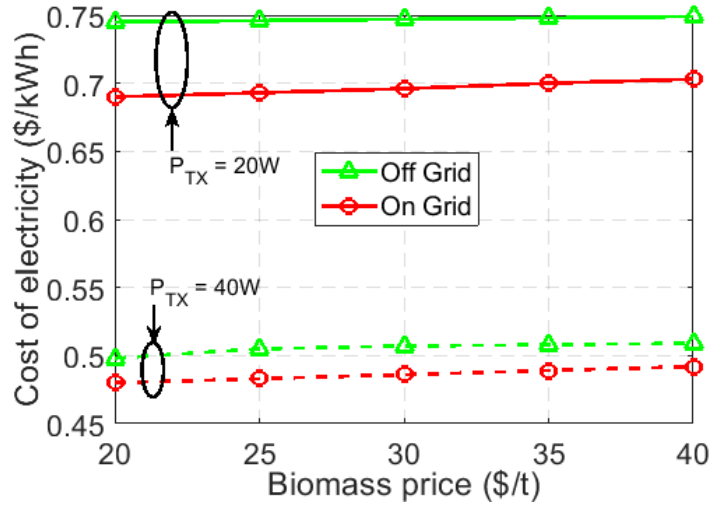
Figure 4.38: Cost of electricity vs. biomass price for the proposed system.

Table 4.8: Pollutants for $P_{TX} = 20W$, and BW=10MHz.

Pollutants	Emissions (Kg/Yr)	
	20W	40W
Carbon dioxide	2.36	0.0815
Carbon monoxide	0.0105	0.00364
Unburned hydrocarbons	0.00117	0.000403
Particulate matter	0.000794	0.000274
Nitrogen oxides	0.094	0.0325

4.7 Greenhouse Gas Emission Analysis

Due to the technological advancement, the higher volume carbon footprint of RES (especially biomass) can be maintained at a lower value. The premier carbon contents emanated by the proposed system for 10MHz bandwidth are counted in Table 4.8. Among the different pollutants, CO_2 is the main contributor to the GHG emission. Fig. 4.39 counts the pollution rate as well as annual GHG emissions for different network settings. In a hybrid solar PV/BG system, solar as an ideal energy source produces zero carbon contents where all of the GHG is emitted by the biomass generator only. The hybrid solar PV/BG system emits the highest amount of greenhouse gas for 10MHz and 15MHz bandwidth because of higher energy contribution by the biomass generator as seen from Fig. 4.39. Additionally, the impact of toxic-intensive GHG generated by the biomass generator is expressed in Fig. 4.40, which implies that a higher BG operating time promotes the carbon footprints, although there is a significant betterment in reliability and QoS. In general, solar radiation rate and solar cell size have a conducive effect on pollution minimization with upgrading the energy generated by the solar PV panel.
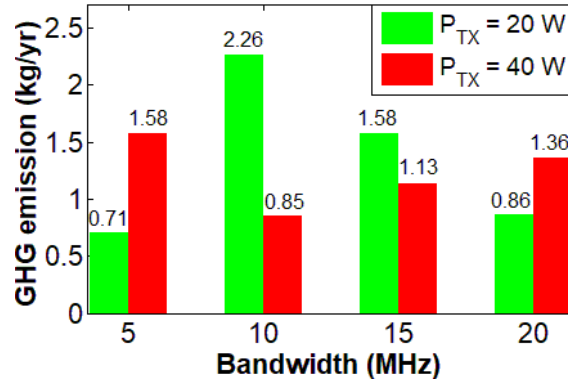
Figure 4.39: GHG emissions vs. system bandwidth for average solar radiation.
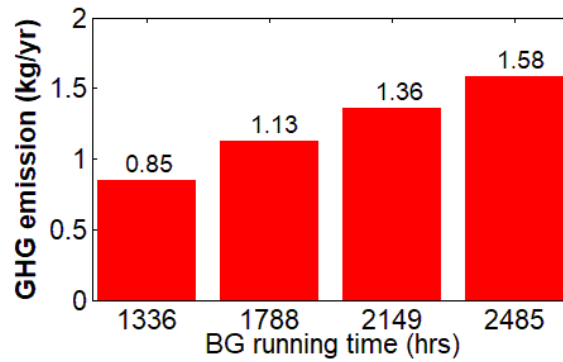
Figure 4.40: GHG emissions vs. BG running time for average solar radiation.

An extensive comparison of greenhouse gas emissions for the off-grid and on-grid configurations of solar PV/BG is shown in Fig. 4.41. The figure depicts that the GHG emission is close to zero for the off-grid system. However, it will show a slight surge with the increment of P_{TX} and BW. On the other hand, the grid-tied arrangement of the hybrid solar PV/BG the system exhibits negative emissions because of transferring a greater amount of excess electricity to the grid. This transfer of green energy will directly reduce the GHG emissions of the fossil fuel-based grid system. Finally, the proposed system can indirectly reduce the carbon contents by minimizing the burning of fossil fuel and biomass.

4.8 Network Performance Analysis

In this subsection, the performance of the wireless network has been critically analyzed in terms of the throughput, spectral efficiency, energy efficiency, and energy efficiency gain matrics considering the temporospatial variation of incoming traffic density as shown in Fig. 2.10. The network has been simulated in the context of 2 tiers, of 19 BSs with hexagonal shape for identifying the inter-cell interference (ICI), and of achieving 4G/5G communications.
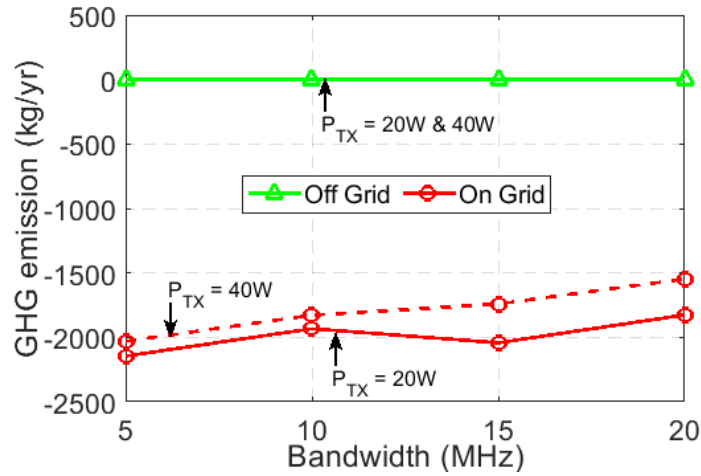
Figure 4.41: Greenhouse gas emissions vs. biomass price for the proposed system.

Fig. 4.42 illustrates the variation of throughput performance over 24 hours for the introduced network taking ICI into account. Additionally, the throughput performances under different system bandwidth and transmission power are presented in Table 4.9. A higher value of throughput performance is always desirable, which is a function of resource blocks (RB), and the quantity of RBs is directly retaliated to the traffic profile. For ensuring better performance, it is assumed that each user is linked to at least one RB and that this number changes with traffic arrival rate. Noticeably, all the throughput curves follow a similar pattern of incoming traffic profile and a significant amount of throughput gap is found between the low density and high density of traffic demand. It is worthy to mention that a large number of RBs is allocated while BSs are run in high BW. Therefore, throughput performance at BW = 20 MHz reveals an optimistic nature compared to others as evident from Table 4.9. It is also remarkable that the throughput performances for P_{TX} = 20 W and P_{TX} = 40 W are very insignificant. This is due to the fact that ICI power increases simultaneously with the received signal power, resulting in consistent throughput performance. The spectral efficiency (SE) comparison of the considered mobile network under different BW is summarized in Table 4.9. As a matter of fact, SE mainly depends on throughput and system BW.

Table 4.9: Throughput and spectral efficiency performance of the wireless network.

BW	Throughput (Kbps)				Spectral Efficiency (Kbps/Hz)			
	On-grid		Off-grid		On-grid		Off-grid	
	20 W	40 W	20 W	40 W	20 W	40 W	20 W	40 W
5 MHz	46,651	46,531	46,651	46,531	9.33×10^{-3}	9.30×10^{-3}	9.33×10^{-3}	9.30×10^{-3}
10 MHz	95,421	100,128	95,421	100,128	9.54×10^{-3}	9.50×10^{-3}	9.54×10^{-3}	9.50×10^{-3}
15 MHz	147,917	146,253	147,917	146,253	9.86×10^{-3}	9.65×10^{-3}	9.86×10^{-3}	9.65×10^{-3}
20 MHz	194,582	198,759	194,582	198,759	9.72×10^{-3}	9.93×10^{-3}	9.72×10^{-3}	9.93×10^{-3}
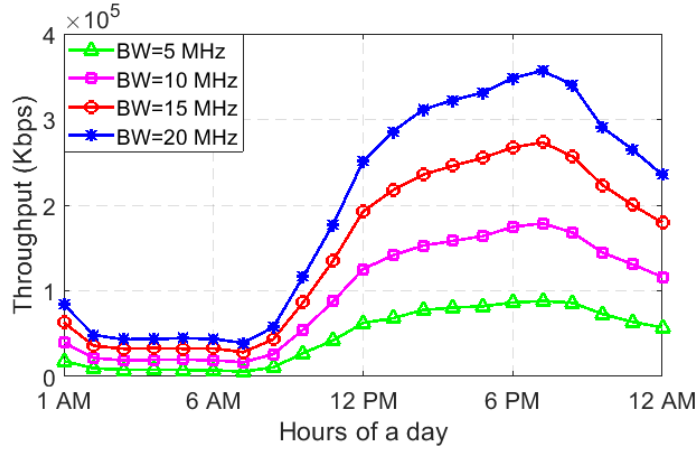
Figure 4.42: A quantitative comparison of throughput performance under different system bandwidth.
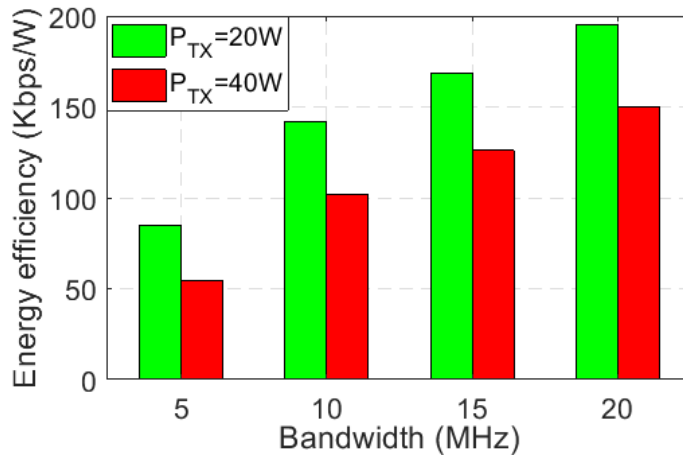
Figure 4.43: A quantitative comparison of EE performance under different system bandwidth.

The energy-efficiency and energy-efficiency gain metrics of the proposed network in consideration with the realistic traffic pattern are respectively depicted in Fig. 4.43 and Fig. 4.44. According to (3.25) and (3.26), a higher value of throughput and a lower value of power consumption have a positive impact on EE performance. Moreover, throughput performance is directly related to the RBs, and higher system BW uses more RBs. In contrast, higher system BW and transmission power are liable to increasing the net power consumption. As a consequence, a better energy efficiency performance can be achieved by running the suggested network at $P_{TX} = 20$ W and BW = 10 MHz. On the other hand, energy efficiency gain measures the improvement of energy efficiency performance by the selected hybrid PV/BG enabled network compared to the reference off-grid hybrid PV/BG enabled system. To the end, Fig. 4.44 implies that the proposed network can attain EE improvement by about 20% with effective modeling of the hybrid PV/BG system.
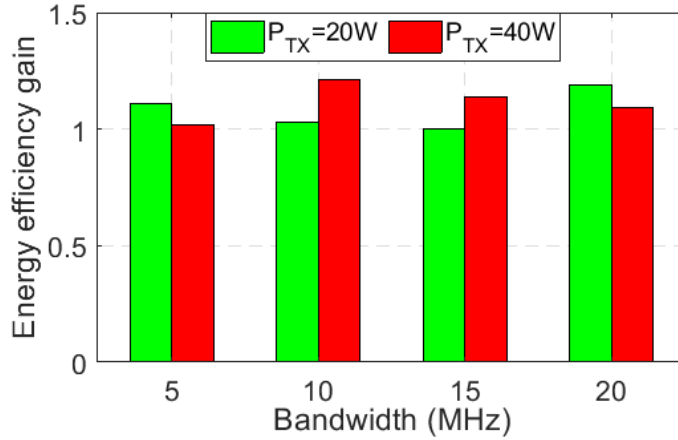
Figure 4.44: A quantitative comparison of EE gain performance under different system bandwidth.

4.9   Outage Probability and Spectral Efficiency via Load Balancing

In a cellular network, voice is the major part of the data demand [67]. The maximum number of voice over LTE (VoLTE) users that can be carried by the wireless network depends on various factors such as physical resource blocks (PRBs), channel quality indicator (CQI), system bandwidth (BW), SINR, etc [67]. The maximum number of the simultaneous users (N_{su}) that can efficiently be supported by the network is calculated as: (Number of Available PRB)/ (Number of PRB per VoLTE call) $\times$ 20. According to [67], the number of required resource blocks and carried VoLTE users under different system bandwidth and CQI are summarized in Table 4.10. However, a base station can support a specific number of users/traffic based on the designed parameters. If the users/ traffic rates increase beyond this value, the performance of the network may decrease. For instance, with the increment of traffic intensity beyond the threshold value, the spectral efficiency of the network decreases, and the outage probability of the network increases. To overcome these problems, load balancing is an efficient technique. By proper modeling and implementing the load balancing technique, the spectral efficiency performance of the wireless network can significantly be improved as shown in Fig. 4.45, where 0% shifted load indicates the spectral efficiency and outage probability of the network without applying the load balancing technique. Fig. 4.45 implies that a 5% shifting of peak load to the neighboring low-density base station can improve the spectral efficiency up to around 4%.
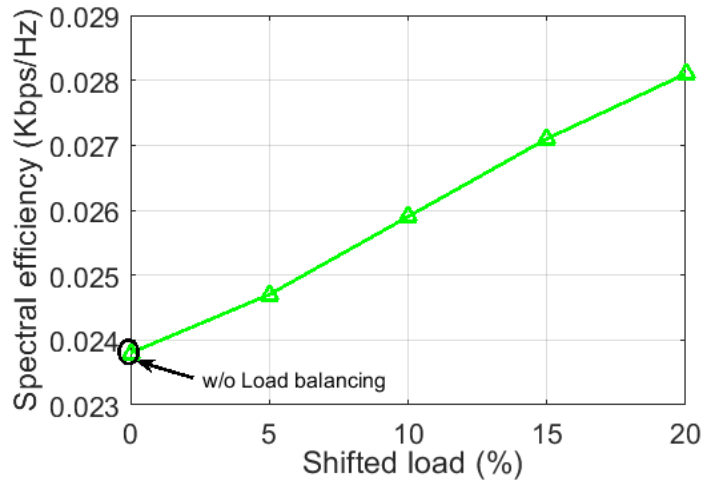
Figure 4.45: Spectral efficiency via load balancing technique under 10 MHz bandwidth.

Table 4.10: Number of VoLTE users for different CQI and system bandwidth.

System Bandwidth (BW)	5 MHz	10 MHz	15 MHz	20 MHz
No. of Resource Blocks (RBs)	25	50	75	100
CQI =15 (1 PRB) no. VoLTE User	500	1000	1500	2000
CQI =7 (2 PRB) no. VoLTE User	250	500	750	1000
CQI =1 (16 PRB) no. VoLTE User	31	63	94	125

An extensive comparison of outage probability of the wireless network for with and without load balancing technique is shown in Fig. 4.46, Fig. 4.47 and Fig. 4.48 under different network conditions. All the figures have been drawn shifting the load from 0% to 5%, where shifted load 0% means without load balancing and shifted load greater than 0% means by applying load balancing. Fig. 4.46 represents the outage probability for three different additional users (additional users are 25, 50, and 75) beyond the standard user of CQI=7 and BW=10 MHz which is mentioned in Table 4.10. The outage probability for different CQI is presented in Fig. 4.47 under 10 MHz bandwidth. On the other hand, Fig. 4.48 outlines the outage probability for different system bandwidth under CQI=7. All the curves follow a similar pattern of the downward trend which implies that balancing the load among the neighboring lower density BSs can significantly reduce the outage probability. To the end, Fig. 4.46 has been drawn to find out the effect of additional users, Fig 4.47 has been drawn to calculate the effect of CQI, and Fig. 4.48 has been drawn to observe the effect of system bandwidth on the simultaneous users. For all the cases, a better value of probability has been found by applying the load balancing technique.
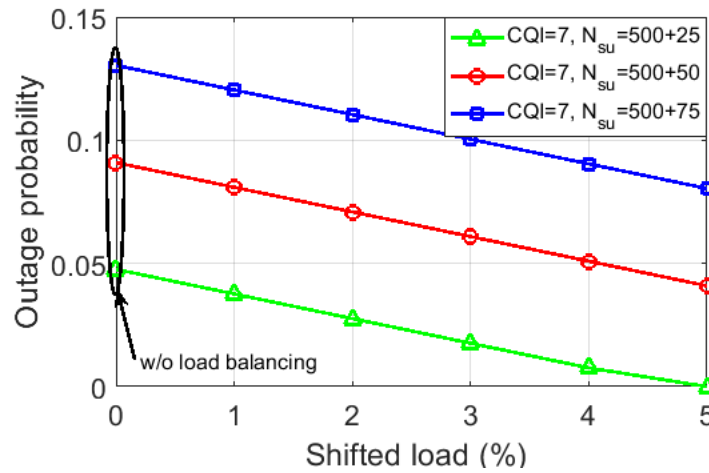
Figure 4.46: Outage probability via load balancing technique for different users under 10 MHz BW.
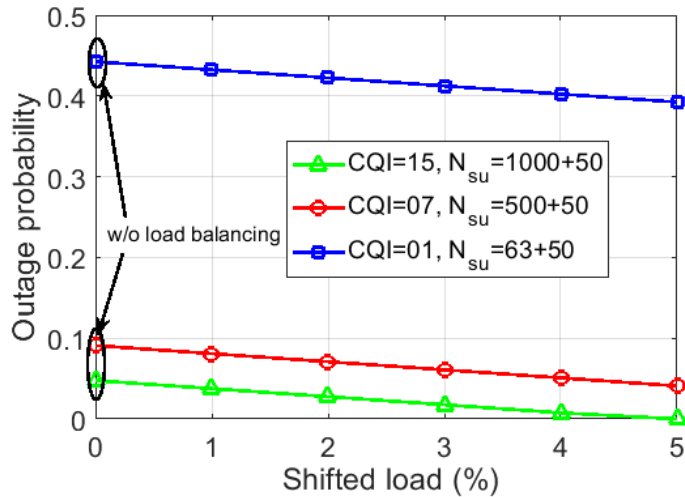
Figure 4.47: Outage probability via load balancing technique for different CQI under 10 MHz BW.
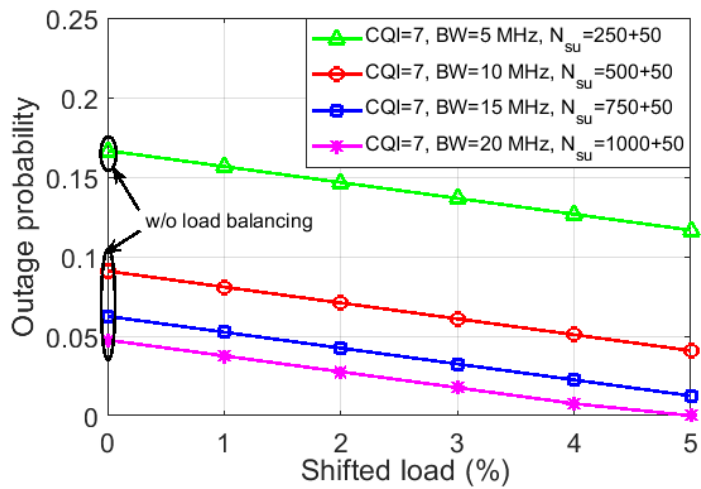
Figure 4.48: Outage probability via load balancing technique for different system BW.

4.10 Conclusion

In this chapter, we examined the feasibility of deploying a combined solar PV and biomass-focused sustainable supply system for powering the LTE macro-base stations in order to reduce both net present cost and carbon contents. The sensitivity of the suggested system has been evaluated using the HOMER software in terms of optimal architecture, energy production, capital cost, and pollution rate varying system parameters such as transmission power and system bandwidth. The outcomes of the simulation depict that the hybrid solar PV/BG system can independently support the BS energy requirement without sacrificing the quality of services. The battery bank can provide sufficient backup power which explicitly conforms to the reliability issue. Numerical results also demonstrate that the energy sharing mechanism can save a significant amount of energy by ensuring the zero percent energy shortage/outage. Moreover, the performance of the wireless network has been evaluated in terms of throughput, spectral efficiency, and energy efficiency metrics. A significant improvement of spectral efficiency can be achieved and a considerable amount of outage probability can be reduced by proper balancing the load among the neighboring base stations. In summary, the hybrid solar PV/BG-powered cellular networks with an energy sharing facility to the interconnected base station (for off-grid condition) or to the electrical grid is an effective way of developing an energy-efficient green mobile communication with affordable cost. In the next chapter, the outcomes of the hybrid solar PV/BG system have been compared with those of other supply schemes for justifying the system validity.

CHAPTER 5

BREAKEVEN POINT ANALYSIS AND FEASIBILITY COMPARISON

5.1 Introduction

In this chapter, the breakeven point of the hybrid solar PV/BG system is estimated for ensuring economic feasibility. Moreover, the outcomes of the proposed system are compared with the standalone solar PV, hybrid PV/WT, and hybrid PV/DG scheme keeping in mind the technical criteria namely, economic analysis, energy yield analysis, and greenhouse gas emissions for ensuring the network sustainability. For presenting a clear view, different power providing schemes have been simulated under the same network setting considering the average solar intensity and biomass profile. Finally, the performance parameters of the introduced system are compared with the previously published research work.

5.2 Breakeven Point Calculation

The breakeven point is the period in which the capital cost of the project is expected to get back by the selling of generated energy. The breakeven point (C_{BP}) is also known as the payback period and can be calculated as follows [69, 70]

$$C_{BP} = \frac{C_{TI}}{C_{AR}} \tag{5.1}$$

where C_{TI} is the total investment (\$) for the hybrid supply system and C_{AR} is the annual return (\$) by selling the generated green energy. The annual return of the system is found by subtracting the annual operational cost from the annual income. In this work, we estimated the breakeven point considering the consumption of generated energy at a rate of \$0.559/kWh, around 10% higher than the generation cost. The detail calculations of the payback period under 10 MHz system bandwidth is shown in below

Total investment =\$42,447

Selling rate of energy=\$0.559/kWh

Sold energy=7724kWh/yr

Fuel cost/kWh=0.560 tones/yr × \$30/tones=\$0.0418/kWh

Operation and maintenance cost=704kWh/yr

Replacement cost=944kWh/yr

Table 5.1: Breakeven point calculation.

Energy rate ($/kWh)	Investment ($)	Return ($/Yr)	Profit ($)	Breakeven point (Yr)
0.559	42,447	2652.7	10607	16
0.610	42,447	3046.6	18485	14
0.636	42,447	3247.4	22501	13

Table 5.2: Summary of technical criteria for the different scheme under P_{TX}=20W and BW=10MHz.

Supply Scheme	PV (kW)	BG (kW)	DG (kW)	WT (kW)	Conv. (kW)	N_{batt} (Units)	B_{loss} (kWh/yr)	B_{aut} (hrs)	C_{loss} (kWh/yr)	E_{Excess} (kWh/yr)
PV	2.5	*	*	*	0.1	64	463	162	14	1949
PV/WT	1	*	*	1	0.1	64	164	162	14	878
PV/DG	4	*	1	*	0.1	64	476	162	14	2911
PV/BG	3	1	*	*	1.5	64	16	162	493	1002
* = Not applicable										

Thus, annual return=($0.559 × $7724)-$17-$944-$704=$2652.7

According to the 5.1, the breakeven point of the solar PV/BG is 16 years. Moreover, if we increase the energy rate from $0.559 to $0.636/ kWh, increases the return and decreases the breakeven period from 16 years to 13 years as summarized in Table 5.1. Table 5.1 represents that a higher value of the energy selling rate steps down the breakeven point leading to enhancement in economic feasibility. This implies that the sample payback period is dependent predominantly on the energy selling rate.

5.3 Feasibility Comparison

5.3.1 Comparison among the different types of supply system

A quantitative comparison of technical criteria including the optimal size is summarized in Table 5.2 for the aforementioned supply system that is obtained from the HOMER software. As is seen, the optimal architecture of the proposed system is in a feasible range and remains almost close to the other supply schemes, which ensure the effectiveness of the system. Noticeably, a large number of solar PV panels are required in order to satisfy the BS energy demand for both standalone solar PV and hybrid PV/DG-powered systems, leading to a remarkable enhancement in NPC and COE.

A detailed comparison of the cost of electricity under different supply schemes is illustrated in Fig. 5.1 and Fig. 5.2 along with the variation of system bandwidth and transmission power. It is observed that the COE curves are in the lower position for the grid-tied system, which implies that the grid-connected hybrid PV/BG scheme attains optimistic results
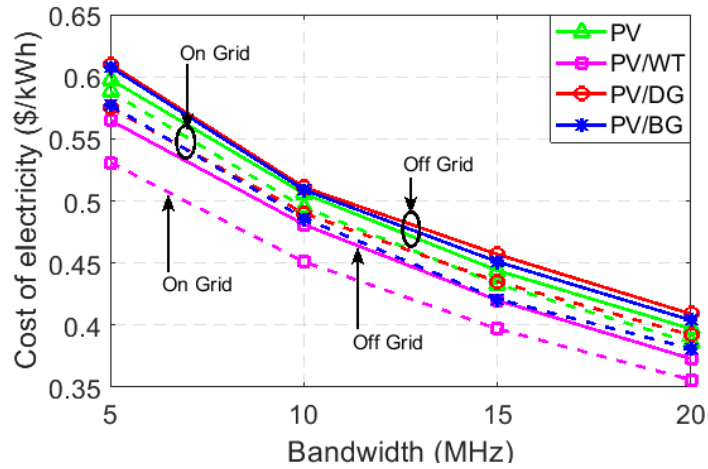
Figure 5.1: Comparison of COE between on-grid and off-grid under different system BW.
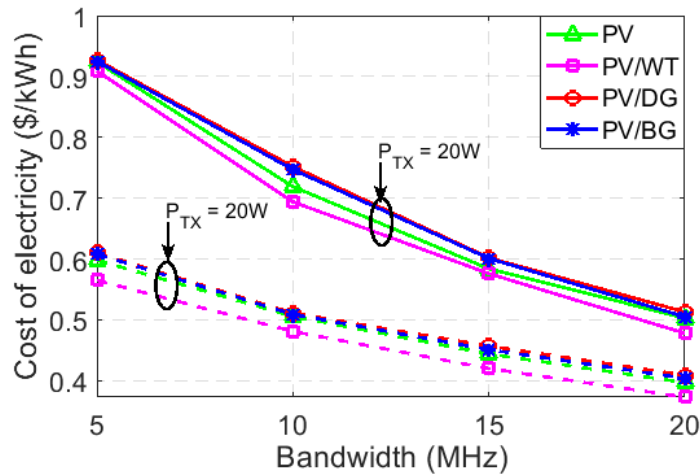
Figure 5.2: Comparison of COE under different transmission power.

wherein standalone solar PV exhibits average results. In line with our expectation, the hybrid PV/DG scheme provides poor value and hybrid PV/WT represents superior performance. Though results show the best output for the hybrid PV/WT system configuration, this hybrid system is not feasible because of the complicacy of the WT setup and low-speed wind graph in the selected location. On the other hand, the hybrid PV/BG system provides greater reliability compared to the standalone solar PV system because the single energy technology source solar energy generation may be outage depending on the weather condition. As a consequence, the hybrid PV/BG system is an attractive solution for powering the macro-BS.

Fig. 5.3 and Fig. 5.4 compare the net present cost among the various supply system likewise in the events discussed in the COE comparison section. It is found that hybrid PV/WT and standalone solar PV involve lower NPC for all cases, whereas the hybrid PV/BG
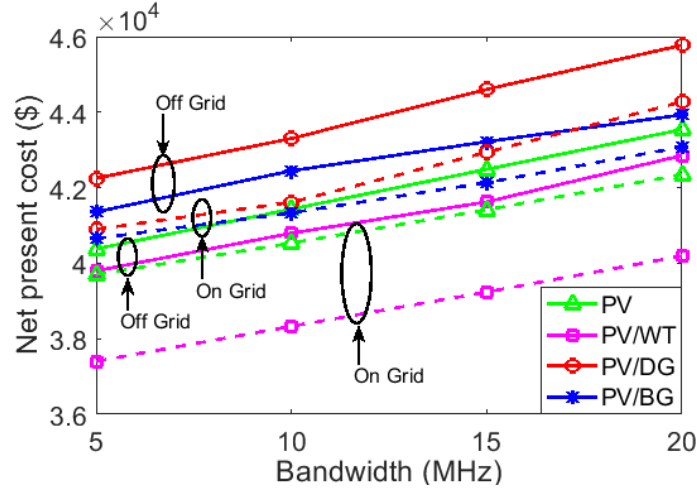
Figure 5.3: Comparison of NPC between on-grid and off-grid under different system BW.
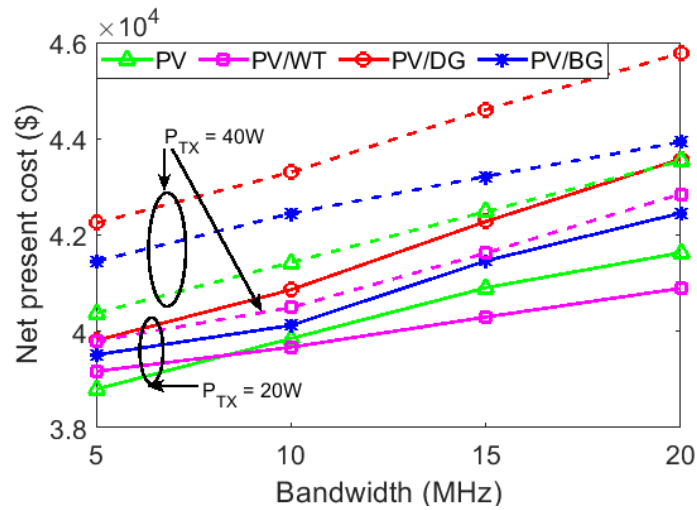
Figure 5.4: Comparison of NPC under different transmission power.

exhibits a medium level of NPC. At the same time, the hybrid PV/DG provides poor NPC because of the continuous requirement of a higher amount of OMC and fuel cost. However, the grid-tied hybrid PV/BG has better NPC performance due to the unavailability of the required wind speed.

A quantitative comparison of energy efficiency performance among the different supply systems taking the effect of dynamic traffic profile into accounts is demonstrated in Fig. 5.5 and Fig. 5.6. These two graphs illustrate that the hybrid solar PV/BG scheme provides a satisfactory level of EE performance as compared to the hybrid solar PV/DG and hybrid solar PV/WT system. It is also observed that the standalone solar PV provides superior EE performance than the other supply schemes due to the smaller amount of losses and excess electricity. Finally, the lower system bandwidth and transmission power (P_{TX}) uplift the EE
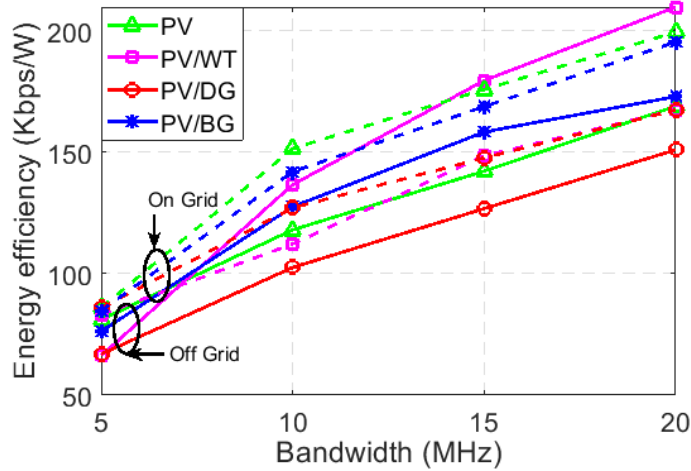
Figure 5.5: Energy efficiency performance comparison among the PV, PV/DG, PV/WT, and PV/BG.
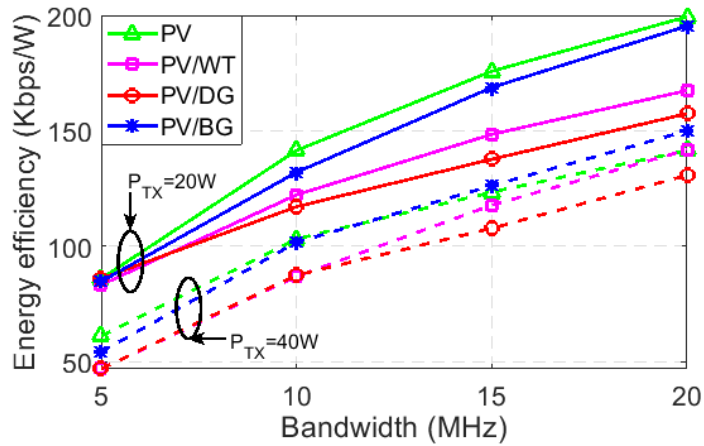
Figure 5.6: Energy efficiency comparison performance among the PV, PV/DG, PV/WT, and PV/BG.

performance of the system under all cases.

An extensive comparison of carbon footprints among the aforementioned supply schemes is illustrated in Fig. 5.7. Remarkably, solar PV and hybrid PV/WT do not contain any carbon contents whereas hybrid PV/BG emits a negligible amount of greenhouse gas. On the other hand, hybrid PV/DG produces a huge amount of GHG due to the burning of a large amount of diesel during the entire project. It is also seen that hybrid PV/DG consumes more fossil fuel to cope up with higher system BW and contributes a greater amount of carbon pollutants. Though the hybrid solar PV/BG system emits a small amount of GHG, environmental degradation can be decreased by reducing the use of biomass in the cooking process.
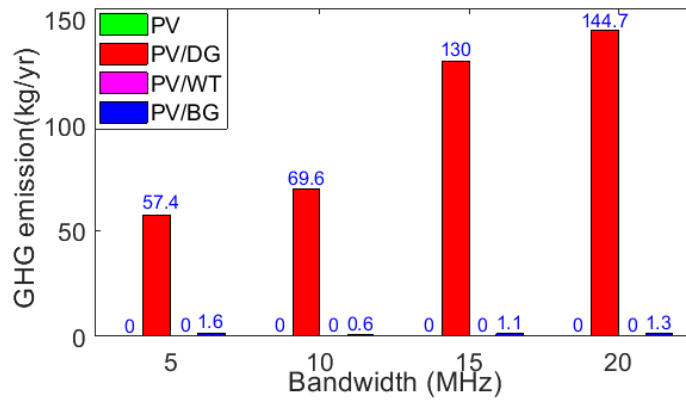
Figure 5.7: Comparison of greenhouse gases (GHG) among the PV, PV/DG, PV/WT, and PV/BG.

Table 5.3: Emissions by different sources [21].

Fuels	Emissions (Kg/Kg fuel)
Rice Husk	1.49
Bituminous Coal	2.46
Natural Gas	1.93

Despite the very small amount of GHG emissions, the hybrid solar PV/BG system is superior to the stand-alone solar PV and hybrid solar PV/DG system because of the following reasons: (i) PV/BG system provides greater sustainability due to the complementary effect of solar PV and BG; and (ii) PV/BG system indirectly minimizes CO_2 emission by reducing the biomass burning in cooking purpose. In other words, biomass burning has a hostile impact on the environment which is shown in Table 5.3 [25]. However, the proposed hybrid solar PV/BG system can save a significant amount of GHG emissions as compared to the hybrid solar PV/DG.

5.3.2 Comparison with the previous research work

In order to compare the performance of the proposed system, Table 5.4 summarizes the relevant references that have discussed similar projects in different countries.

Recently, the renewable energy-focused supply system has been considered as a promising solution for developing a green cellular network. As a consequence, harvesting energy from the locally available renewable energy sources has been extensively analyzed by telecom operators and researchers. Being inspired by the above potential benefits Nokia Siemens has already developed a hybrid solar PV and wind turbine (WT) powered green cellular BS in the rural areas of Germany [77]. Ericsson [78] has also installed wind energy focused off-grid BS for avoiding the grid energy. Besides, a diesel generator based hybrid supply system has been established by the Huawei technology in remote areas of Africa and the Middle East [20].

Table 5.4: Comparison of our system with some other suggested system

Case Study	Software Used	Outcomes
India [71]	HOMER	The hybrid solar PV/WT and solar PV/WT/fuel cell (FC) system can be a feasible solution for powering the cellular BSs with the lowest net present cost (NPC) as there are no emissions of harmful GHG emissions. Moreover, the hybrid solar PV/WT/FC system is the most economically feasible configuration for Global System for Mobile communication (GSM) BSs with NPCs of $75,515, 2 kW PV, 3 kW WT, and 2 kW FC. The hybrid supply system produces excess energy 3926 kWh/year which is stored in the battery bank for providing backup power in the case of shortage or outage of renewable energy.
Pakistan [72]	HOMER	The hybrid solar PV/WT/DG system is the most economically feasible configuration for GSM base stations with an energy cost of $0.839/kWh, 5 kW PV, 1 kW WT, 16 units of batteries, and 3 kW DG. This hybrid system can produce excess annual electricity of 3792.9 kWh per year to maintain continuity of power supply.
Malaysia [73]	HOMER	The hybrid solar PV/WT system is the most economically feasible configuration for LTE BSs in urban areas with 2 kW PV, 1 kW WT, 3 units of batteries, 1 kW electric grid, and annual OPEX savings of up to 39%. On the other hand, the stand-alone solar PV system for LTE BSs in remote areas has annual OPEX savings of up to 43%, with 2 kW PV, 4 units of batteries, and 1 kW DG for backup power.
South Korea [68]	HOMER	The hybrid solar PV/WT and stand-alone solar PV are the feasible solutions for powering the cellular network. The stand-alone solar PV system is a more feasible solution for developing a green cellular network in terms of cost, sustainability, and GHG issue with a 9 kW PV, 64 units battery with NPC of $30,366. The operational expenditure can be saved up to 56.99%, and 56.13% respectively if the DG is replaced by the hybrid solar PV/WT and solar PV system.
Nigeria [74]	HOMER	The hybrid solar PV/DG system is the most economically feasible configuration for GSM BSs with NPC of $69,811, the energy cost of $0.409/kWh, 10 kW PV, 64 units of batteries, and 5.5 kW DG. The sensitivity result implies that the hybrid system can save GHG emissions of 1.4 tons per yare as compared to the stand-alone DG system.
Spain [75]	HOMER	The hybrid solar PV/DG system is the most economically feasible configuration for GSM BSs with an energy cost of €5432 0.436/kWh, NPC of €5432 88,463, 2.5 kW PV, 12 units of batteries, and 2 kW DG.
Bangladesh [76]	HOMER	The solar PV/battery system along with small size DG is the most economic feasible configurations for powering the off-grid GSM BSs with an energy cost of $1.657/kWh, 5 kW PV, 16 batteries in 2 parallel string, and 4 kW DG. In this model, the solar PV/battery bank provides primary power and the backup power is supplied by the DG.
Bangladesh [Proposed]	HOMER MATLAB	The main contribution of this work is to develop a hybrid solar PV/BG powered green cellular network along with a sufficient battery bank. We introduced a green energy sharing and load balancing technique for increasing the network performance by optimal use of renewable energy sources. The optimal criteria of the proposed system are 3 kW PV, 1 kW BG, 64 units of batteries, and the cost of energy is $0.509/kWh under 10 MHz system bandwidth. The optimal system architecture, economic feasibility, and GHG emissions of this work have been examined using HOMER optimization software. On the other hand, the performance of the wireless network has been (throughput, energy efficiency, spectral efficiency, and outage probability) evaluated with the help of Matlab based Monte Carlo simulations.

However, most of the authors examined the key challenges of developing a green cellular network using the solar PV and wind turbines along with a backup system (such as battery bank and DG). They examined the techno-economic feasibility with the help of HOMER ignoring the dynamic behavior of traffic intensity. Moreover, many of them didn't present an energy sharing model or no algorithm at all. To the best knowledge, we are the first to develop the energy efficiency analysis integrating load-balancing scheme and energy cooperation policies for the envisaged green wireless networks.

5.4 Conclusion

This chapter primarily compares the techno-economic criteria of the hybrid solar PV/BG system with other power providing schemes in the context of energy-efficient green mobile communication. With the augmentation of harvesting renewable energy, cellular base stations (BSs) are progressively being powered by the locally available renewable energy sources (RES) to reduce the energy crisis, carbon contents, and its dependency on fossil fuel. Thus, the combination of solar PV with the biomass generator or the integration of solar PV/BG system with the electrical grid system is proving to be a more realistic option for developing an energy-efficient as well as an eco-sustainable system considering the geographical location of Bangladesh. It is revealed that the proposed system performs a lot better than the hybrid solar PV/DG. It has also achieved better reliability as compared to the solar PV system. Moreover, a significant improvement of energy efficiency can be achieved and a considerable amount of carbon content can be saved if the off-grid hybrid PV/BG system is replaced by the grid-tied system.

CHAPTER 6

CONCLUSIONS AND FUTURE WORKS

6.1 Conclusions

This work examined the feasibility and effectiveness of the integration of a solar PV system with the biomass resource generator for powering the macro base stations in Bangladesh to minimize the net present cost and greenhouse gas emissions. Green energy sharing mechanism has also been incorporated for enhancing the energy efficiency by maximum utilization of renewable energy sources. For ensuring long term sustainability and reliability, the performance of the renewable energy-based system along with sufficient energy storage devices has been analyzed in terms of various key aspects such as: (i) Optimal system architecture, (ii) energy yield analysis, (iii) Economic yield analysis, and (iv) Greenhouse gas emission analysis. Extensive simulation are carried out over the entire project time using the HOMER software in order to determine the optimal system architecture, energy-saving, capital cost, carbon footprint and assess the quantitative benefits of the proposed scheme along with energy sharing mechanisms considering the effect of solar radiation, and bandwidth variation. It is observed that the optimal use of harvested green energy with a fruitful energy sharing mechanism has enough potential to fulfill the own energy demand of BSs maintaining the guaranteed continuity of power supply in both off-grid and grid-tied systems. The total energy generated (under P_{TX}=20W, and BW=10MHz) from the off-grid hybrid system is 6,566 kWh (82% from solar PV and 18% from BG) and provides excess electricity of 1,034 kWh, which indicates the increased level of reliability ensuring zero outage. For off-grid conditions, the inter BSs green energy sharing mechanism can save energy up to 2%. On the other hand, for the grid-tied system, the energy sharing facility to the electrical grid can sell an average of 793.07 kWh energy per year, which can reduce the grid pressure and save capital cost around \$7,194/year. The simulation results also shows that the energy storage systems can carry the load demand for around 162 hours without any external sources, which is enough time to fix the renewable energy sources. Though the hybrid solar PV/BG system releases a small number of carbon footprints, the biomass generator acts as a sustainable waste management system by reducing the burning of biomass (agriculture residue) in cooking and heating purpose.

The proposed system exhibits a satisfactory level of throughput, energy efficiency, and spectral efficiency performance that are extensively analyzed considering the tempo-spatial variation of traffic intensity and system bandwidth. Moreover, the spectral efficiency and outage probably of user equipment's are thoroughly investigated by employing the load balancing technique under different system conditions such as different user conditions, different channel quality indicators (CQI), and different transmission bandwidth. Numerical results demonstrate that the integration of load balancing provides better spectral efficiency and outage probability as compared to those without load balancing condition. A significant improvement of energy efficiency can be achieved and a considerable amount of carbon content can be saved if the off-grid hybrid PV/BG system is replaced by the grid-tied system. It is revealed that the proposed system performs a lot better than the hybrid solar PV/DG. It has also achieved better reliability as compared to the solar PV system. In summary, the proposed renewable energy-focused hybrid supply system along with the proper balancing of the load among the neighboring BSs can improve the outage probability of the user equipment and the green energy sharing mechanism can overcome the loss of power supply probability. Countries like Bangladesh are in dire need of establishing such a hybrid power system to meet the increasing energy demand, save the environment, and ensure continual services to the users. Finally, the hybrid solar PV/BG system is an attractive solution to develop a sustainable green mobile communication in Bangladesh for her position as the tropical and fourth rice (the main source of biomass) producing country in the world.

6.2   Suggestions for Future Works

At the current stage of the proposed research, developed renewable energy-focused macro cellular network under load balancing and energy sharing mechanisms have much room for being improved and extended in several interesting directions. Future extension of this research work are summarized as below:

i) Developing a generalized algorithm and mathematical modeling under heterogeneous cellular networks for sharing green energy among the neighboring BSs by maximum utilization of renewable energy.

ii) Developing a cell zooming algorithm for operating the heterogeneous cellular networks according to the generated green energy and incoming traffic rate.

iii) A renewable energy cooperation of C-RAN heterogeneous networks paradigm can be explored for improving energy efficiency performance.

iv) An optimized resource scheduling algorithm can be incorporated for a better tradeoff between data rate and fairness.

RELATED PUBLICATIONS

Journal Papers

[J1] **M. S. Hossain**, A. Jahid, K. Z. Islam and M. F. Rahman, "Solar PV and biomass resources-based sustainable energy supply for off-grid cellular base stations," *IEEE Access*, vol. 8, pp. 53817–53840, Mar 2020.

[J2] **M. S. Hossain**, A. Jahid, K. Ziaul Islam, M. H. Alsharif, and M. F. Rahman, "Multi-objective optimum design of hybrid renewable energy system for sustainable energy supply to a green cellular networks," *Sustainability*, vol. 12, no. 9, pp. 3536, Apr 2020.

[J3] **M. S. Hossain**, and M. F. Rahman, "Hybrid solar PV/Biomass powered energy efficient remote cellular base stations," *International Journal of Renewable Energy Research*, vol. 10, no. 1, pp. 329–342, Mar 2020.

[J4] A. Jahid, **M. S. Hossain**, M. K. H. Monju, M. F. Rahman and M. F. Hossain, "Techno-economic and energy efficiency analysis of optimal power supply solutions for green cellular base stations," *IEEE Access*, vol. 8, pp. 43776–43795, Feb 2020.

[J5] **M. S. Hossain**, A. Jahid, K. Z. Islam, M. H. Alsharif, K. M. Rahman, M. F. Rahman, M. F. Hossain, "Towards energy efficient load balancing for sustainable green wireless networks under optimal power supply," *IEEE Access*, vol. 8, pp. 200635–200654, Nov 2020.

Conference Papers

[C1] **M. S. Hossain**, A. Jahid, and M. F. Rahman, "Dynamic load management framework for off-grid base stations with hybrid power supply," *IEEE International Conference on Electrical Engineering and Information & Communication Technology (iCEEiCT)*, Dhaka, Bangladesh, Sep 2018, pp. 336–341.

[C2] **M. S. Hossain**, A. Jahid, and M. F. Rahman, "Quantifying potential of hybrid PV/WT power supplies for off-grid LTE base station," *IEEE International Conference on Computer, Communication, Chemical, Material and Electronic Engineering (IC4ME2)*, Rajshahi, Bangladesh, Sep 2018, pp. 1–5.

[C3] A, Jahid, K. Z. Islam, **M. S. Hossain**, M. K. Hasan Monju and M. F. Rahman, "Performance evaluation of cloud radio access network with hybrid power supplies," *IEE International Conference on Sustainable Technologies for Industry 4.0 (STI)*, Dhaka, Bangladesh, Dec 2019, pp. 1–5.

[C4]   **M. S. Hossain**, M. N. S. K. Shabbir, and M. F. Rahman, "Control of power factor and reduction of THD for a three phase grid connected inverter, "*IEEE International Conference on Electrical & Electronic Engineering (ICEEE)*, Rajshahi, Bangladesh, Dec 2017, pp. 1–4.

REFERENCES

[1] Y. Li, H. Zhang, J. Wang, B. Cao, Q. Liu, and M. Daneshmand, "Energy-efficient deployment and adaptive sleeping in heterogeneous cellular networks," *IEEE Access*, vol. 7, pp. 35 838–35 850, Mar 2019.

[2] D. N. Luta and A. K. Raji, "Renewable hydrogen-based energy system for supplying power to telecoms base station," *International Journal of Engineering Research in Africa*, vol. 43, pp. 112–126, Jul 2019.

[3] "Ericsson. Mobile subscriptions First Quarter 2019," [Online]. Available: https://www.ericsson.com/en/mobility-report/reports/ june-2019/mobile-subscriptions-q1-2019.

[4] "GSMA. Country overview: Bangladesh," [Online]. Available: https://www.gsmaintelligence.com/research/? file=a163eddca009553979bcdfb8fd5f2ef0&download.

[5] "GSMA, London, UK, community power: Using mobile to extend the grid," [Online]. Available: https://www.gsma.com/mobilefordevelopment/wp-content/uploads/2012/05/Community-Power-Using-Mobile-to-Extend-the-Grid-January-2010.pdf.

[6] J. Wu, Y. Zhang, M. Zukerman, and E. K.-N. Yung, "Energy-efficient base-stations sleep-mode techniques in green cellular networks: A survey," *IEEE communications surveys & tutorials*, vol. 17, no. 2, pp. 803–826, Apr 2015.

[7] A. M. Aris and B. Shabani, "Sustainable power supply solutions for off-grid base stations," *Energies*, vol. 8, no. 10, pp. 10 904–10 941, Sep 2015.

[8] "GSMA. Extending the grid: Bangladesh market analysis," [Online]. Available: http://www.gsma.com/mobilefordevelopment/wp-content/uploads/2013/03/GPM-MarketAnalysis-Bangladesh.pdf.

[9] "World energy outlook 2018," [Online]. Available: https://www.iea.org/weo2018/.

[10] M. H. Alsharif and J. Kim, "Hybrid off-grid SPV/WTG power system for remote cellular base stations towards green and sustainable cellular networks in south korea," *Energies*, vol. 10, no. 1, p. 9, Dec 2016.

[11] M. Ismail, W. Zhuang, E. Serpedin, and K. Qaraqe, "A survey on green mobile networking: From the perspectives of network operators and mobile users," *IEEE Communications Surveys & Tutorials*, vol. 17, no. 3, pp. 1535–1556, Aug 2015.

[12] S. Zhang, N. Zhang, S. Zhou, J. Gong, Z. Niu, and X. S. Shen, "Energy-sustainable traffic steering for 5G mobile networks," *IEEE Communications Magazine*, vol. 55, no. 11, pp. 54–60, Nov 2017.

[13] C. A. Chan, W. Li, S. Bian, I. Chih-Lin, A. F. Gygax, C. Leckie, M. Yan, and K. Hinton, "Assessing network energy consumption of mobile applications," *IEEE Communications Magazine*, vol. 53, no. 11, pp. 182–191, Nov 2015.

[14] V. Chamola and B. Sikdar, "Solar powered cellular base stations: current scenario, issues and proposed solutions," *IEEE Communications magazine*, vol. 54, no. 5, pp. 108–114, May 2016.

[15] Y. Zhang, M. Meo, R. Gerboni, and M. A. Marsan, "Minimum cost solar power systems for LTE macro BSs," *Computer Networks*, vol. 112, pp. 12–23, Jan 2017.

[16] M. H. Alsharif, "Optimization design and economic analysis of energy management strategy based on photovoltaic/energy storage for heterogeneous cellular networks using homer model," *Solar Energy*, vol. 147, pp. 133–150, May 2017.

[17] A. Chauhan and R. Saini, "A review on integrated renewable energy system based power generation for stand-alone applications: configurations, storage options, sizing methodologies and control," *Renewable and Sustainable Energy Reviews*, vol. 38, pp. 99–120, Oct 2014.

[18] "NASA, Surface meteorology and solar energy: A renewable energy resource." [Online]. Available: https://eosweb.larc.nasa.gov/sse/.

[19] M. Alam Hossain Mondal and A. Sadrul Islam, "Potential and viability of grid-connected solar pv system in bangladesh," *Renewable Energy*, vol. 36, no. 6, pp. 1869–1874, Jun 2011.

[20] "Huawei, Mobile networks go green," [Online]. Available: http://www.huawei.com/en/abouthuawei/publications/ communicaite/hw-082734.htm.

[21] P. Halder, N. Paul, and M. Beg, "Assessment of biomass energy resources and related technologies practice in bangladesh," *Renewable and Sustainable Energy Reviews*, vol. 39, pp. 444–460, Nov 2014.

[22] A. K. Hossain and O. Badr, "Prospects of renewable energy utilisation for electricity generation in Bangladesh," *Renewable and Sustainable Energy Reviews*, vol. 11, no. 8, pp. 1617–1649, Oct 2007.

[23] M. S. Islam, R. Akhter, and M. A. Rahman, "A thorough investigation on hybrid application of biomass gasifier and PV resources to meet energy needs for a northern rural off-grid region of Bangladesh: A potential solution to replicate in rural off-grid areas or not?" *Energy*, vol. 145, pp. 338–355, Feb 2018.

[24] A. Huda, S. Mekhilef, and A. Ahsan, "Biomass energy in Bangladesh: Current status and prospects," *Renewable and Sustainable Energy Reviews*, vol. 30, pp. 504–517, Feb 2014.

[25] M. Ahiduzzaman and A. Sadrul Islam, "Energy utilization and environmental aspects of rice processing industries in Bangladesh," *Energies*, vol. 2, no. 1, pp. 134–149, Mar 2009.

[26] "Food and agriculture organization: Rice market monitor (Apr 2018)," [Online]. Available: http://www.fao.org/3/I9243EN/i9243en.pdf.

[27] I. B. Sofi and A. Gupta, "A survey on energy efficient 5G green network with a planned multi-tier architecture," *Journal of Network and Computer Applications*, vol. 118, pp. 1–28, Sep 2018.

[28] R. Mahapatra, Y. Nijsure, G. Kaddoum, N. Ul Hassan, and C. Yuen, "Energy efficiency tradeoff mechanism towards wireless green communication: A survey," *IEEE Communications Surveys Tutorials*, vol. 18, no. 1, pp. 686–705, First Quarter 2016.

[29] K. Kanwal, G. A. Safdar, M. Ur-Rehman, and X. Yang, "Energy management in LTE networks," *IEEE Access*, vol. 5, pp. 4264–4284, Jan 2017.

[30] M. H. Alsharif, "Techno-economic evaluation of a stand-alone power system based on solar power/batteries for global system for mobile communications base stations," *Energies*, vol. 10, no. 3, p. 392, Mar 2017.

[31] T. Han and N. Ansari, "On optimizing green energy utilization for cellular networks with hybrid energy supplies," *IEEE Transactions on Wireless Communications*, vol. 12, no. 8, pp. 3872–3882, Aug 2013.

[32] V. A. Ani and A. N. Emetu, "Simulation and optimization of hybrid diesel power generation system for GSM base station site in Nigeria," *Electronic Journal of Energy & Environment*, vol. 1, no. 1, pp. 37—-56, Apr 2013.

[33] M. H. Alsharif, R. Nordin, and M. Ismail, "Energy optimisation of hybrid off-grid system for remote telecommunication base station deployment in Malaysia," *EURASIP Journal on Wireless Communications and Networking*, vol. 2015, no. 64, pp. 1–15, Dec 2015.

[34] D. Bezmalinović, F. Barbir, and I. Tolj, "Techno-economic analysis of PEM fuel cells role in photovoltaic-based systems for the remote base stations," *International Journal of Hydrogen Energy*, vol. 38, no. 1, pp. 417–425, Jan 2013.

[35] V. A. Ani and A. N. Nzeako, "Potentials of optimized hybrid system in powering off-grid macro base transmitter station site," *International Journal of Renewable Energy Research*, vol. 3, no. 3, pp. 861—-87, Dec 2013.

[36] S. Singh, M. Singh, and S. Kaushik, "A review on optimization techniques for sizing of solar-wind hybrid energy systems," *International Journal of Green Energy*, vol. 13, no. 15, pp. 1564–1578, Dec 2016.

[37] A. Jahid, M. K. H. Monju, M. E. Hossain, and M. F. Hossain, "Renewable energy assisted cost aware sustainable off-grid base stations with energy cooperation," *IEEE Access*, vol. 6, pp. 60 900–60 920, Oct 2018.

[38] A. Jahid, A. B. Shams, and M. F. Hossain, "Dynamic point selection comp enabled hybrid powered green cellular networks," *Computers & Electrical Engineering*, vol. 72, pp. 1006–1020, Nov 2018.

[39] B. Xu, Y. Chen, J. Requena Carrión, J. Loo, and A. Vinel, "Energy-aware power control in energy cooperation aided millimeter wave cellular networks with renewable energy resources," *IEEE Access*, vol. 5, pp. 432–442, Jan 2017.

[40] A. B. Shams, A. Jahid, and M. F. Hossain, "A CoMP based LTE-A simulator for green communications," in *2017 International Conference on Wireless Communications, Signal Processing and Networking (WiSPNET)*, 2017, pp. 1751–1756.

[41] A. Jahid, A. B. Shams, and M. F. Hossain, "Energy efficiency of JT CoMP based green powered LTE-A cellular networks," in *2017 International Conference on Wireless Communications, Signal Processing and Networking (WiSPNET)*, 2017, pp. 1739–1745.

[42] H. Hung, T. Ho, S. Lee, C. Yang, and D. Yang, "Relay selection for heterogeneous cellular networks with renewable green energy sources," *IEEE Transactions on Mobile Computing*, vol. 17, no. 3, pp. 661–674, Mar 2018.

[43] C. Liu and B. Natarajan, "Power management in heterogeneous networks with energy harvesting base stations," *Physical Communication*, vol. 16, pp. 14–24, Sep 2015.

[44] A. Jahid, A. B. Shams, and M. F. Hossain, "PV powered CoMP based green cellular networks with standby grid supply," *Journal of Photoenergy*, vol. 2017, pp. 1–14, Apr 2017.

[45] Y.-K. Chia, S. Sun, and R. Zhang, "Energy cooperation in cellular networks with renewable powered base stations," *IEEE Transactions on Wireless Communications*, vol. 13, no. 12, pp. 6996–7010, Dec 2014.

[46] A. Antonopoulos, E. Kartsakli, A. Bousia, L. Alonso, and C. Verikoukis, "Energy-efficient infrastructure sharing in multi-operator mobile networks," *IEEE Communications Magazine*, vol. 53, no. 5, pp. 242–249, May 2015.

[47] A. Bousia, E. Kartsakli, A. Antonopoulos, L. Alonso, and C. Verikoukis, "Game-theoretic infrastructure sharing in multioperator cellular networks," *IEEE Transactions on Vehicular Technology*, vol. 65, no. 5, pp. 3326–3341, May 2016.

[48] M. J. Farooq, H. Ghazzai, A. Kadri, H. Elsawy, and M.-S. Alouini, "A hybrid energy sharing framework for green cellular networks," *IEEE Transactions on Communications*, vol. 65, no. 2, pp. 918–934, Feb 2017.

[49] Y. Li, H. Zhang, J. Wang, B. Cao, Q. Liu, and M. Daneshmand, "Energy-efficient deployment and adaptive sleeping in heterogeneous cellular networks," *IEEE Access*, vol. 7, pp. 35 838–35 850, Apr 2019.

[50] K. Son, E. Oh, and B. Krishnamachari, "Energy-aware hierarchical cell configuration: From deployment to operation," in *2011 IEEE Conference on Computer Communications Workshops (INFOCOM WKSHPS)*, 2011, pp. 289–294.

[51] V. Prithiviraj, S. Venkatraman, and R. Vijayasarathi, "Cell zooming for energy efficient wireless cellular network," *Journal of Green Engineering*, vol. 3, no. 4, pp. 421–434, Jul 2013.

[52] Q. Ye, B. Rong, Y. Chen, M. Al-Shalash, C. Caramanis, and J. G. Andrews, "User association for load balancing in heterogeneous cellular networks," *IEEE Transactions on Wireless Communications*, vol. 12, no. 6, pp. 2706–2716, Jun 2013.

[53] I. Siomina and D. Yuan, "Load balancing in heterogeneous lte: Range optimization via cell offset and load-coupling characterization," in *2012 IEEE International Conference on Communications (ICC)*, 2012, pp. 1357–1361.

[54] H. Ghazzai, E. Yaacoub, A. Kadri, H. Yanikomeroglu, and M.-S. Alouini, "Next-generation environment-aware cellular networks: Modern green techniques and implementation challenges," *IEEE Access*, vol. 4, pp. 5010–5029, Sep 2016.

[55] M. H. Alsharif and M. Ismail, "A solar energy solution for sustainable third generation mobile networks," *Energies*, vol. 10, no. 4, pp. 1–17, Mar 2017.

[56] M. H. Alsharif and R. Nordin, "Comparative analysis of solar-powered base stations for green mobile networks," *Energies*, vol. 10, no. 8, pp. 1–25, Aug 2017.

[57] J. Leithon, T. J. Lim, and S. Sun, "Energy exchange among base stations in a cellular network through the smart grid," in *2014 IEEE International Conference on Communications (ICC)*, 2014, pp. 4036–4041.

[58] M. F. Hossain, K. S. Munasinghe, and A. Jamalipour, "Energy-aware dynamic sectorization of base stations in multi-cell OFDMA networks," *IEEE Wireless Communications Letters*, vol. 2, no. 6, pp. 587–590, Dec 2013.

[59] K. Son, R. Guruprasad, S. Nagaraj, M. Sarkar, and S. Dey, "Dynamic cell reconfiguration framework for energy conservation in cellular wireless networks," *Journal of Communications and Networks*, vol. 18, no. 4, pp. 567–579, Aug 2016.

[60] L. Xiang, X. Ge, C.-X. Wang, F. Y. Li, and F. Reichert, "Energy efficiency evaluation of cellular networks based on spatial distributions of traffic load and power consumption," *IEEE Transactions on Wireless Communications*, vol. 12, no. 3, pp. 961–973, Mar 2013.

[61] G. Auer, V. Giannini, C. Desset, I. Godor, P. Skillermark, M. Olsson, M. A. Imran, D. Sabella, M. J. Gonzalez *et al.*, "How much energy is needed to run a wireless network?" *IEEE Wireless Communications*, vol. 18, no. 5, Oct 2011.

[62] H. Holtkamp, G. Auer, V. Giannini, and H. Haas, "A parameterized base station power model," *IEEE Communications Letters*, vol. 17, no. 11, pp. 2033–2035, Nov 2013.

[63] R. Ayop, N. M. Isa, and C. W. Tan, "Components sizing of photovoltaic stand-alone system based on loss of power supply probability," *Renewable and Sustainable Energy Reviews*, vol. 81, pp. 2731–2743, Jan 2018.

[64] A. Rahil, R. Gammon, and N. Brown, "Techno-economic assessment of dispatchable hydrogen production by multiple electrolysers in Libya," *Journal of Energy Storage*, vol. 16, pp. 46–60, Apr 2018.

[65] A. Tabak, M. Ozkaymak, M. T. Guneser, and H. O. Erkol, "Optimization and evaluation of hybrid PV/WT/BM system in different initial costs and LPSP conditions," *International Journal of Advanced Computer Science and Applications*, vol. 8, Nov 2017.

[66] S. M. Hasan, M. A. Hayat, and M. F. Hossain, "On the downlink sinr and outage probability of stochastic geometry based lte cellular networks with multi-class services," in

2015 18th International Conference on Computer and Information Technology (ICCIT), 2015, pp. 65–69.

[67] "Volte cell capacity- calculating packet size, prbs and no. of users," [Online]. Available: file:///D:/M%20Sc%20Thesis/New%20Journal/AJSE/VoLTE%20Cell%20 Capacity-%20Calculating%20Packet%20Size,%20PRBs%20and%20No. %20of%20Users%20-%20Techplayon.html.

[68] M. Alsharif, J. Kim, and J. Kim, "Energy optimization strategies for eco-friendly cellular base stations," *Energies*, vol. 11, no. 6, pp. 1–22, Jun 2018.

[69] S. Ahammad, A. H. Khan, T. E. Nur, and S. Ghose, "A hybrid of 30 kw solar pv and 30 kw biomass system for rural electrification in bangladesh," in *in 2015 International Conference on Green Energy and Technology (ICGET)*, 2015, pp. 1–5.

[70] K. Singh and S. S. Sooch, "Comparative study of economics of different models of family size biogas plants for state of punjab, india," *Energy Conversion and Management*, vol. 45, no. 9, pp. 1329–1341, Jun 2004.

[71] W. M. Amutha and V. Rajini, "Techno-economic evaluation of various hybrid power systems for rural telecom," *Renewable and Sustainable Energy Reviews*, vol. 43, pp. 553–561, Mar 2015.

[72] R. M. Asif and F. Khanzada, "Cellular base station powered by hybrid energy options," *International Journal of Computer Applications*, vol. 115, pp. 35–39, Apr 2015.

[73] M. H. Alsharif, R. Nordin, and M. Ismail, "Green wireless network optimisation strategies within smart grid environments for long term evolution (LTE) cellular networks in Malaysia," *Renewable Energy*, vol. 85, pp. 157–170, Jan 2016.

[74] L. Olatomiwa, S. Mekhilef, A. S. N. Huda, and K. Sanusi, "Techno-economic analysis of hybrid PV–diesel–battery and PV–wind–diesel–battery power systems for mobile BTS: the way forward for rural development," *Energy Science & Engineering*, vol. 3, no. 4, pp. 271–285, Jul 2015.

[75] M. Martínez-Díaz, R. Villafafila-Robles, D. Montesinos-Miracle, and A. Sudriá-Andreu, "Study of optimization design criteria for stand-alone hybrid renewable power systems," in *in 2013 International Conference on Renewable Energies and Power Quality (ICREPQ'13), Bilbao, Spain,*, 2013, pp. 1–5.

[76] S. Moury, M. Nazim Khandoker, and S. M. Haider, "Feasibility study of solar pv arrays in grid connected cellular bts sites," in *2012 International Conference on Advances in Power Conversion and Energy Technologies (APCET)*, 2012, pp. 1–5.

[77] "E-plus, Nokia siemens networks build Germany first off-grid base station," [Online]. Available: http://www.nokiasiemensnetworks.com.

[78] "Sustainable energy use in mobile communications, Ericsson inc., White paper, 2007," [Online]. Available: https://www.techonline.com/electrical-engineers/education-training/tech-papers/4136182/Sustainable-Energy-Use-in-MobileCommunications.